**Title**
UNC93B1 Mediates Differential Trafficking of Endosomal Toll-like Receptors



**Author**
Lee, Bettina

**Publication Date**
2013

Peer reviewed|Thesis/dissertation

# UNC93B1 Mediates Differential Trafficking of Endosomal Toll-like Receptors

By

Bettina Lauren Lee

A dissertation submitted in partial satisfaction of the

requirements for the degree of

Doctor of Philosophy

in

Molecular and Cell Biology

in the

Graduate Division

of the

University of California, Berkeley

Committee in charge:

Professor Gregory M. Barton, Chair
Professor Nilabh Shastri
Professor Randy Schekman
Professor Richard S. Stephens

Spring 2013

Abstract

UNC93B1 Mediates Differential Trafficking of Endosomal Toll-like Receptors

by

Bettina Lauren Lee

Doctor of Philosophy in Molecular and Cell Biology

University of California, Berkeley

Professor Gregory M. Barton, Chair

UNC93B1, a multipass transmembrane protein required for TLR3, TLR7, TLR9, TLR11, TLR12, and TLR13 function, controls trafficking of TLRs from the endoplasmic reticulum (ER) to endolysosomes. In this dissertation, I introduce the field of innate immunity, endosomal TLRs, and the known roles of UNC93B1. Furthermore, I discuss results from our studies to understand the mechanism by which UNC93B1 mediates its regulatory effects. Our results demonstrate that UNC93B1 enters the secretory pathway and directly controls the packaging of TLRs into COPII vesicles that bud from the ER. Unlike other COPII loading factors, UNC93B1 remains associated with the TLRs through post-Golgi sorting steps. Unexpectedly, these steps are different among endosomal TLRs. TLR9 requires UNC93B1-mediated recruitment of adaptor protein complex 2 (AP-2) for delivery to endolysosomes while TLR7, TLR11, TLR12, and TLR13 utilize alternative trafficking pathways. In addition, we established several assays to determine UNC93B1 function and describe a mouse model to better understand the regulation of an endogenous nucleic acid sensing TLR, TLR9. Our studies describe mechanisms for differential sorting of endosomal TLRs by UNC93B1, which may explain the distinct roles played by these receptors in certain autoimmune diseases.

This manuscript is dedicated to
T. C. Li

# Table of Contents

## List of Figures and Tables

# List of Abbreviations

**AP** – Adaptor protein complex
**CD** – Cluster of differentiation
**DOTAP** – N-[1-(2,3-Dioleoyloxy)propyl]-N,N,N-trimethylammonium methyl-sulfate
**DNA** – Deoxyribonucleic acid
**ERGIC** – Endoplasmic Reticulum to Golgi intermediate compartment
**ES** – Embryonic stem cells
**ESCRT** – Endosomal sorting complex required for transport
**HMBG1** – High-mobility group protein B1
**HRS** – Hepatocyte growth factor related tyrosine kinase substrate
**HSV** – Herpes simplex virus
**IFN** – Interferon
**IL** – Interleukin
**IRAK** – Interleukin-1 receptor associated kinase 1
**IRF** – Interferon Regulatory Factor
**LAMP** – Lysosomal associated membrane protein
**LRO** – Lysosome related organelle
**LRR** – Leucine Rich Repeat
**LPS** – Lipopolysaccharide
**MCMV** – Murine cytomegalovirus
**MHC** – Major histocompatibility complex
**MyD88** – Myeloid differentiation primary gene (88)
**NEO** - Neomycin
**NF-κB** – Nuclear Factor kappa B
**NOD** – Nucleotide-binding oligomerization domain-containing protein 1
**ODN** – Oligodeoxynucleotide
**ORN** – Oligoribonucleotide
**PAMP** – Pathogen Associated Molecular Patterns
**pDC** – Plasmacytoid dendritic cell
**PolyI:C** – Polyinosinic:polycytidylic acid
**PRR** – Pattern Recognition Receptor
**RIG-I** – Retinoic acid-inducible gene 1
**RNA** – Ribonucleic acid
**SLE** – Systemic lupus erythematosus
**TBK1** – TANK binding kinase 1
**TGN** – Trans-Golgi Network
**TIR** – Toll Interleukin-1 domain
**TIRAP** – TIR domain containing adaptor protein
**TLR** – Toll- Like Receptor
**TNF** – Tumor necrosis factor
**TRAF** – TNF-receptor associated factor
**TRAM** – TRIF-related adaptor molecule
**TRIF** – TIR-domain-containing adapter-inducing interferon-β
**VSV** – Vesicular stomatitis virus

# Acknowledgements

I came to graduate school in hopes of developing into a confident, well-trained, and knowledgeable scientist. I have to thank my mentor, Greg Barton, who helped me achieve this goal. Joining his lab wasn't always clear, but looking back it was the best decision I could have made. Greg genuinely cares about the people in his lab – in research, career and personal life. I feel special to have received his support throughout the years. Despite of my shyness and insecurities (and inappropriate use of commas!), he has always seen my potential and pushed me to reach it. I thank him for being confident in my abilities and helping me find my confidence.

I would not be in graduate school if it were not for Averil and Barbara. Averil offered me the opportunity to work in his lab right out of college and it was there that I learned what it was like to work in academic research. This experience inspired me go to graduate school. I thank both Averil and Barbara for being my friends and also supportive "science parents."

I was extremely lucky to be surrounded by the amazing members of the Barton lab. They are the most supportive and importantly, inclusive group of people I know. They made my experience fun and exciting while their intelligence and amazing talent motivated me to think more critically and work harder. I thank the first group of graduate students that brought me into their family - Sarah, Maria, Nick, Roman, and Laura. Sarah patiently trained me in the early days, and Nick took care of me like no one else. I thank my baymate, Alex, for being so kind and patient with me. Kelsey, Zaq, Allison, Meghan, April, Jacques, Gaby, Olivia, Bo, thank you for making the so lab fun! I also thank my extremely talented undergraduate, Joanne and our tech, Bling (Jeff) for helping me with my project.

I would not have been able to graduate without the tremendous support of my graduate school friends. If I had to take one thing away with me from graduate school, it would be the life-long friendships with my grad school classmates. Elena, Patty, and MT were my going-out buddies, while Kwan was my chillin'-at-a-coffee shop buddy. All were my travel buddies. Together, we shared unforgettable adventures in Italy, Spain, Poland, Iceland and Japan. I will miss the "wine down Wednesdays", coffee breaks, and cardio kickboxing classes together. I thank Elena for being such an amazing friend, for always telling me "don't stress," and for planning all social activities, period. I thank Patty for always having a bright smile and for always being there to chat about anything. I thank MT for being so outgoing and showing me that fun and dancing is an essential part of life. I thank Kwan for being the most sweetest and dependable person ever. My buddies in the hallways, Jenny and Kristin, were my go-to gals to have a longer than expected chat. I thank them for making me feel like I was not alone and that graduate school *is* hard. I also thank Soo-Jung her friendship and late night lab dinners, and Lara and Brandon for SFS. All together, these made grad school worth it!

I would like to especially thank Will. He is my best friend and my favorite companion. He has shown me that there is life outside of lab and it has to be explored! I thank him for opening my eyes to new experiences and for his loving and everlasting support.

Lastly, but most importantly, I thank my loving family for their support and sacrifices. My family is THE most important part of my life, and I feel privileged to have my family's support and encouragement to make *my happiness* a priority. Mom, Dad and Melody and Xiao (our dog) are my foundation and I would not have pursued my career goals without their support. I miss my grandparents and wish they could be here today to see my accomplishments. I thank all of my family (my aunts and uncles and cousins), who positively influenced who I am today.

# Chapter 1: Introduction to Toll-like receptors and immunity

## A history of innate immunity and microbial pattern recognition

The vertebrate immune system is comprised of distinct cell types that coordinate to enable sensing and effective elimination of microbial infections. The immune system can be further partitioned into two branches: the innate immune system and the adaptive immune system. The adaptive immune system is comprised of B and T cells and mounts a specific, clonal response to foreign antigen. This response requires rearrangement of receptors expressed by B and T cells and leads to clearance of infection through secretion of antibodies, cytokines, or cell-mediated responses (Figure 1.1). Importantly, unlike the innate immune system, the adaptive immune system is capable of establishing immunological memory. The innate immune system is a more rapid, ancient immune defense system and relies on recognition of microbes through broad specificity, non-rearranging receptors expressed on innate immune cells such as macrophages and dendritic cells. The innate immune system can be thought of as a first line of defense against microbial infection but also carries importance in the initiation of an effective adaptive immune response.

The idea that the innate immune system could influence the adaptive immune response came to light in Charles Janeway's introduction to the 1989 Cold Spring Harbor Symposium [1]. Janeway proposed the existence of evolutionarily conserved receptors, which he termed pattern recognition receptors (PRRs) that would recognize conserved molecular features of microbes. He then suggested that these receptors, expressed on innate immune cells like dendritic cells, could elicit a rapid, non-clonal response and provide a second signal for adaptive immune cells to initiate a specific clonal response. This notion was supported by what Janeway called "immunologist's dirty little secret," in which a strong adaptive immune response required prior mixing of an antigen with an adjuvant containing dead microbes [1]. Janeway's model is summarized in Figure 1.1, in which recognition of microbial products by innate immune cells such as macrophages and dendritic cells leads to up-regulation of co-stimulatory molecules, cytokine secretion and antigen presentation; this innate immune response in turn is necessary for the activation of the adaptive immune response.

Toll-like Receptors (TLRs) are an ancient, evolutionarily conserved family of PRRs. The *drosophila* Toll, was originally identified as a key gene important for the establishment of the dorsal-ventral axis in the developing *drosophila* embryo [2]. It was later shown by Lemaitre et al. that Toll participated in immunity against fungal infection in the adult fly [3]. The following year, Medzhitov and Janeway discovered the existence of a human orthologue of Toll, later shown to be TLR4, and provided the name Toll-like Receptor (TLR) [4]. This TLR was expressed on antigen presenting cells and lead to the induction of cytokines and co-stimulatory molecules. Independently, Beutler and colleagues identified murine Toll-like Receptor 4 as the receptor recognizing lipopolysacharride (LPS), a component of gram-negative bacteria cell walls [5]. Subsequent discoveries of other members of the TLR family and their role in innate immunity have paved the way for the immense volume of research over the next 20 years that has elucidated the importance of TLRs in microbial sensing and disease pathogenesis [2, 6]. Although TLRs are indisputably important for innate immunity, other pattern recognition receptors have also been discovered as critical components of the innate immune response, for

example, the NOD-like receptors, RIG-I-like receptors and potential DNA sensors [7]. While their importance cannot be understated, it is beyond the focus of this dissertation and will not be further discussed.

Together our understanding of the innate immune system is comprised of a vast number of receptors including TLRs that recognize distinct molecular characteristics of microbes. This allows the immediate recognition and initiation of immune responses necessary for the successful clearance of microbial infection. Today, research aims to further understand the mechanisms of regulation that lead to the critical outcomes that trigger the innate immune response and influence the adaptive immune system.

## Toll-like Receptors

### TLR Function and Expression

Presently, thirteen TLRs have been discovered between human and mice; mice lack expression of TLR10, while humans lack expression of TLR11, 12 and 13. The conserved microbial derived molecules they recognize are summarized in Table 1.1. Recognition of these pathogen associated molecular patterns, or PAMPs, have been shown to lead to a variety of critical downstream responses [8].

TLRs are expressed on many different cell types and participate in important immune functions. As mentioned previously, TLRs expressed on dendritic cells and macrophages, play a role in the induction of host defense mechanisms, such as secretion of anti-viral and pro-inflammatory cytokines, as well as communication with the adaptive immune system through antigen presentation and up-regulation of co-stimulatory molecules. TLRs are also expressed on B cells and T cells and can play a direct role in activating these cells [9]. Additionally, expression on intestinal epithelial cells and skin cells is essential for the maintenance of commensal bacteria and sensing of microbial infection [10]. Other immune functions in a variety of other specialized cells types have also been reported but are not mentioned here [9]. Currently, identifying additional cell types expressing specific TLRs has been a difficult task, in part due to the lack of TLR-specific antibodies and reliance on mRNA transcript detection or signaling in response to identified ligands [9].

The distribution of nucleic acid-sensing TLRs is of particular interest to our broader understanding of the roles of nucleic acid sensing TLRs in an immune response and the mechanisms to regulate their activity. For example, plasmacytoid dendritic cells (pDCs), a specialized type I interferon (IFN)-producing cell, express only TLR7 and TLR9 but not TLR3 [11]. TLR9 in the mouse is specifically expressed in pDCs, B cells, macrophages and dendritic cells, while TLR7 can have a more broad expression pattern [9]. In contrast, human TLR9 is restricted to pDCs and B cells [9]. This could imply an evolutionary mechanism to prevent unnecessary inflammatory responses by restricting activation to certain specialized cell types.

### TLR Structure

Toll-like receptors are a family of type I transmembrane proteins with an extracellular domain, or ectodomain, a transmembrane domain, and an intracellular domain containing a signaling

adaptor interacting domain called Toll-Interleukin-1 Receptor (TIR) domain [12]. Additional critical regions include the area between the transmembrane and TIR domain, referred to as the 'linker' region [13]. (Figure 1.2A)

Over the past ten years, crystal structures have provided immense insight into how TLRs bind their cognate ligand. However, it is important to note that these crystal structures were solved using truncated TLRs and may not reflect the natural conformation of a full-length membrane bound receptor. The following TLR structures have been solved: TLR1/2 and TLR2/6 hetero-dimers, TLR4 (with co-receptor MD2), TLR3, TLR5 and most recently TLR8 homo-dimers [14-20]. Importantly, these structures confirm that the ectodomain forms a horseshoe-like structure and support a model in which TLRs form homo-dimers or hetero-dimers upon ligand binding (Figure 1.2B). Additionally, each TLR recognizes ligand using unique binding sites. TLRs 2, 4, and 5 each have one site for ligand binding, while TLR3 has two binding sites for dsRNA. Although the structure of TLR9 has yet to be solved, one study demonstrated that TLR9 exists as a dimer in the ER and traffics to endolysosmes in a dimerized state [21, 22]. In addition, a conformational change occurs upon ligand recognition which likely confers recruitment of signaling adaptors to promote signaling [21]. Furthermore, nucleic acid sensing TLRs, such as TLR7 and TLR9, exist as functional proteolytically processed forms in endosomes [23, 24]. The current model identifies this proteolytic cleavage event as a necessary step to induce a conformational change to allow recruitment of downstream signaling adaptors upon ligand binding. In line with this hypothesis, the full-length receptor, though capable of binding ligand, cannot promote recruitment of signaling adaptors [24].

The TLR ectodomain contains a series of leucine-rich repeats (LRRs), which consist of repeated regions characterized by a LxxLxLxxN amino acid sequence motif [12]. Notably, other PRRs such as NOD-like Receptors also contain LRRs [25]. While LRRs are thought to promote protein-protein interactions, the LRRs in TLRs seem to mostly participate in the binding of various non-protein ligands [12]. All TLRs contain a conserved cysteine residue, near the start of the transmembrane however defining the region transmembrane domains of TLRs has been difficult and controversial. The "linker" region may have important information for TLR trafficking, however, these residues again depend on defining the position of the transmembrane [13]. TIR domains are present on both TLRs and signaling adaptors such as MyD88 and TRIF, as well as TIRAP and TRAM, and interact through TIR-TIR interactions [12]. The signaling adaptors recruit downstream signaling molecules leading to transcription factor activation. TLRs may recruit the signaling adaptor MyD88 directly, as in TLR9, or interact with TIRAP to recruit MyD88, as in TLR4 and TLR2. Moreover, TLR3 TIR domain interacts directly with signaling adaptor TRIF, while TLR4 interacts with TRAM to recruit TRIF [26].

**TLR Signaling Pathways**

MyD88- and TRIF-dependent downstream signaling can lead to distinct immunological outcomes. Both signaling pathways rely on a signaling cascade consisting of the molecules IRAKs, TRAFs, TBK1, TAK1 to activate transcription factors such as NF-κB and IRFs, to up-regulate various genetic programs and lead to specific immune responses. These pathways are summarized in Figure 1.3. MyD88 signaling can lead to the activation of NF-κB resulting in the production of pro-inflammatory cytokines, such as TNFα, IL-6 and IL-12p40, while it is also possible that signaling can lead to the activation of IRF7 and promote production of type I

interferons (IFN), such as IFNα/β. Similarly, TRIF signaling can lead to IRF3 and NF-κB activation to achieve type I IFN and pro-inflammatory responses. Downstream signaling from each TLR can be unique. All TLRs, with the exception of TLR3, can signal through MyD88. TLR3 relies on TRIF mediated signaling while TLR4 is capable of signaling through MyD88 and TRIF. [7]

Differential signaling through a TLR can be influenced its cellular localization. For example, TLR4 signals via MyD88 at the plasma membrane while internalization of TLR4 into endosomes leads to TRIF mediated signaling [27, 28]. Moreover, TLR9 leads to type I IFN responses at early endosomal compartments while promoting pro-inflammatory responses from late endosomes [29]. Differential signaling seems to depend on the cell type and the specific molecules recruited to the signaling complexes. For example, upon engagement of TLR7 or TLR9 ligands, conventional dendritic cells do not produce type I IFNs, while plasmacytoid dendritic cells (pDCs) can secrete large amounts of type I IFNs. This difference is in part due to the preferential recruitment of IRF7 to MyD88 signaling complexes to early endosomes in pDCs [29]. Additionally, lysosome-related organelles were demonstrated to be another specialized compartment from which TLR9 can signal and lead to type I IFN responses in pDCs [30, 31]. Finally, TLR2 has also been shown to initiate type I IFN responses in inflammatory monocytes after internalization [31]. Thus, signaling from a "specialized" subcellular compartment seems to be important for induction of type I interferon responses.

## Toll-like Receptors in pathogen recognition

TLRs play a critical role in initiation of host defense against microbial infection. For example, TLR4 recognizes lipopolysaccharides (LPS) and is important in the detection of gram-negative bacteria that can lead to septic shock. TLR5, and now TLR11, recognize a range of bacteria through recognition of flagellin [8]. Additionally, TLRs 3, 7 and 9 have been shown to play a vital role in viral clearance, as in the case of murine cytolomegalovirus (MCMV) and Herpes Simplex Virus (HSV1) infection [32]. Additionally, TLR9 participates in the recognition of hemozoin from *Plasmodium falcicarum* in malarial infection [33]. Furthermore, activation of TLR2 can triggered in response to viral, bacteria, fungal and parasitic infections, such as VSV, mycobacteria, *Candida albicans*, and *Trypanosoma* infections [8]. TLR11 and TLR12 recognize profilin-like proteins and are critical for defense against *Toxoplasma gondii* and uropathogenic bacterial infection [34]. Finally, TLR13 recognizes bacterial RNA such as that from S. Aureus [34-37]. More recently it seems apparent that TLRs also play a role in recognition of non-pathogens, such as gut commensals. The regulation of how TLRs distinguish between pathogen and non-pathogen is under active research.

## Toll-like Receptors in disease

Intriguingly, several TLRs have been shown to recognize host-derived ligands triggering inflammation [7]. In some cases, this is thought to be a mechanism to detect 'danger' in the presence tissue damage, cell death or cellular stress caused by invading pathogens or tumor progression. For example, TLR2 and TLR4 can recognize heat-shock proteins Hsp60/70 derived

from dying cells. HMGB1, a nuclear non-histone protein, can be released by necrotic cells or during inflammation and recognized by TLR2, 4, and 9 [7]. Additionally, HMGB1 can act as a co-receptor, as it has also been shown to bind DNA to activate TLR9 [38]. Sterile inflammation triggered by TLR can lead to certain pathologies. For example, recognition of oxidized LDL is linked to atherosclerosis and recognition of amyloid beta is linked to Alzheimer's disease [7].

In other cases, self-recognition may be due to uncontrolled regulation of TLR recognition and can be detrimental for the host. Because TLRs 3, 7, 8, and 9 all recognize nucleic acid ligands, it seems critical for the host to establish regulatory mechanisms to avoid recognition of self-nucleic acid. Regulation is accomplished in part by compartmentalization of the receptors to intracellular compartments [39, 40]. Self-nucleic acids, present in the extracellular space, are unstable and susceptible to nucleases, and thus, are unable to freely enter the endocytic pathway to reach TLRs in endosomes. Viral particles containing nucleic acids, however, are able to enter the endocytic pathway leaving nucleic acid relatively intact for recognition by nucleic acid sensing TLRs [41]. In the case of apoptotic cell clearance, macrophages may internalize dying cells through specific receptors and potentially expose endosomal TLR to self-nucleic acids. However, it is likely that other, currently unidentified mechanisms are in place to avoid recognition by nucleic acid sensing TLRs.

Breakdown of this regulatory pathway can lead to potential autoimmunity. For example, LL37, an antimicrobial cationic peptide, binds to host-derived RNA and DNA, and mediates its uptake into endocytic compartments in pDCs, leading to activation of TLR7 and TLR9. Increased expression or secretion of LL37 has been linked to the autoimmune-like disease, psoriasis [42]. Systemic lupus erythematosus (SLE), an inflammatory autoimmune disease, is also linked to the recognition of nucleic acid complexes by nucleic acid sensing TLRs 7 and 9 [43]. In SLE, ribonucleoproteins-RNA and histone DNA complexes are recognized by autoantibodies. These nucleic acid-protein complexes can be internalized by FcγRIIa on dendritic cells or by B cell antigen receptors in B cells, thus facilitating recognition of self-DNA and -RNA by TLR9 and 7, respectively. Additionally, DNAse I-deficient mice are unable to clear self-DNA leading a to lupus-like syndrome [44].

Interestingly, although it is clear that both TLR7 and TLR9 can lead to autoantibody production and inflammation associated with SLE, they may in fact play distinct roles. In a specific mouse model of SLE (MRL lpr/lpr), researchers have demonstrated that while TLR7 deficiency protects against disease progression, TLR9 deficiency can exacerbate disease [43, 45]. Moreover, a duplication or over-expression of TLR7 in a mouse model can lead to SLE-like disease [46]. Thus, while TLRs are necessary to detect presence of invading microbes, potential recognition of self-ligands pose a threat to the host and may lead to various pathologies.

| TLR | Ligand | Pathogen recognition |
|---|---|---|
| **TLR 1/2** | triacyl lipopeptides | bacteria and mycobacteria |
| **TLR 2** | bacterial peptidoglycan | gram-positive bacteria |
| **TLR 3** | dsRNA | viruses |
| **TLR 4** | LPS | gram-negative bacteria |
| **TLR 5** | flagellin | flagellated bacteria |
| **TLR 2/6** | diacyl lipopeptides, zymosan | mycoplasma |
| **TLR 7** | ssRNA, R848, loxoribine, imiquimod | RNA viruses |
| **TLR 8*** | ssRNA, R848 | RNA viruses |
| **TLR 9** | DNA, unmethylated CpG | viruses, plasmodium |
| **TLR 10*** | unknown | unknown |
| **TLR 11** | profilin, flagellin | Toxoplasma gondii |
| **TLR 12** | profilin | Toxoplasma gondii |
| **TLR 13** | ssRNA | Staphylococcus Aureus |

**Table 1.1 Toll-like Receptors and recognized ligands[8]**

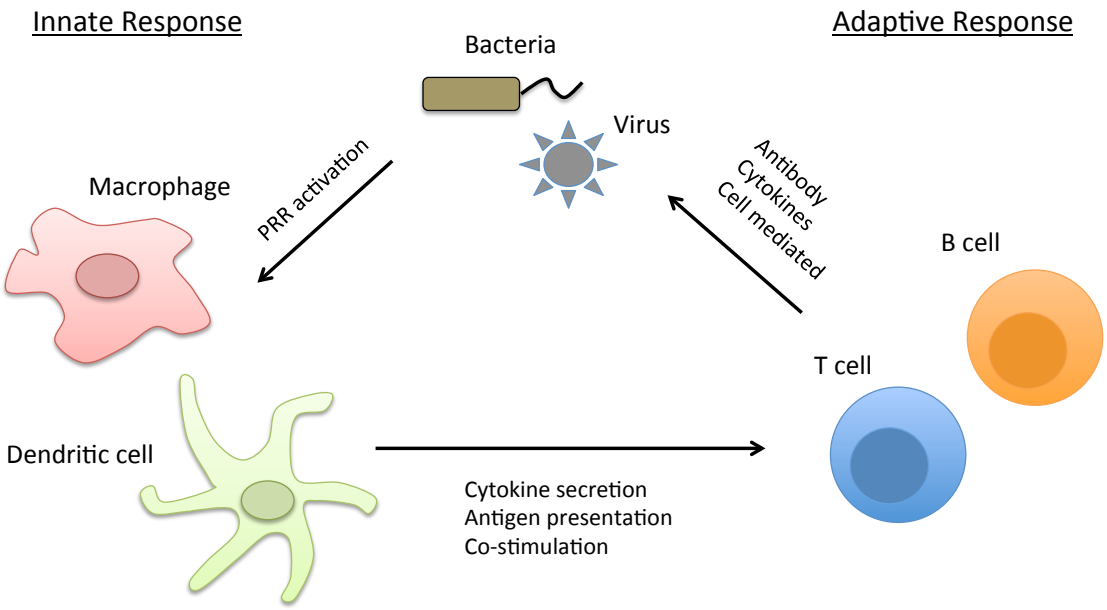


**Figure 1.1. Simplified schematic of microbial recognition and immune response**
The immune system can be subdivided into the innate and adaptive immune responses. The two have distinct roles but work together to efficiently clear microbial infections. Recognition of microbial products by innate immune cells, such as macrophages and dendritic cells, through their pattern recognition receptors (PRRs), can lead to the up-regulation of co-stimulatory molecules, cytokine secretion and antigen presentation, all of which are necessary to activate of the adaptive immune response. The adaptive immune system is comprised of B and T cells and mounts a specific, clonal response against foreign antigen. B and T cells must rearrange their receptors to afford specific detection of microbes. By receiving signals from the innate immune system, B and T cells are then instructed to secrete antibodies, cytokines, or mediate cell-mediated responses, appropriately.

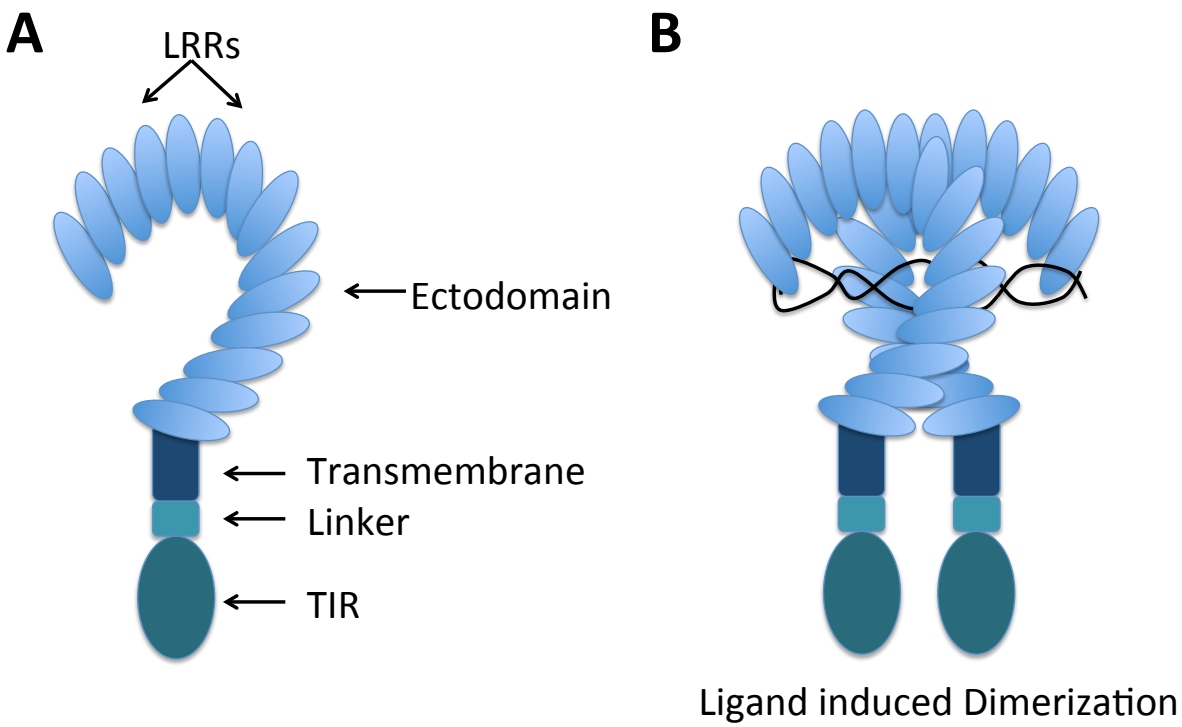


**Figure 1.2. Structure of Toll-like receptors**
(A) Schematic of a generic Toll-like receptor (not drawn to scale). Toll-like receptors consist of an extracellular domain, also called an ectodomain, a transmembrane domain, and an intracellular region containing the Toll-Interleukin-1 Receptor (TIR) domain, important for interaction with signaling adaptors. The ectodomain contains several leucine-rich repeats (LRRs) and are important for ligand binding. Additional critical regions include the area between the transmembrane and TIR domain, referred to as the 'linker' region. (B) Ligand recognition and dimerization. TLRs may bind ligand through receptor dimerization. While some TLRs may form pre-dimers before ligand recognition and undergo a conformational change upon ligand binding to induce signaling.

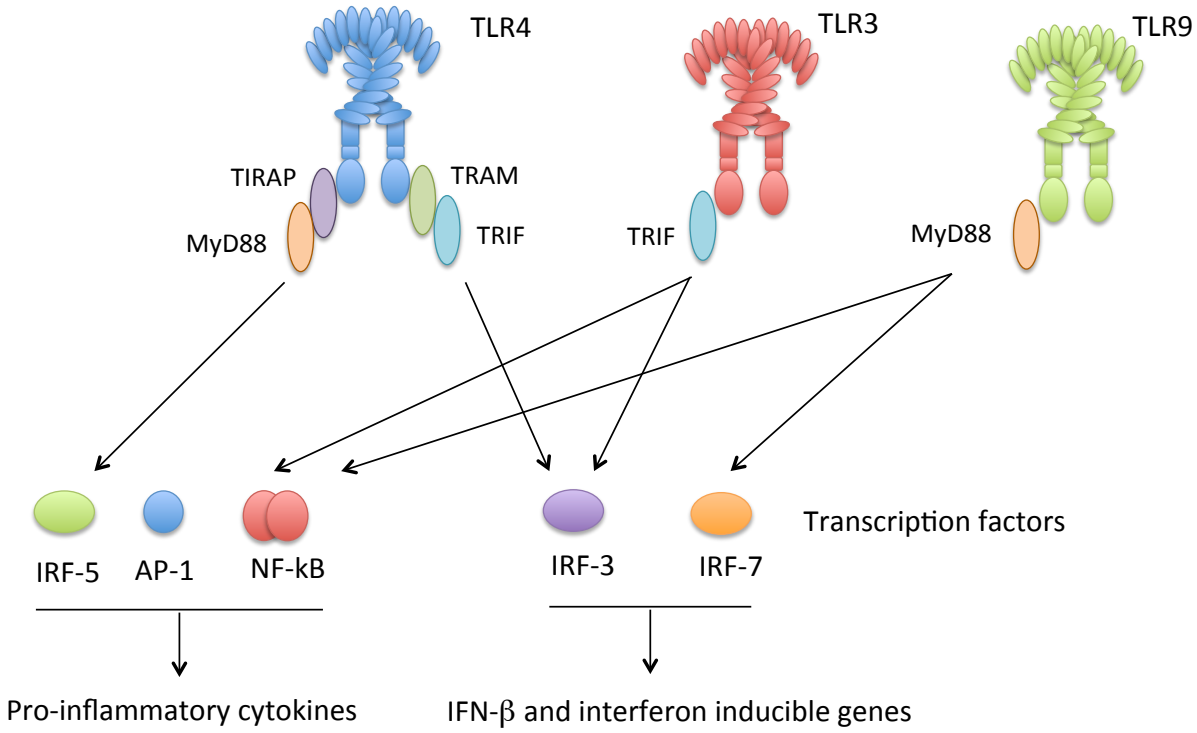


**Figure 1.3 Toll-like Receptor Signaling**
MyD88- and TRIF-mediated signaling utilizes several signaling adaptors (not shown here) and transcription factors, NF-κB and IRFs, to induce specific transcriptional programs. MyD88-mediated signaling can lead to the activation of NF-κB resulting in the production of pro-inflammatory cytokines, such as TNFα, IL-6 and IL-12p40. In addition, MyD88 can lead to recruitment and activation of IRF7 to promote production of type I interferons (IFNs), such as IFNα/β. Alternatively, TRIF-mediated signaling can leads to activation of IRF3 and induce type I IFN responses, as well as NF-κB to induce pro-inflammatory responses. All TLRs, with the exception of TLR3, can use MyD88. TLR3 only signals through TRIF, while TLR4, the only other TLR that can signal through TRIF uses both MyD88 and TRIF.

# Chapter 2: Regulation of subcellular localization of endosomal Toll-like receptors

## Endosomal TLRs

The focus of this dissertation is to understand how endosomal TLRs are regulated with an emphasis on the role of UNC93B1. The following chapter delves into the importance of each endosomal TLR in greater detail, the models of endosomal TLR localization, the roles of UNC93B1 and general mechanisms of intracellular trafficking.

### Nucleic acid sensing TLRs 3, 7, 8 and 9

**TLR3** recognizes double stranded RNA structures, such as the synthetic analog polyinosine-polycytidylic acid (PolyI:C) [47]. Indeed, TLR3-/- mice are unresponsive to PolyI:C [48]. Of note, polyI:C present in the cytosol is also a ligand for the RNA sensor, RIG-I [49]. Replication intermediates in viral infections by ssRNA viruses or from transcription of DNA viruses can generate dsRNA structures [50]. Interestingly, TLR3 deficiency fails to result in an increased susceptibility to various viruses such as VSV and LCMV, suggesting other anti-viral mechanisms are dominant in these viral infections [51]. However, genetic studies in humans and mice have demonstrated a role for TLR3 in controlling of HSV1/2 infection of the central nervous system [52, 53]. Why TLR3 is important for some viruses and not others may be due to differences in cellular expression. While conventional dendritic cells and various epithelial cells express TLR3, pDCs lack TLR3 expression, despite expressing other nucleic acid sensing TLRs 7 and 9 [11]. In addition, the localization of TLR3 is not well established. One report suggests that TLR7, 9 and TLR3 are in similar compartments [54, 55]. While another report suggests that TLR3 may also localize to the plasma membrane [56], in addition to its presence in endosomes. TLR3 also exists as a proteolytically processed form, a common feature of nucleic acid sensing TLRs [57, 58]. The mechanism of ligand binding is still controversial. Structural studies conclude that TLR3 binds polyI:C as a full-length homo-dimer with binding sites present at both N- and C-terminal regions of the TLR3 ectodomain [59]. However, the N-terminal portion of the ectodomain is cleaved off from the C-terminal receptor and has been reported to shed or be secreted[60]. Additionally, recent evidence suggests that the N terminal and C terminal fragments remain associated after proteolytic processing [58]. A unifying model is still necessary to understand the specific mechanisms of ligand binding and signaling.

**TLR7** recognizes single stranded RNA species derived from bacteria and viruses [61, 62]. Indeed, TLR7 knockout mouse studies have demonstrated a role against ssRNA viruses such as VSV and influenza [61]. Moreover, TLR7 is thought to be responsible for the control of endogenous retroviruses[63]. The small molecular compounds R-837 (imiquimod) and R848 (resiquimod) and 3M-001 activate TLR7 [62, 64]. Additional ligands include loxoribine, a substituted guanosine nucleoside, and ssRNA40, a phosphothioate-protected RNA oligonucleotides based on a GU-rich sequence from HIV complexed with a cationic lipid such as DOTAP [65, 66]. Interestingly, while ssRNA40 stimulates mouse TLR7, it does not stimulate human TLR7 but does stimulate human TLR8 [66]. Thus, there are species differences in

recognition of ssRNA ligands. Additionally, oligoribonucleotide sequences were discovered to trigger both TLR7 and TLR13 [35]. TLR7 is expressed by dendritic cells, macrophages and plasmacytoid dendritic cells, but may play additional roles in different cell types. For example, TLR7 plays a role in neurological outcomes [67].

**TLR8** shares the closest homology, structurally and in sequence, to TLR7. Human TLR8 was shown to recognize the small molecule agonists (imidazoquinolines) like TLR7 [64, 68]. In a study comparing several small molecules, human TLR8, but not TLR7, responded to 3M-002. Interestingly, all human TLR8 small molecule agonists were unable to stimulate mouse TLR8 [64]. This has led to the conclusion that mouse TLR8 is defective or nonfunctional. However, a combined delivery of polyT oligodeoxynucleotides and small molecule agonists (3M-002 and 3M-003) has been shown to activate mouse TLR8 [69]. Additionally, TLR8-/- mice develop spontaneous autoimmunity, a phenotype in part due to an increase in TLR7 expression [70]. Together, these studies leave open the possibility that mouse TLR8 is a functional receptor and suggests a role in controlling aberrant TLR7 levels that lead to rampant autoimmunity.

**TLR9** was identified as a receptor that recognizes bacterial DNA and stimulatory CpG oligonucleotides (ODN) [71]. However, it plays a critical role in immunity against many viruses, including HSV-1/2 and MCMV. TLR9 expression in pDCs is critical for clearing these viral infections [72-74]. Studies examining TLR9 function often use CpG ODNs to activate the receptor. Two classes of stimulatory CpG ODN are commonly used [29, 75]. Class A ODNs (CpG-A), characteristically form higher order structures and use both phosphodiester and phosphothiorate backbones. Class B ODNs (CpG-B) are naturally monomeric with a complete phosphothiorate backbone. While CpG-A can stimulate pDCs to produce type I IFNs, CpG-B leads to a pro-inflammatory cytokine response. Notably, TLR9 recognizes the sugar backbones of ODNs in addition to the nucleotide base sequence [76]. Binding does not necessarily correlate with stimulation, as inhibitory CpG ODNs can still bind but prevent receptor signaling [77]. Thus, TLR9 maintains preferences for certain unmethylated CpG sequences for potent activation [78, 79]. Since the majority of mammalian CpG sequences are methylated, this feature has been suggested to be a discriminating feature between microbial DNA from host cell DNA. However, not all CpG sites in the mammalian cell are methylated, and accordingly, several reports have shown that TLR9 is capable of engaging genomic DNA [40, 80]. As mentioned previously, TLR9 is proteolytically processed to generate a C-terminal fragment that functions as the receptor to bind ligand and recruit MyD88 [24]. However, others have suggested a role for the N-terminal portion of the ectodomain for signaling [81]. It remains to be determined how the N-terminus participates in ligand sensing and signaling and whether it plays a role before or after the proteolytic processing event. Thus, it may be possible that association of the N-terminal fragment with the C-terminal receptor occurs after proteolytic processing, much like that hypothesized for TLR3. Thus, both N and C terminal fragments may be required to bind ligand while the conformational change induced by cleavage is still required for signaling adaptor recruitment. A crystal structure will be necessary to bridge the data describing TLR9 ligand binding.

**Other endosomal TLRs 11 and 13**

**TLR11** is expressed in mice, but not humans [82]. Although TLR11 was thought to reside at the surface, several reports now suggest that TLR11 has an intracellular presence [36]. It is currently the only known endosomal TLR that recognizes a protein rather than a nucleic acid. TLR11 was originally discovered to recognize a profilin-like protein, involved in motility of *Toxoplasma gondii* [83]. TLR11 plays a crucial role in *T. gondii* infection, but also in uropathogenic bacterial infections [84]. Its role in uropathogenic infections could be explained by a more recent observation that TLR11 recognizes flagellin, a protein important for the motility of some bacteria. Flagellin recognition by TLR11 was demonstrated to be crucial in *Salmonella Typhimurium* and *Salmonella Typhi* infections [85]. Thus, lack of TLR11 in humans may explain why humans are susceptible to *S. Typhi* while mice are naturally resistant. Flagellin was first recognized as a ligand for TLR5, therefore it is not surprising that TLR11 and TLR5 share strong homology [82, 85]. Unlike TLR11, TLR5 is not expressed in macrophages, however both are expressed in dendritic cells [85]. It remains to be determined whether TLR11 and TLR5 need to form heterodimers for function and whether they have non-overlapping roles in bacterial infection models. In addition, TLR12 has been shown to form heterodimers with TLR11 for the recognition of parasitic profilin-like protein [34]. Accordingly, TLR12 was also shown to play a prominent role in the clearance of *T. gondii* infection [86].

**TLR13** has been identified as a receptor for single stranded RNA [35, 87, 88]. Like TLR11, TLR13 is not expressed in humans. Short oligoribonucleotide (ORN) sequences have been identified to specifically stimulate TLR13 [35]. TLR13 participates in bacterial and viral sensing, such as *staphylococcus aureus* and vesicular stomatitis virus [35, 37]. TLR13 is likely localized intracellularly, however the study of this TLR is still in its infancy. It remains to be determined whether TLR13 has prominent or redundant roles in bacterial or viral ssRNA sensing.

## Trafficking of endosomal TLRs

Localization of Toll-like receptors seems to have evolved for the optimal ligand recognition. TLRs can reside at the plasma membrane or take residence in acidic intracellular compartments like endosomes and lysosomes, or endo-lysosomes. TLRs 1, 2, 4, 5, 6, 10, 12 are proposed to localize to the plasma membrane while TLRs 3, 7, 9, and more recently, TLR11 and 13, are present in intracellular acidic compartments [36, 37, 89, 90]. Surface TLRs commonly recognize features of microbes present extracellularly, such as LPS or lipoproteins components of bacterial cell walls, while intracellular TLRs tend to recognize ligands present inside microbes such as nucleic acids. Surface or endosomal residence is not permanent, as surface localized TLRs can also function in endolysosomal compartments. As mentioned previously in Chapter 1, TLR4 signals through a TRIF-dependent pathway only upon internalization by a CD14-Syk-PLCγ endocytosis pathway from the plasma membrane into endosomes[28]. Additionally, surface localized TLR2 is found in phagosomes and initiates a type I IFN signaling pathway after internalization in inflammatory monocytes [31, 90]. The specific mechanisms that determine residence at a surface location versus endosomal location are still unclear.

Importantly, a clearer picture of the trafficking route of intracellular TLRs, such as TLR9 and 7, has emerged in recent years (Figure 2.1). TLR9, once thought to traffic through an ER to endolysosome by a direct route bypassing the Golgi [22], is now thought to enter the

conventional secretory pathway from the ER to the Golgi to endolysosome [23, 24, 41]. In the first report to describe this pathway, Ewald et al. investigated the trafficking of TLR7 and TLR9 through biochemical approaches. They showed that TLR9 transits through the Golgi prior to reaching endolysosomes. In addition, TLR9 is proteolytically processed from a 150kDa protein to generate a functional 80kDa form of the receptor that recruits MyD88 upon signaling [24]. Proteolytic cleavage occurs in a step-wise manner, where an initial cleavage is achieved by an asparagine endopeptidase or cathepsin followed by further trimming by various cathepsins [23]. Of note, TLR9 is thought to exit the ER as a dimer and experiences a conformational change upon ligand binding, rather than induced dimerization, for signal transduction [21, 22]. The regulation of TLR9 and other endosomal TLR trafficking is still unclear and whether TLR9 traffics at steady state or upon stimulation to endolysosomes is under debate.

The transmembrane domain and/or linker region was demonstrated to contain information for determining cellular destinations [13, 55]. However, defining the residues that make up the transmembrane and linker regions has been difficult and disputed in the literature. Nevertheless, swapping these regions can affect the trafficking of TLRs. For example, attaching the transmembrane and cytosolic region of TLR4 onto the ectodomain of TLR9 can confer trafficking to the surface [40]. Additionally, replacing the transmembrane of TLR3 with that of TLR9 can disrupt normal trafficking of TLR9 [80]. Moreover, it was demonstrated that TLR3 depends on its linker region for intracellular localization, while TLR7 relies on its transmembrane domain [54].

Trafficking determinants on each TLR may be important for associating with trafficking factors. For example, TLRs 3, 7, and 9 require interaction with the trafficking chaperone, UNC93B1, for transport from ER to endolysosomes [91]. Indeed, UNC93B1 interacts with the transmembrane domains of TLRs 3, 7 and 9 but not surface TLR4 [92]. Other co-factors have been reported for TLR trafficking. For example, CD14 originally thought of as a co-factor for LPS, has been shown to facilitate trafficking of TLR4 to endosomes upon stimulation [28]. Of note, CD14 may also be involved in TLR 3, 7, and 9 function [93, 94]. Additionally, all TLRs are folded in the endoplasmic reticulum (ER) with the help of ER folding chaperones such as gp96 and PRAT4A [95]. For example, both gp96 and PRAT4A are involved in the maturation of TLR4 and co-receptor MD2 in the ER [95]. Other TLRs, including TLR9 have also been reported to use gp96 and PRAT4A for trafficking out of the ER [95]. TLRs are then exported from the ER and traffic to their final destinations either surface or endosome. Thus, although several factors are required for trafficking of TLRs, UNC93B1 seems uniquely specific for trafficking of endosomal TLRs.

Roles of the ectodomain or cytosolic regions in determining trafficking cannot be excluded. Trafficking factors have been reported to be important for trafficking or responses downstream of TLR9 and TLR7 and rely on interactions with the cytosolic regions. AP-3 is a heterotetrameric complex that is responsible for clathrin mediated sorting of cargo into lysosome related organelles [30, 96]. AP-3 was demonstrated to play a role in type I IFN production but not pro-inflammatory cytokines in pDCs upon TLR7 and TLR9 stimulation [30]. AP-3 seems to sort TLR9 into specialized organelles capable of recruiting MyD88-IRF7 complex and drive type I IFN production [30] (Figure 2.2). Furthermore, through a unbiased siRNA screen, Chiang et al. reported the role of HRS in trafficking TLR7 and TLR9 to endolysosomes [97]. HRS is part of the “endosomal sorting complex required for transport” (ESCRT), which recognizes ubiquitin bound cargo and packages cargo into multivesicular bodies. Chiang et al propose that TLR9 is

packaged into multivesicular bodies and proceeds through a non-conical pathway, where instead of being targeted for degradation, TLR9 is maintained in lysosomes [97].

Proper endosomal localization is important for ligand recognition and downstream responses. TLR9 is thought to bind DNA at an optimal pH between 5 and 6.5 found within endosomes and lysosomes [78]. Therefore, intracellular localization in acidic compartments is critical for signaling. Early endosomes mature to late endosome then to lysosomes (Figure 2.2). Signaling from these distinct organelles can lead to different responses (Figure 2.2). For example, as mentioned in Chapter 1, multimeric CpG-A can be retained in early endosome longer, and able to recruit MyD88-IRF7 signaling complex to drive type I interferon responses in pDCs [29]. In contrast, monomeric CpG-B accesses late endosomes rapidly and induces MyD88-NFkB signaling axis to stimulate proinflammatory cytokines [29]. Interestingly, complexing CpG-B with DOTAP (a cationic lipid) can retain CpG-B in early endosomes and induce a type I interferon response through MyD88-IRF7 axis in pDC s[29]. Thus, localization of TLRs and the location of receptor-ligand recognition can determine the type of responses after receptor engagement.

## UNC93B1: a trafficking factor for endosomal TLRs

Endosomal TLRs are dependent on UNC93B1 for proper trafficking. UNC93B1 was first identified through a forward genetic screen in mice. This initial study demonstrated that UNC93B1 is involved in the function of TLRs 3, 7, and 9 [98]. It was therefore referred to as "triple defect" or *3d* [98]. Subsequently, TLRs 11 and 13 were also shown to require UNC93B1 for function [35-37]. The *3d* mutation (His to Arg mutation at position 412) renders the protein non-functional [98]. UNC93B1 is most highly expressed in cell types expressing TLR9, such as dendritic cells, macrophages, and B cells (www.biogps.org). Not surprising, *Unc93b1*$^{3d/3d}$ mice were found to be highly susceptible to viral, bacterial and parasitic infections. A lengthy list includes mouse cytomegalovirus (MCMV), HSV-1/2, *Listeria monocytogenes, Leishmania major, Toxoplasma gondii* and *Trypanosoma cruzi* infections [36, 98-102]. Susceptibility is largely attributable to the lack of UNC93B1-dependent TLR function. Lack of UNC93B1 expression in humans also confers increased susceptibility to viral infections [99]. Although studies in human cells expressing nonfunctional UNC93B1 have demonstrated impaired cellular type I IFN response leading to HSV-1 encephylitis, UNC93B1 deficiency surprisingly did not compromise immune responses to other pathogens[53]. *Unc93b1*$^{3d/3d}$ mice were reported to have a deficiency in exogenous antigen presentation such as cross-presentation and MHC II presentation [98, 103]. However, our group has not been able to reproduce this data (data not shown) suggesting that UNC93B1 major defect is the lack of endosomal TLR function. In addition, human cells knocked down for UNC93B1 had normal MHC II presentation [104]. Due to its role in nucleic acid sensing TLR function, UNC93B1 is also linked to autoimmunity. In support of this, increased expression of UNC93B1 has been linked to SLE in humans [105] and moreover, UNC93B1 deficiency in a mouse model of SLE can alleviate disease [106]. Furthermore, an UNC93B1 mutation at position 34 from Asp to Ala in mice leads to a spontaneous autoimmune disease, driven by increased levels of TLR7 [107].

Structurally, UNC93B1 is thought to fold as a twelve-pass transmembrane protein [92]. It has 30% homology to a potassium ion channel regulator first identified in C. Elegans and

contains a domain with weak homology to the bacterial ABC-2 type transporter [108]. The UNC-93 protein family contains characteristic acidic clusters at terminal ends [108].

The current model for the control of TLR trafficking by UNC93B1 proposes that UNC93B1 directly interacts with intracellular TLRs 3, 7, and 9 through transmembrane associations in the ER and together, traffic to endolysosomal compartments [92]. Therefore, UNC93B1 plays a key role in regulation of intracellular TLR trafficking to endolysosomes while dysregulation may cause the development of autoimmune disease. Thus, it will be critical to determine the mechanism of regulation and better understand the control of intracellular TLR trafficking.

## Mechanisms of protein trafficking

General trafficking mechanisms can be applied toward understanding TLR cell biology. Our knowledge of Toll-like receptor cell biology is only beginning to develop. Below are some general mechanisms of intracellular trafficking described for various proteins, which may be useful in defining the trafficking mechanisms of endosomal TLRs.

### Endoplasmic reticulum export of transmembrane proteins

Levels of endosome resident TLRs may be controlled by mechanisms of ER export. TLRs are folded in the ER and, through unknown mechanisms, leave the ER traffic to endolysosomal compartments. Importantly, one school of thought suggests that TLR9 is transported from the ER to endolysosome in a stimulation dependent manner [22]. Although our group has shown the existence of steady state trafficking to endolysosomes [24], we cannot rule out the possibility that increase ER export may occur upon stimulation. Together, these support the idea of a regulated mechanism for TLR9 transport out of the ER.

Proteins destined to leave the ER, also called cargo proteins, may be exported by two broad mechanisms: (1) a selective, active transport mechanism, or (2) a bulk flow mechanism [109]. Transmembrane cargo proteins are incorporated into COPII vesicles that bud from the ER and traffic to ER to Golgi intermediate compartments (ERGIC) [110]. It is at the ERGIC where cargo proteins are released from COPII vesicles and can enter the Golgi apparatus [110]. While a bulk flow mechanism suggests that cargo proteins are passively incorporated into budding COPII vesicles, the selective ER export mechanism suggests cargo proteins are concentrated and recognized by Sec24, one of the several COPII coat proteins, to support entry into COPII vesicles [110]. Initiation of COPII vesicle formation begins by the activity of Sec12, an ER resident protein, to initiate activation of Sar1 into a GTP state. Sar1-GTP can then dock on ER membranes and catalyze the recruitment of Sec23/24. This is followed by the recruitment of Sec13/31 to the forming vesicle and completion of the COPII coat to allow budding from ER membranes [111].

Sec24 proteins bind motifs present on the cytosolic facing portion of cargo transmembrane proteins, or can bind motifs present on escort chaperones that are associated with cargo proteins [110]. There are four isoforms of Sec24s each in mice and humans, named Sec24 A, B, C, and D. Human Sec24A and B have a preference for D/ExE/D motifs while Sec24C and D have a preference for IxM motifs, however, Sec24 specificity can also vary among all four isoforms [112, 113]. For example, Sec24 isoforms have been shown to recognize variety of

diacidic and dihydrophobic motifs [114, 115]. Thus, active transport provides a way for the cell to control the levels of proteins leaving the ER through exposure of Sec24 binding motifs or presence of escort chaperones.

An interesting example of regulated ER export in the control of sterol regulatory element binding protein (SREBP) in lipid homeostasis [116]. Scap is a polytopic escort protein that binds SREBP, a membrane bound transcription factor, directly and offers a Sec24 binding site to mediate ER export of the Scap-SREBP complex. Under high cholesterol condition, Scap is inhibited by Insig through the direct binding of Insig to Scap. In absence of cholesterol, association with Insig is disrupted and Scap is able to bind Sec24 and initiate ER export of SREBP [116]. Thus, regulation may occur through ER retention mechanisms in response to differential stimuli.

### Sorting transmembrane proteins to endolysosomes

Regulation of trafficking may also occur at trans-Golgi compartments and post-Golgi compartments. Transmembrane proteins that enter the conventional secretory pathway reach the trans-Golgi network (TGN) and may be directed to the plasma membrane or enter endosomal or lysosomal sorting pathways [117]. Sorting occurs through recognition of sorting signals present in cytosolic regions of transmembrane proteins; however, length of the transmembrane domain[118], glycosylation status of luminal domains[119], and post-translational modifications[117], have also been reported as a potential mechanisms.

There are multiple routes to entering endosomal and lysosomal compartments. Receptors present at the plasma membrane may be internalized through endocytosis to downregulate signaling, while other proteins, such as MHC II or LAMP-1/2, traffic to the surface and internalize to achieve residence in lysosomes [120-122]. Still others can traffic to directly to endolysosomes from the trans-Golgi [117]. Components of vesicle coats include the adaptor protein (AP) complexes and GGA. Adaptor proteins mediate recognition of motifs such as NPXY, [DE]XXXL[LI], or YXXΦ, where Φ represents a bulky hydrophobic group [117]. Trafficking of cargo can be mediated through AP -1, -2, -3, -4 complexes through clathrin dependent or independent mechanisms [117]. Clathrin-dependent endocytosis is mediated by AP-2 complex [123, 124], while other AP complexes seem to be involved in intracellular sorting directly from Golgi to endo-lysosomal compartments or between endosome or lysosome compartments [117]. Ubiqutination can also serve as a sorting signal and is recognized by proteins such as ubiquitin interacting motif (UIM) containing proteins and GGA proteins [117]. Another mechanism to consider is a pathway direct from ER to phagosome (compartment formed from phagocytosis) [125]. A recent report suggests that a regulatory protein, Sec22B, may mediate this pathway[126]. Thus, it will be interesting to determine whether TLRs also utilize these pathways to enter endosomal compartments.

## Forward Perspectives

Studying the mechanisms involved in trafficking endosomal TLRs will be important in understanding the regulation involved in avoiding autoimmune disease pathology. Additionally, investigating the trafficking of TLRs to specific compartments may provide crucial information about how microbes are handled versus endogenous material such as apoptotic cells. It remains to be determined whether any of these steps are achieved by specific cell types or perhaps, in a stimulus dependent manner. To gain insight into how cells achieve the precise trafficking of

endosomal TLRs, we focused our efforts on the protein UNC93B1. The following chapters of this dissertation describe work aimed at further identifying mechanisms of UNC93B1 in endosomal TLR trafficking.

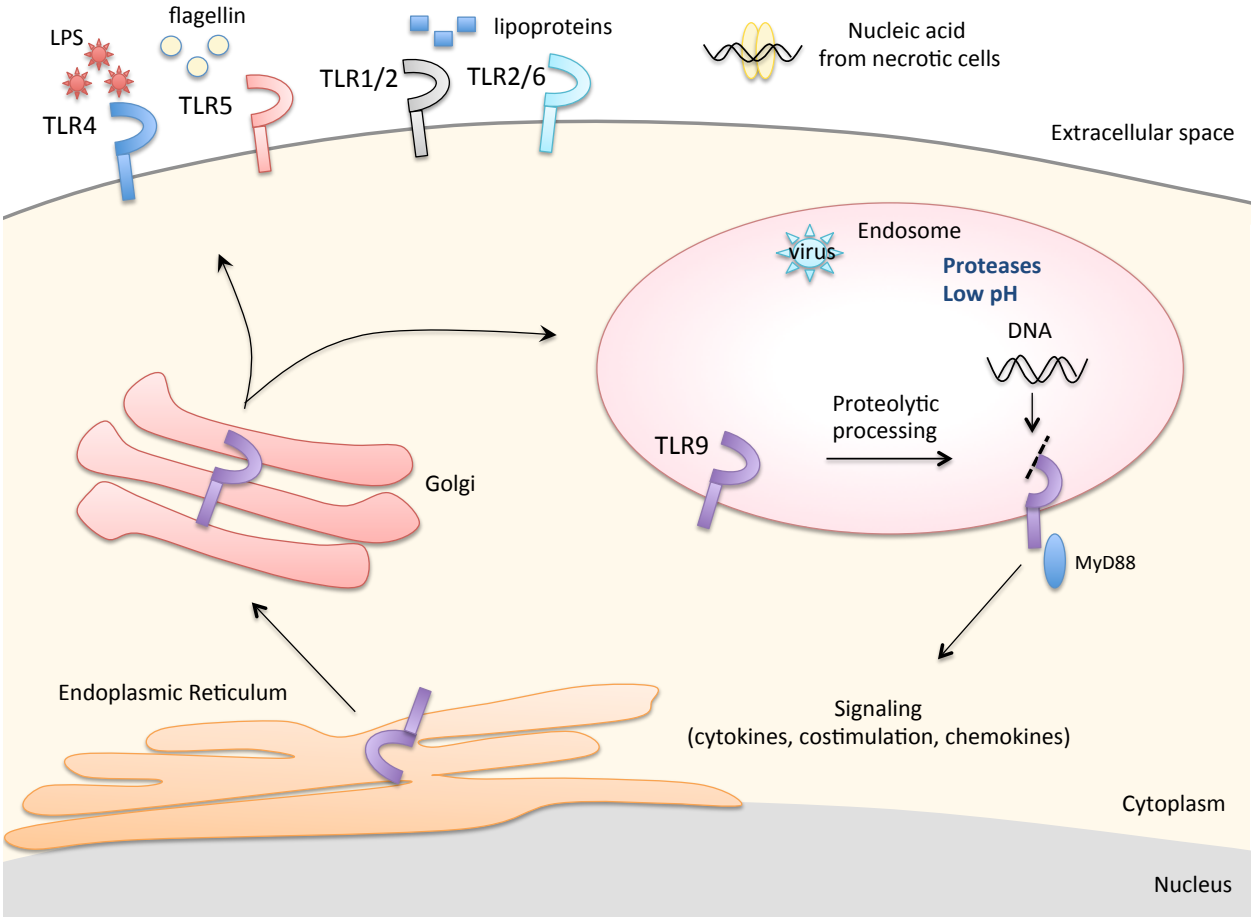


**Figure 2.1 Trafficking of nucleic acid sensing Toll-like Receptors.**
A schematic of nucleic acid sensing TLR trafficking. As opposed to surface localized TLRs, 1,2,4, 5, and 6, nucleic acid sensing TLRs, such as TLR9, reside intracellularly. Because TLR9 senses DNA, it can recognize foreign DNA from viruses, and potentially self-DNA present in the extracellular from dying cells. TLR9 trafficking is regulated in several ways to discriminate between self/non-self ligands. TLR9 is folded in the ER and transits through the Golgi. From there, TLR9 is sorted into endosomal compartments to avoid the surface where self-nucleic acids can be accessed. Endosomal residence also serves several other purposes. For one, TLR9 needs to be proteolytically cleaved to form an active receptor. Second, unprotected DNA (such as that from dying cells) are quickly degraded in the acidic and DNase-rich compartments, thus ensuring that only DNA encapsulated from viral particles can reach TLR9 receptor. Third, TLR9 binding has been shown to be optimal at low pH. Thus, these mechanisms provide a way to prevent self-DNA recognition and optimal recognition of foreign DNA.

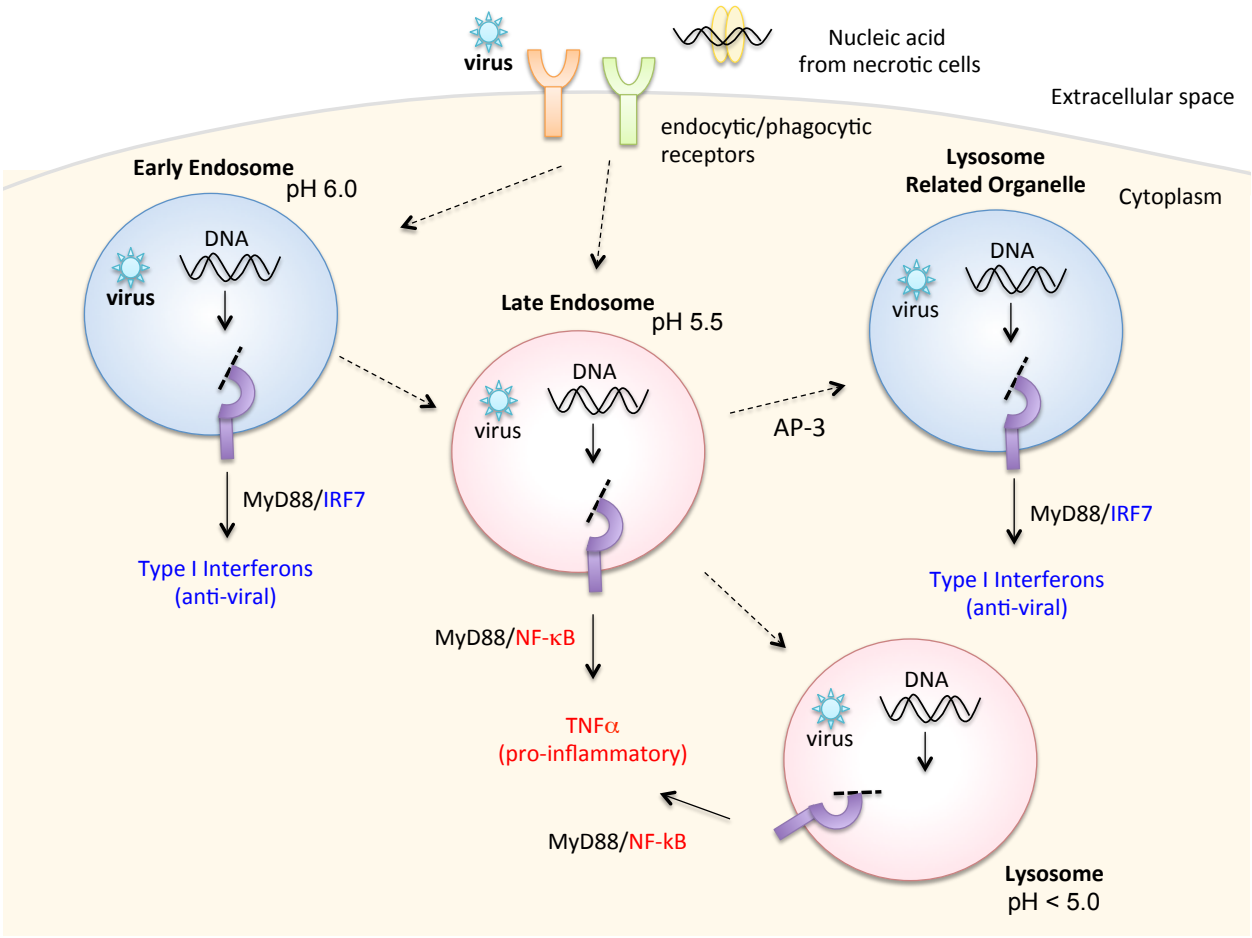


**Figure 2.2 Differential signaling by TLR9 from different endosomal compartments**
Early endosomes (pH ~6.0) mature to late endosome (pH~5.5) then to lysosomes (pH >5.0). Lysosome related organelles (LROs) are distinct set of organelles. AP-3 mediates trafficking of molecules from late endosomes to LROs. Signaling from these distinct organelles can lead to differential responses by the same receptor. TLR9 signaling in early endosomes recruits the MyD88-IRF7 signaling complex and drives type I interferon responses in pDCs. In contrast, ligand recognition in late endosomes leads to the MyD88-NFkB signaling axis and induces proinflammatory cytokines. Additionally, AP-3 can sort TLR9 from late endosomes into LROs, where TLR9 can recruit the MyD88-IRF7 complex and drive type I IFN production.

# Chapter 3: The ER export of endosomal TLRs by UNC93B1

## Background

Toll-like receptors (TLRs) recognize conserved microbial features and initiate signals critical for induction of immune responses to infection. A subset of TLRs (TLR3, TLR7, TLR8, and TLR9) recognizes forms of nucleic acids, including double-stranded RNA, single-stranded RNA, and DNA [49]. This specificity facilitates recognition of a broad array of microbes but introduces the potential for recognition of self-nucleic acids. TLR7 and TLR9 recognition of self-RNA and self-DNA, respectively, contributes to autoimmune diseases such as systemic lupus erythematosus (SLE) [43, 45].

TLR9 and other intracellular TLRs must traffic from the endoplasmic reticulum (ER) to endolysosomes before responding to ligands. UNC93B1, a multi-pass transmembrane protein localized to the ER, appears to facilitate this trafficking[91, 92]. Mice homozygous for a nonfunctional *Unc93b1* (H412R) allele (*Unc93b1*$^{3d/3d}$) fail to respond to TLR3, TLR7, or TLR9 ligands, and mice and humans deficient in UNC93B1 are highly susceptible to viral infection[53, 98, 99]. More recently, UNC93B1 has been implicated in the function of TLR11, TLR12, and TLR13[34-37]. UNC93B1 is not required for responses by surface localized TLRs such as TLR2 and TLR4[98]. UNC93B1 associates with endosomal TLRs, and in cells with defective UNC93B1, TLR9 and 7 fail to leave the ER [91, 92]. However, the mechanism by which UNC93B1 facilitates TLR trafficking to endosomal compartments remains enigmatic, especially considering its reported direct translocation from the ER to endolysosomes [91]. This pathway is inconsistent with our findings that TLR9 and TLR7 traffic through the general secretory pathway en route to endosomes[23, 24]. In addition, mice expressing an aspartic acid to alanine mutation at amino acid position 34 in UNC93B1 (*Unc93b1*$^{D34A/D34A}$) were recently shown to develop spontaneous autoimmunity due to enhanced TLR7 responses and diminished TLR9 responses [107, 127]. These findings suggest that regulation of TLRs by UNC93B1 can influence the relative thresholds of receptor activation. For these reasons, we have sought to define the molecular basis by which UNC93B1 controls endosomal TLR trafficking and function.

Beyond the implied role for UNC93B1 discussed above, little is known about the molecular mechanisms that mediate proper localization of endosomal TLRs and no other factor required specifically for endosomal TLR trafficking has been identified. Nevertheless, several reports suggest that endosomal TLR trafficking may be influenced at the ER. Gp96 functions as an ER folding chaperone for many TLRs, including TLR9, and PRAT4A has been implicated in TLR trafficking from the ER, including the nucleic acid sensing TLRs [128-130]. Whether UNC93B1 behaves similarly or functions through a different mechanism has yet to be determined. Moreover, whether trafficking of UNC93B1 and associated TLRs occurs through the Golgi or through a direct ER to endolysosome pathway is still an open question.

Here, we describe a direct role for UNC93B1 in facilitating the ER exit of TLRs en route to Golgi. Furthermore, we identify additional TLRs that expand the repertoire of TLRs requiring UNC93B1 for trafficking. And finally, to gain mechanistic insight, we used a mutagenesis approach and report a role for an N-terminal region of UNC93B1 for ER export of TLRs. Thus, we find that UNC93B1 plays a direct role in controlling the ER exit of all endosome bound TLRs.

## Results

### UNC93B1 traffics to phagosomes via the Golgi compartment

UNC93B1 has been described as an ER-resident trafficking chaperone that translocates TLRs directly from the ER to endolysosomes upon TLR activation [91]. This model is based in part on the observation that UNC93B1 never acquires Endoglycosidase H (EndoH)-resistant glycans [92], which are acquired only when proteins traffic through the medial Golgi [24]. Because this proposed function for UNC93B1 conflicts with our model of TLR9 trafficking [23, 24], we first examined whether UNC93B1 is present in endolysosomal compartments in unstimulated cells. Wildtype (WT) UNC93B1 but not the nonfunctional (H412R) mutant was detectable in phagosomes purified from unstimulated RAW264 cells (Figure 3.1A). Moreover, a portion of UNC93B1-WT gained EndoH-resistance in multiple cell types, while UNC93B1-H412R was entirely EndoH-sensitive (Figure 3.1B-F). These results agree with a previous report that the H412R mutant fails to leave the ER[91]. To formally demonstrate that the increased molecular weight of WT UNC93B1 is due to N-linked glycans, we mutated Asn-251, which is within a consensus N-glycosylation site, and this mutant failed to acquire EndoH-resistant glycans (Figure 3.1G). Based on the acquisition of EndoH-resistant glycans by UNC93B1, we examined whether UNC93B1 is detectable within COPII vesicles, which mediate transport of cargo between the ER and Golgi [112]. Using an *in vitro* COPII budding assay [131, 132], we compared levels of UNC93B1-WT and -H412R in purified vesicles. UNC93B1-WT, but not H412R, was clearly present within the vesicles, further supporting a model in which UNC93B1 exits the ER through the general secretory pathway (Figure 3.1H). Altogether, these data indicate that a pool of UNC93B1 protein exits the ER and traffics through the Golgi in unstimulated cells. Moreover, transit from the ER to the Golgi may be important for UNC93B1 function, as the nonfunctional UNC93B1-H412R mutant fails to enter COPII vesicles and does not reach the medial Golgi.

### UNC93B1 facilitates TLR9 loading into COPII vesicles

Our previous work reported that three species of TLR9 can be detected within macrophages, representing distinct maturation stages: an initial150kDa species with EndoH-sensitive glycans corresponding to the ER-resident protein (TLR9-ER), a larger species with EndoH-resistant glycans corresponding to full-length receptor that has passed through the Golgi (TLR9-Precursor), and a 80kDa band with EndoH-resistant glycans corresponding to the mature, cleaved receptor within endolysosomes (TLR9-Cleaved) (Figure 3.2A, lane 1) [24]. To examine how UNC93B1 function impacts TLR9 localization, we compared these three forms of TLR9 in immortalized macrophages derived from *Unc93b1*$^{3d/3d}$ mice and complemented with UNC93B1-WT or UNC93B1-H412R. While all three bands were present in macrophages with functional UNC93B1, only the ER-resident form was detectable in cells expressing the UNC93B1-H412R mutant (Figure 3.2A), consistent with our previous analysis of TLR9 in UNC93B1 shRNA knockdown cells. These data indicate that TLR9 does not reach the medial Golgi in the absence of functional UNC93B1. Because a pool of UNC93B1 can traffic from ER to Golgi by entering COPII vesicles (Figure 3.1B), we considered whether UNC93B1 regulates this aspect of TLR9 trafficking. Indeed, analysis of TLR9 loading into COPII vesicles revealed that TLR9 was only detectable in the presence of functional UNC93B1 whereas a control traffic protein, ERGIC/p58,

was packaged independently of UNC93B1 (Figure 3.2B).

Quality control mechanisms ensure that only properly folded proteins can exit the ER, and one mechanism by which UNC93B1 could regulate ER exit of TLR9 is through regulation of TLR9 folding, as has been reported for gp96[130]. To address whether UNC93B1 serves as a folding chaperone, we tested whether a chimeric CD4-TLR9 protein, consisting of the ectodomain of CD4 fused to the transmembrane and cytosolic regions of TLR9 (Figure 3.2C left), required UNC93B1 function. Because trafficking of CD4 is not UNC93B1-dependent (Figure 3.2D), this chimera can be used to test whether TLR9 requires UNC93B1 to ensure correct folding of the TLR9 ectodomain. CD4-TLR9 acquired EndoH-resistant glycans when expressed with UNC93B1-WT but not when expressed with mutant UNC93B1-H412R (Figure 3.2C right). Thus, the requirement for UNC93B1 is not based on TLR9 ectodomain folding. Furthermore, the transmembrane domain and cytosolic regions of TLR9 are sufficient to mediate UNC93B1-dependent trafficking.

Taken together, these data indicate that UNC93B1 regulates ER to Golgi transport of TLR9. While we cannot rule out that a pool of UNC93B1 bypasses the Golgi en route to endosomes as suggested by others [91, 92], this route does not seem relevant for UNC93B1-dependent TLR9 trafficking. Instead, UNC93B1 appears to control TLR9 entry into COPII vesicles.

**UNC93B1 is required for proper trafficking of TLR3, TLR7, TLR9, TLR11, and TLR13 from the ER**

We next sought to determine whether the dependence on UNC93B1 for ER exit is a general property of endosomal TLRs. We generated a panel of CD4-TLR fusion proteins and tested whether they required UNC93B1 to exit the ER, based on acquisition of EndoH-resistant glycans. As expected, ER exit of both CD4-TLR3 and CD4-TLR7 required UNC93B1, which is consistent with defective TLR3 and TLR7 signaling in *Unc93b1*$^{3d/3d}$ mice [98], whereas CD4-TLR4 trafficked independently of UNC93B1 (Figure 3.2E). CD4-TLR11 and CD4-TLR13 also required UNC93B1 for ER exit (Figure 3.2E). Less is known about the localization or trafficking of these TLRs, although biochemical studies have suggested that these TLRs can associate with UNC93B1 [36, 92, 133]. Our results are the first to show that UNC93B1 regulates the trafficking of TLR11 and TLR13 by controlling ER exit. Altogether, our data indicate that the role for UNC93B1 in controlling ER exit extends to all known endosomal TLRs (TLR3, TLR7, TLR9) as well as TLR11 and TLR13.

**Mutational analysis reveals distinct regions of UNC93B1 required for ER exit and post-Golgi trafficking of TLR9**

To define regions within UNC93B1 necessary for ER export of TLRs, we generated a series of N-and C-terminal truncation mutants. Based on the predicted topology of UNC93B1 [92], the N- and C-termini face the cytosol, so we reasoned that these regions would be most likely to interact with putative trafficking factors (Figure 3.3A). Interestingly, N-terminal truncations resulted in a strong defect in TLR9 trafficking from the ER as evidenced by significantly reduced or absent precursor and cleaved forms of TLR9 in cells expressing the Δ50 and Δ57 UNC93B1 truncations (Figure 3.3B). This defective trafficking resulted in impaired responses to TLR9 ligands in macrophages, while TLR2 responses remained intact (Figure 3.3C). Taken together, our data indicate that the N-terminal region of UNC93B1 contains residues important for trafficking of

TLR9 and UNC93B1 from the ER to endolysosomes. These findings are in agreement with a previous study showing that TLR9 responsiveness is strongly dependent on the N-terminus of UNC93B1, although this study did not directly examine TLR9 trafficking [127]. Furthermore, an UNC93B1 point mutant (D34A), which reduced TLR9 signaling but enhanced TLR7 signaling [107, 127], reduced TLR9 transport and cleavage (Figure 3.3D).

The preceding findings were documented in the publication "UNC93B1 controls the differential trafficking of endosomal TLRs" *eLife* 2013; 2: e00291

## Discussion

The studies presented here address a poorly understood aspect of TLR cell biology. We describe a mechanism by which UNC93B1 can regulate trafficking. Here we show UNC93B1 controls exit of at least 5 TLRs (TLR3, TLR7, TLR9, TLR11, and TLR13) from the ER by regulating their loading into COPII vesicles.

Previous work has demonstrated that TLR9 and TLR7 fail to reach endosomes in the absence of functional UNC93B1 [91]. Interactions between UNC93B1 and TLRs appear necessary for proper trafficking [92], but until our work it was unclear how UNC93B1 mediated delivery of TLRs to endosomal compartments. The most direct examination of UNC93B1 function concluded that the protein translocates with TLRs from the ER to endolysosomes without passing through the Golgi apparatus [91, 92]. In contrast, we propose that UNC93B1 is required for loading of TLR9 into COPII vesicles, which direct transport from the ER to the cis-Golgi [112]. Multiple lines of evidence support the conclusion that UNC93B1 regulates this essential aspect of ER exit. First, UNC93B1 is detected within COPII vesicles, but the nonfunctional UNC93B1-H412R mutant is not. Second, a fraction of UNC93B1 protein acquires EndoH-resistant glycans, indicative of trafficking through the medial-Golgi. Again, the UNC93B1-H412R mutant does not acquire EndoH resistance. Third, in cells lacking UNC93B1, TLR9 is not detected within COPII vesicles. Fourth, the EndoH-resistant precursor and cleaved forms of TLR9 are absent in cells not expressing functional UNC93B1. Importantly, we ruled out the possibility that UNC93B1 functions as a folding chaperone by showing that CD4-TLR fusion proteins require UNC93B1 for ER exit. Altogether, these results argue that UNC93B1 regulates TLR passage through the general secretory pathway, instead of controlling direct translocation between the ER and endosomes. We cannot formally rule out that a pool of UNC93B1 uses this non-canonical route, but it would seem to have little if any relevance for TLR trafficking. The recent identification of Sec22b as a factor required for ER to endosome translocation may allow for further investigation of this possibility[126].

Regulation of ER exit of TLR11 and TLR13 by UNC93B1 is not completely unexpected, as these TLRs were previously linked to UNC93B1 [35, 36, 92, 133], however, to our knowledge we are the first to report the direct role of UNC93B1 to control trafficking of these TLRs. The determinants of UNC93B1 binding to each of these TLRs remain poorly defined. Residues within the first 50 amino acids of UNC93B1 appear necessary for export of TLR9 but not for export of TLR7. This result suggests that distinct regions of UNC93B1 are required for association with TLR9 and TLR7, although measuring how these mutations impact TLR/UNC93B1 interactions has been challenging for us and for other groups [127]. The fact that UNC93B1-D34A- expressing mice exhibit enhanced TLR7 responses and develop SLE suggests that UNC93B1 is limiting in the ER, at least for TLR7[107]. Presumably, the inability of UNC93B1-D34A to interact with TLR9 results in greater TLR7 export and enhanced signaling

What are the precise mechanisms of UNC93B1 control of ER export? Considering interaction is a required step, we propose two possible mechanisms that require further exploration. One, in which UNC93B1 interaction with individual TLRs is required to concentrate TLRs at sites of ER exit. UNC93B1 could assume the role of an escort chaperone where ER export sites that interact with Sec24 are available on UNC93B1, and through association with TLRs, facilitates incorporation of the UNC93B1-TLR complex into COPII vesicles [110]. Alternatively, interaction with UNC93B1 could expose ER export motifs present on the TLRs

that are sterically hindered prior to UNC93B1 association. A second possible model predicts the existence an undetermined inhibitory factor, which could retain endosomal TLRs in the ER. UNC93B1 may be required to displace this factor and release inhibition to allow exit of TLRs from the ER. The mechanisms that proceed to allow ER export may rely on Sec24 binding sites on either UNC93B1 or TLR as described in the first model. Thus, the two models described here are not mutually exclusive and may, in fact, be complementary. Additional biochemical studies will be needed to establish the precise mechanism, including identifying any interacting inhibitory factor that binds TLRs in the ER and the determinants on UNC93B1 or the TLRs that mediate incorporation into COPII vesicles.

It will be important to determine whether ER export can be regulated at the level of UNC93B1 in the face of changing conditions or stimuli. Changes in the levels of UNC93B1 may be a way to enhance or prevent trafficking of TLRs. For example, stimulation has been shown to induce the up-regulation of UNC93B1 [56]. This could enhance the trafficking of TLRs and increase the pool of functional receptors in endolysosomes. In absence of stimuli, down-regulation of UNC93B1 expression may be mechanism to decrease the levels of function receptor in the cell and mute responses. Additionally, UNC93B1 may be post-translationally modified or interact with additional factors that could support its ER export function. Studies of UNC93B1 mutants may reveal these mechanisms.

Controlling the levels of TLR at the level of ER export is an intriguing regulatory mechanism. Defining the mechanisms that contribute to the control of individual TLRs will help us understand the regulatory mechanisms in place to maintain proper responses toward microbial infection and avoid a dysregulated self-recognition leading to autoimmunity.

## Materials and Methods

### Antibodies and Reagents

The following antibodies were used for immunoblots, immunoprecipitations, or flow cytometry: anti-HA as purified antibody or matrix (3F10, Roche), anti-FLAG as purified antibody or matrix (M2 and M5, Sigma), anti-GFP (JL-8, Clontech), anti-GFP as purified or matrix (RQ2, MBL International), anti-*myc* (purified mouse, Invitrogen), anti-CD4 (RM4-5, BD Biosciences), anti-Lamp-1 (1D4B, BD Biosciences), anti-calnexin (rabbit polyclonal, Enzo Life), anti-ERGIC/p58 (rabbit) has been previously described[132], anti-TNFα-PE or -APC (MP6-XT22, eBiosciences), goat anti-mouse IgG-AlexaFluor647 (Invitrogen), goat anti-rat-HRP, sheep anti-mouse-HRP, and donkey anti-rabbit-HRP (GE Healthcare). For immunofluorescence: rabbit anti-HA (Y11, Santa Cruz), goat anti-mouse Cy3 (Jackson Immunoresearch), goat anti-rabbit-AlexaFluor647 (Invitrogen). The following TLR ligands were used to stimulate cells: CpG ODN (TCCATGACGTTCCTGACGTT, all phosphorothioate linkages), R848 (Invivogen), and Pam3CSK4 (Invivogen). 3XFLAG peptide was purchased from Sigma. Digitonin was purchased from Wako or Calbiochem. Lipofectamine-LTX reagent (Invitrogen) was used for transient transfection of plasmid DNA. OptiMEM-I (Invitrogen) was used as media to form nucleic acid complexes for transient transfections.

### Mice

*Unc93b1*$^{3d/3d}$ mice[98] were obtained from the MMRRC at UC Davis. C57Bl/6 were purchased from The Jackson Laboratory. All mice were housed in the animal facilities at the University of California, Berkeley according to guidelines of the Institutional Animal Care and Use Committee.

### Plasmid Constructs

Pfu Turbo polymerase (Agilent) was used according to manufacturer's instructions for site directed mutagenesis. The following mouse stem cell virus (MSCV)-based retroviral vectors were used to express UNC93B1, TLR9, and TLR7 in cell lines: MSCV2.2 (IRES-GFP), MSCV-Thy1.1 (IRES Thy1.1), MIGR2 (IRES-hCD2). The following epitope tags were fused to the C-terminus of UNC93B1: 3XFLAG (DYKDHDGDYKDHDIDYKDDDDK), Myc (EQKLISEEDL), HA (YPYDVPDYA) and entire eGFP cDNA derived from pIRES-eGFP plasmid (Clonetech). TLR9 was fused to HA at the C-terminal end as previously described [24]. UNC93B1 shRNA and control were generated in MSCV-Lmp, as previously described[24]. CD4-TLR chimeras were generated in pCDNA3.1 (Invitrogen). CD4 extracellular domain (mouse 1-390 a.a.) was fused to transmembrane domain and cytosolic regions of the following TLRs and C-terminally tagged with HA: TLR4 (620-835 a.a.), TLR9 (mouse 803-1032 a.a.), TLR3 (human 691-904 a.a.), TLR7 (human 825-1049), TLR11 (mouse 703-926 a.a.) TLR13 (mouse 770-991 a.a.).

### Cell lines and Tissue culture conditions

HEK293T cells were obtained from American Type Culture Collection (ATCC). GP2-293 packaging cell lines were obtained from Clonetech. Phoenix-Eco (ØNX-E ) cells were provided by G. Nolan, Stanford University. Mouse embryonic fibroblasts (MEFs) are TLR2/TLR4 double knockout genotype immortalized with SV40 large T-antigen. COS7 were obtained from the Berkeley cell culture facility. The above cell lines were cultured in DMEM supplemented with

10% (vol/vol) FCS, L-glutamine, penicillin-streptomycin, sodium pyruvate, and HEPES (pH 7.2) (Invitrogen). RAW264 macrophage cell lines (ATCC) and immortalized macrophages (generated as described below) were cultured in RPMI 1640 (same supplements as above).

To generate immortalized macrophage cell lines, bone marrow from *Unc93b1*$^{3d/3d}$ mice was cultured in RPMI 1640 media supplemented with supernatant containing M-CSF, as previously described[134], as well as virus encoding both v-raf and v-myc[135]. After 8 days, macrophages were removed from M-CSF-containing media and cultured in RPMI 1640 media with added supplements as described above.

**Retroviral transduction**
For retroviral transduction of immortalized macrophages, VSV-G-psuedotyped retrovirus was made in GP2-293 packaging cells (Clontech). GP2-293 cells were transfected with retroviral vectors and pVSV-G using Lipofectamine LTX reagent. 24 hours post-transfection, cells were incubated at 32°C. 48 hours post-transfection viral supernatant (with polybrene at final 5mg/ml) and was used to infect target cells overnight at 32°C and protein expression was checked 48 hours later. Target cells were sorted on MoFlo Beckman Coulter Sorter to match expression.

**Lysate preparation, SDS-PAGE, Immunoblotting**
Cell lysates were prepared with TNT buffer (20 mM Tris [pH 8.0], 200 mM NaCl, 1% Triton X-100, 4mM EDTA and supplemented with EDTA-free complete protease inhibitor cocktail (Roche)) unless otherwise noted. Digitonin lysis buffer (50 mM Tris [pH 7.4], 150 mM NaCl, 5 mM EDTA [pH 8.0], 1% Digitonin added fresh and supplemented with EDTA-free complete protease inhibitor cocktail) was used for co-immunoprecipitations. Lysates were cleared of insoluble material by centrifugation. For immunoprecipitations, lysates were incubated with anti-HA matrix, anti-FLAG matrix, anti-GFP matrix or with purified antibody conjugated to Protein A/G beads (Pierce) and precipitated proteins were denatured in SDS-PAGE buffer separated by SDS-PAGE (Tris-HCl self cast gels or Bio-Rad TGX precast gels), and probed by the indicated antibodies. For anti-FLAG matrix immunoprecipitations, 3XFLAG peptide (Sigma) was used to elute.

**Endoglycosidase H assay**
Immunoprecpitated proteins or total lysate were denatured and treated with Endoglycosidase H or PNGase F according to manufacturer's instructions. All enzymes and buffers were purchased from New England Biolabs.

**Flow cytometry**
To measure TNFa production, we added brefeldinA to cells 30 min after stimulation, and cells were collected after an additional 4h, and cells were stained for intracellular cytokines with a Fixation & Permeabilization kit according to manufacturer's instructions (eBioscience).
All data were collected on LSR II (Becton Dickinson) or FC-500 (Beckman Coulter) flow cytometers and were analyzed with FloJo software (TreeStar).

**Phagosome Isolation**

RAW264 cells were used to isolate phagosomes as previously described [24]. Briefly, cells were incubated with 2 μM latex beads (Polysciences, Inc) for 1 hr. Cells were disrupted by dounce homogenization to release intact phagosomes. Following centrifugation in sucrose step gradient, phagosomes were harvested from the 20–10% sucrose interface. Lysates were analyzed by immunoblot.

***In vitro* COPII budding assay**

COPII vesicle formation was performed as described previously[131, 132]. In brief, RAW264 cells grown in 10x10mm plates or COS7 cells grown in 6 × 100 mm plates were washed in PBS, removed from plates with trypsin, and washed again in PBS containing 10 μg $ml^{-1}$ soybean trypsin inhibitor. Cells were permeablized with 40 μg $ml^{-1}$ digitonin for 5 min in ice-cold KHM buffer (110 mM KOAc, 20 mM Hepes pH 7.2 and 2 mM $Mg(OAC)_2$) and washed and resuspended in 100 μl KHM. Each reaction contained KHM and where indicated an ATP regenerating system (40 mm creatine phosphate, 0.2 mg/ml creatine phosphokinase, and 1 mm ATP), 0.2 mm GTP, and rat liver cytosol (prepared as described previously[131]). Reactions were incubated at 30 °C for 60 min. A 75-μl aliquot of the vesicle fraction was separated from the donor microsomal fraction by centrifugation at 14,000 × *g* for 20 min at 4 °C. Donor fraction was lysed in 75ul of Buffer C (10 mm Tris-HCl (pH 7.6), 100 mm NaCl, 10% (w/v) SDS plus protease inhibitor mixture). The vesicles were collected by centrifugation at 50,000 rpm at 4 °C in a Beckman TLA100 rotor for 30 min. Isolated vesicles were lysed in 20ul of Buffer C. Donor membrane (20% total) and isolated vesicles (75% of total) were separated by SDS-PAGE and analyzed by immunoblotting.

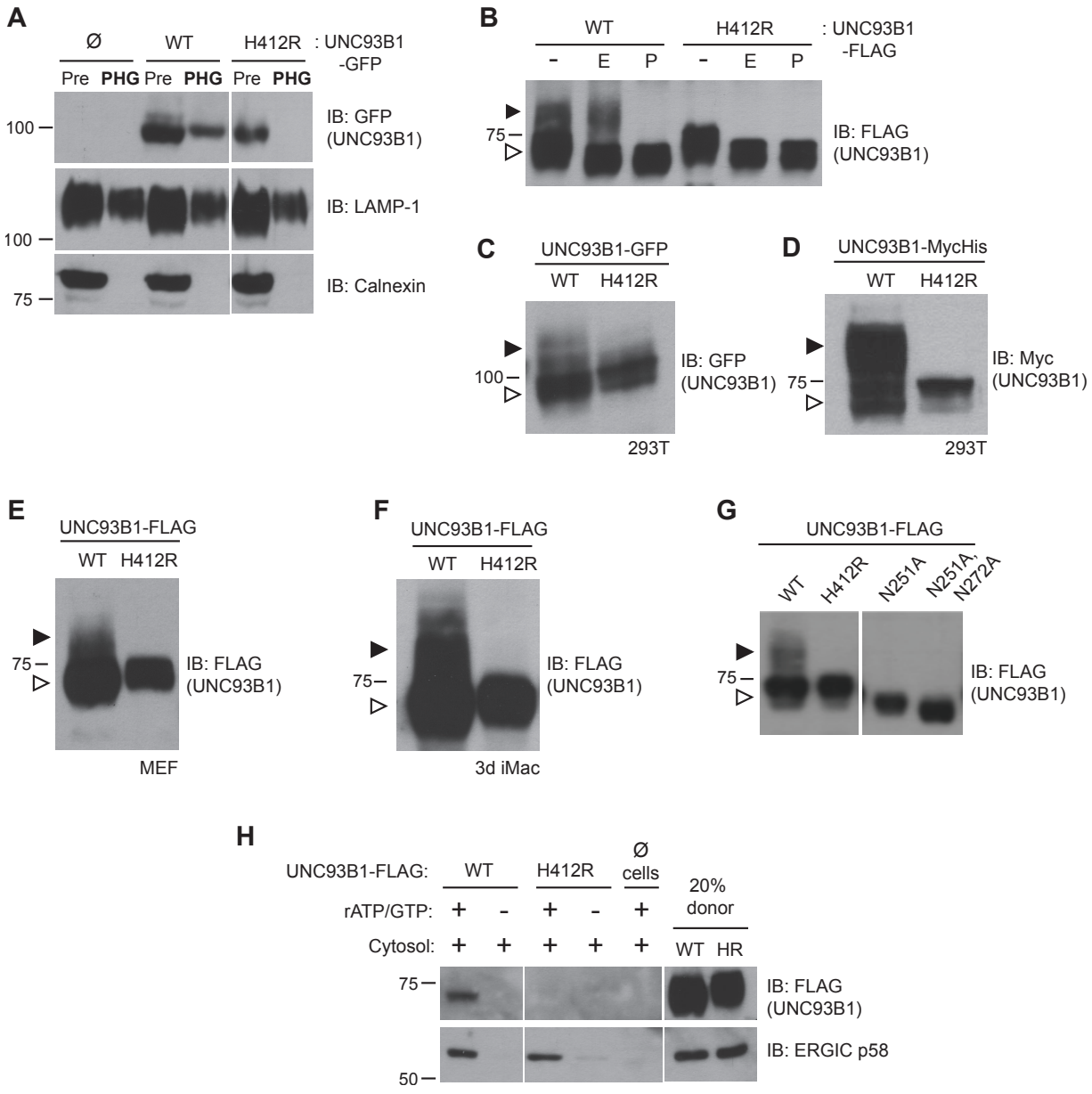
A
Ø
WT
H412R
: UNC93B1 -GFP
Pre PHG Pre PHG Pre PHG
100
IB: GFP (UNC93B1)
IB: LAMP-1
100
IB: Calnexin
75
B
WT
H412R
: UNC93B1 -FLAG
- E P - E P
75
IB: FLAG (UNC93B1)
C
UNC93B1-GFP
WT H412R
100
IB: GFP (UNC93B1)
293T
D
UNC93B1-MycHis
WT H412R
75
IB: Myc (UNC93B1)
293T
E
UNC93B1-FLAG
WT H412R
75
IB: FLAG (UNC93B1)
MEF
F
UNC93B1-FLAG
WT H412R
75
IB: FLAG (UNC93B1)
3d iMac
G
UNC93B1-FLAG
WT
H412R
N251A
N251A, N272A
75
IB: FLAG (UNC93B1)
H
UNC93B1-FLAG:
WT
H412R
Ø cells
20% donor
rATP/GTP: + - + - +
Cytosol: + + + + +
WT HR
75
IB: FLAG (UNC93B1)
50
IB: ERGIC p58

**Figure 3.1. UNC93B1 traffics to the Golgi en route to endolysosomes.**
(**A**) UNC93B1 is present in phagolysosomes of unstimulated cells. Phagosomes (PHG) isolated by flotation from RAW264 cells only (∅) or expressing GFP tagged UNC93B1-WT or UNC93B1–H412R and cells prior to isolation (Pre) were separated by SDS-PAGE, and immunoblotted with anti-GFP, anti-Lamp1 (lysosome), and anti-calnexin (ER). (**B**) A portion of UNC93B1 protein traffics to the Golgi apparatus. Wildtype UNC93B1 (WT) or H412R, each with a C-terminal 3xFLAG tag, were expressed in HEK293Ts by transient transfection. The immunoprecipitated proteins were treated with EndoH (E), PNGaseF (P) or left untreated (-), separated by SDS-PAGE, and visualized by immunoblot with anti-FLAG antibody. Bands representing EndoH-sensitive (white arrow) and resistant (black arrow) forms of UNC93B1 are indicated. (**C-F**) UNC93B1 acquires EndoH-resistant modifications. UNC93B1 tagged with GFP (**C**) or Myc-His (**D**) from transiently transfected HEK293Ts, and FLAG tagged UNC93B1 expressed in MEFs (**E**) or *3d* iMac cells (**F**) were analyzed for the presence of EndoH-resistant glycans. Lysates were separated by SDS-PAGE and immunoblotted with the indicated antibodies. EndoH-sensitive (white arrow) and -resistant (black arrow) forms are indicated. (**G**) Mutation of UNC93B1 glycosylation sites abolishes EndoH resistant forms. Lysates from HEK293Ts transiently transfected with FLAG tagged UNC93B1-WT, -N251A or -N251A/N272A were separated by SDS-PAGE and immunoblotted with anti-FLAG antibody. (**H**) UNC93B1 is loaded into COPII vesicles. Digitonin-permeabilized COS7 cells expressing 3xFLAG-tagged UNC93B1-WT or UNC93B1-H412R, or no cells (∅) were incubated with ATP regenerating system, GTP, and rat liver cytosol, as indicated, in an *in vitro* COPII budding assay. Vesicles purified by ultracentrifugation were analyzed by SDS-PAGE and immunoblot using the indicated antibodies. 20% of the COS7 cells prior to the budding reaction serves as a loading control (20% donor). ERGIC/p58 serves as a positive control for the formation of COPII vesicles. Results are representative of at least three experiments (A-G) or two experiments (H).

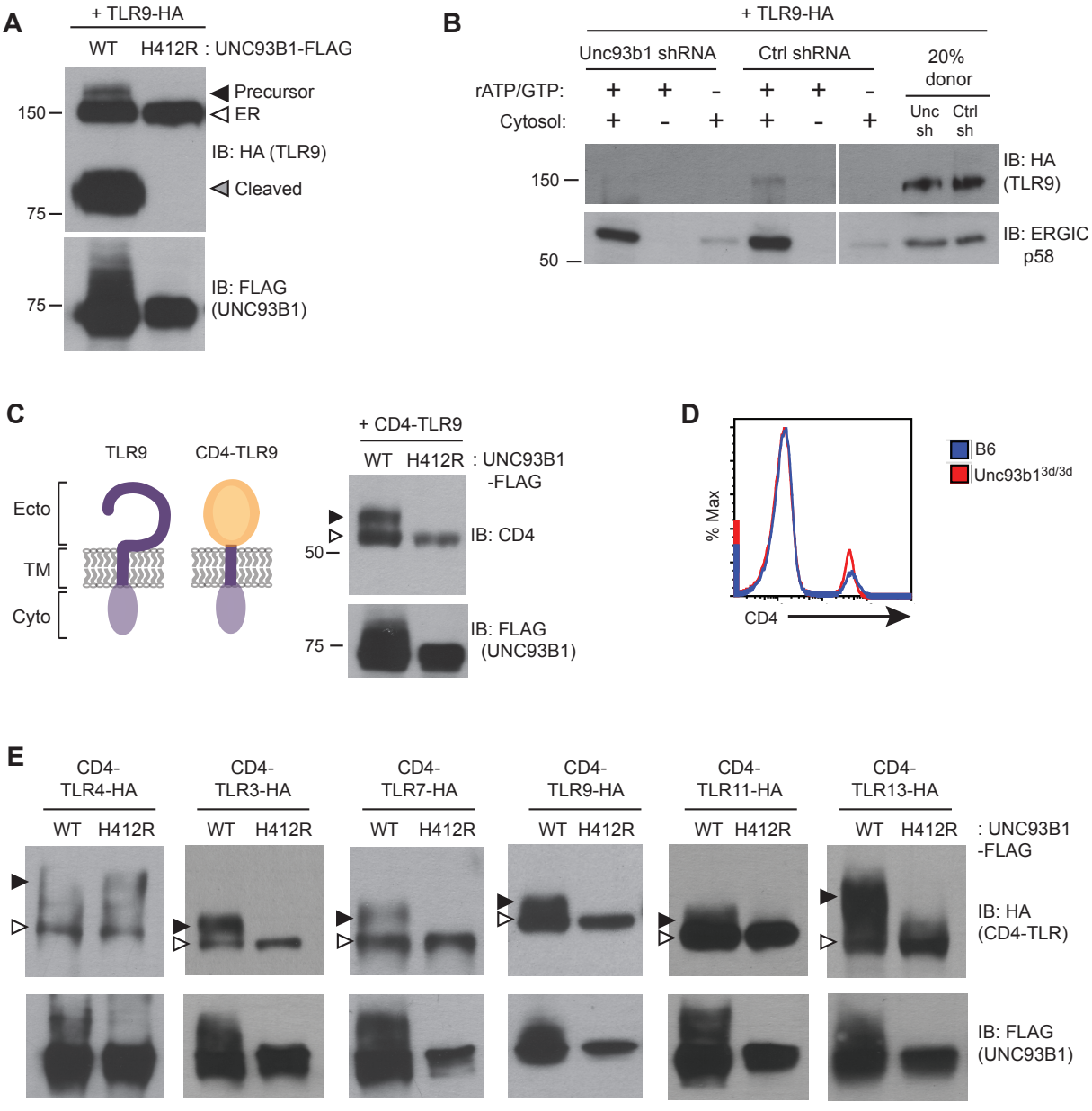
A
+ TLR9-HA
WT H412R : UNC93B1-FLAG
150
75
75
Precursor
ER
IB: HA (TLR9)
Cleaved
IB: FLAG (UNC93B1)
B
+ TLR9-HA
Unc93b1 shRNA
Ctrl shRNA
20% donor
rATP/GTP:
Cytosol:
Unc sh
Ctrl sh
150
50
IB: HA (TLR9)
IB: ERGIC p58
C
TLR9
CD4-TLR9
Ecto
TM
Cyto
+ CD4-TLR9
WT H412R : UNC93B1 -FLAG
50
75
IB: CD4
IB: FLAG (UNC93B1)
D
% Max
CD4
B6
Unc93b1 3d/3d
E
CD4- TLR4-HA
CD4- TLR3-HA
CD4- TLR7-HA
CD4- TLR9-HA
CD4- TLR11-HA
CD4- TLR13-HA
WT H412R
: UNC93B1 -FLAG
IB: HA (CD4-TLR)
IB: FLAG (UNC93B1)

**Figure 3.2. UNC93B1 controls ER exit of TLRs 3, 7, 9, 11, and 13.**
(**A**) TLR9 fails to exit the ER in cells lacking functional UNC93B1. Lysates from *3d* iMac cells complemented with either UNC93B1-WT or UNC93B1-H412R and expressing TLR9-HA were analyzed by SDS-PAGE and immunoblotted with the indicated antibodies. The precursor (black arrow), ER (white arrow) and cleaved (grey arrow) forms of TLR9-HA are indicated. (**B**) UNC93B1 is required for TLR9 loading into COPII vesicles. RAW264 macrophages stably transduced with retroviruses encoding control or Unc93b1-directed shRNA and expressing TLR9-HA were used in an *in vitro* COPII budding assay as described in (**Figure1H**). Lysates of purified vesicles or donor membranes were probed with the indicated antibodies. (**C**) The transmembrane and cytosolic domain of TLR9 is sufficient to confer UNC93B1-dependence. (Left) Schematic of TLR9 and the CD4-TLR9 chimera. Transmembrane (TM), ectodomain (Ecto) and cytosolic domain (Cyto) are indicated. (Right) CD4-TLR9 was expressed in HEK293Ts together with FLAG-tagged UNC93B1-WT or UNC93B1-H412R. Total lysates were analyzed by SDS-PAGE and immunoblotted with anti-CD4 and anti-FLAG antibodies. EndoH-sensitive (white arrow) and resistant (black arrow) forms are indicated. (**D**) CD4 trafficking to the cell surface is normal in Unc93b1$^{3d/3d}$ cells. Splenocytes from C57BL/6 (blue line) or Unc93b1$^{3d/3d}$ (red line) mice were stained with anti-CD4 and analyzed by flow cytometry. (**E**) CD4-TLR chimeric proteins for each of the indicated TLRs were expressed in HEK293Ts together with FLAG-tagged UNC93B1-WT or UNC93B1-H412R. Lysates were separated by SDS-PAGE and visualized by immunoblot with anti-HA and anti-FLAG antibodies. EndoH-sensitive (white arrows) and resistant (black arrows) forms are indicated. The chimeras were constructed as shown in Figure 1E, except with the addition of a C-terminal HA tag. Results are representative of at least three experiments (A, C, and E) or two experiments (B, D).

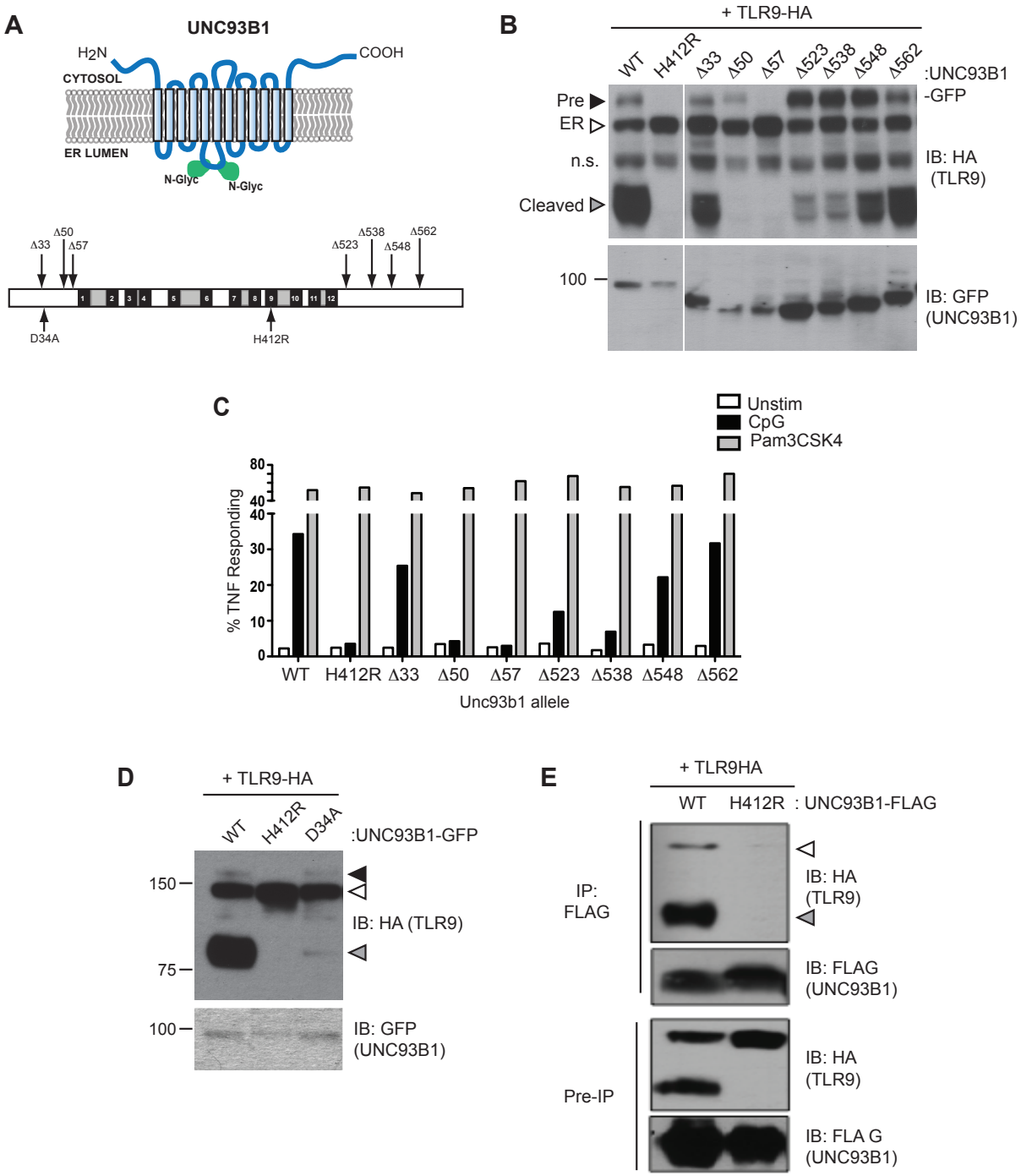
A
UNC93B1
H2N
COOH
CYTOSOL
ER LUMEN
N-Glyc
N-Glyc
Δ33
Δ50
Δ57
Δ523
Δ538
Δ548
Δ562
D34A
H412R
B
+ TLR9-HA
WT
H412R
Δ33
Δ50
Δ57
Δ523
Δ538
Δ548
Δ562
:UNC93B1 -GFP
Pre
ER
n.s.
Cleaved
IB: HA (TLR9)
100
IB: GFP (UNC93B1)
C
Unstim
CpG
Pam3CSK4
% TNF Responding
80
40
30
20
10
0
WT
H412R
Δ33
Δ50
Δ57
Δ523
Δ538
Δ548
Δ562
Unc93b1 allele
D
+ TLR9-HA
WT
H412R
D34A
:UNC93B1-GFP
150
75
IB: HA (TLR9)
100
IB: GFP (UNC93B1)
E
+ TLR9HA
WT
H412R
: UNC93B1-FLAG
IP: FLAG
IB: HA (TLR9)
IB: FLAG (UNC93B1)
Pre-IP
IB: HA (TLR9)
IB: FLA G (UNC93B1)

**Figure 3.3 UNC93B1 mutants reveal two distinct roles in TLR9 trafficking.**
(**A**) Schematic of predicted UNC93B1 topology. UNC93B1 is a twelve pass transmembrane protein with terminal regions facing cytosol. Two putative N-linked glycosylation (N-Glyc) sites are indicated (top). Schematic of UNC93B1 (1-598 a.a.). The black numbered boxes represent predicted transmembrane domains, white boxes represent regions predicted to face the cytosol, and grey boxes represent regions predicted to face the lumen. Truncation and point mutations are indicated with arrows (bottom). (**B**) N- and C- terminal mutants of UNC93B1 have distinct TLR9 trafficking outcomes. Lysates from *3d* iMac cells expressing TLR9-HA and complemented with mutant forms of GFP-tagged UNC93B1 were subjected to SDS-PAGE and immunoblotted with anti-HA and anti-GFP antibodies. The precursor (black arrow), ER (white arrow) and cleaved (grey arrow) forms of TLR9-HA are indicated. (**C**) N- and C-terminal mutants of UNC93B1 have diminished TLR9 signaling. *3d* iMac cells complemented with WT or indicated mutant alleles of UNC93B1 were harvested for intracellular TNFα staining 5h after stimulation with 3μM CpG, 1μg/ml Pam3CSK4 or left unstimulated. Percentages of TNF-producing cells after gating on UNC93B1-GFP positive cells are plotted. (**D**) TLR9 trafficking to endolysosomes is impaired in UNC93B1-D34A cells. *3d* iMac cells were complemented with GFP-tagged UNC93B1-WT, -H412R or -D34A. Lysates were separated by SDS-PAGE and visualized by immunoblot with anti-HA and anti-GFP antibodies. The precursor (black arrow), ER (white arrow) and cleaved (grey arrow) forms of TLR9-HA are indicated. (**E**) UNC93B1 interacts with the cleaved form of TLR9. Immunoprecipitation of FLAG tagged UNC93B1 (WT or H412R) in *3d* iMac cells expressing TLR9-HA was performed in 1% digitonin with anti-FLAG matrix. UNC93B1 associated proteins were analyzed by SDS-PAGE and immunoblot with anti-FLAG and anti-HA antibodies. ER (white arrows) and cleaved (grey arrows) forms of TLR9-HA are indicated. All results are representative of at least three experiments.

# Chapter 4: The post-ER regulation of endosomal TLRs by UNC93B1

## Background

Toll-like receptors (TLRs) are an ancient family of innate immune receptors that recognize conserved microbial structures. Signaling is important for the induction of innate and adaptive immune responses to microbial infection. A subset of TLRs (TLR3, TLR7, TLR8, and TLR9) recognizes nucleic acids structures, including double-stranded RNA, single-stranded RNA, and DNA that are commonly found in microbes. However, this specificity for nucleic acid presents the potential to recognize self-nucleic acids. Indeed, TLR7 and TLR9 recognition of self-RNA and self-DNA, respectively, has been reported to contribute to autoimmune diseases such as systemic lupus erythematosus (SLE) and psoriasis.

Discrimination between self and microbial nucleic acids cannot be achieved solely through recognition of distinct features but instead relies on differential delivery of these potential ligands to TLRs [39]. All of the TLRs capable of nucleic acid recognition localize within endosomal compartments, which sequesters these receptors away from self nucleic acids in the extracellular space [39]. Our previous studies as well as work from other groups indicate that a requirement for ectodomain cleavage of intracellular TLRs further restricts receptor activation to protease-rich acidic compartments [23, 24, 136, 137]. Bypassing this requirement enables responses to extracellular self nucleic acid and leads to fatal inflammatory disease in mice [80]. Moreover, the system appears carefully balanced as simply overexpressing TLR7 in mice causes responses to self-RNA and development of an SLE-like disease [46, 138, 139]. Thus, defining the regulatory steps that control TLR localization and influence the threshold of receptor activation has important implications for self/non-self discrimination.

TLR9 and other intracellular TLRs must traffic from the endoplasmic reticulum (ER) to endolysosomes before responding to ligands. This trafficking seems to depend on a multi-pass transmembrane protein, UNC93B1 [91, 92]. Mice expressing a nonfunctional *Unc93b1* (H412R) allele (*Unc93b1*$^{3d/3d}$) fail to respond to TLR3, TLR7, or TLR9 ligands, while responses by surface localized TLRs such as TLR2 and TLR4 are unimpaired [98]. Importantly, mice and humans deficient in UNC93B1 are highly susceptible to viral infection [53, 98, 99]. UNC93B1 associates with endosomal TLRs, however, this interaction is terminated in the presence of the H412R UNC93B1 mutant [92]. In addition, cells expressing defective UNC93B1 cannot traffic TLR9 and 7 out of the ER [91]. Other groups have implicated UNC93B1 in the function of TLR11, TLR12, and TLR13 without a direct study of its possible role in trafficking [34-37, 98]. As discussed in Chapter 3, we identified a role for UNC93B1 in facilitating the ER export of TLRs 3, 7, 9, 11 and 13 en route to the Golgi. In this chapter, we sought to define additional mechanisms by which UNC93B1 controls endosomal TLR trafficking and function. UNC93B1 traffics to endolysosomes and continues to interact with the cleaved form of TLR9, suggesting a role beyond ER export. Here, we focus on the role of UNC93B1 at a post-ER step.

Several factors have been reported to aid TLR9 in accessing endolysosomal compartments. The HRS/ESCRT pathway is involved in post-Golgi trafficking by sorting ubiquitinated TLR7 and TLR9 to endosomal compartments [97], and the adaptor protein-3 (AP-3) has been reported to target TLR9 and TLR7 to lysosome related organelles specialized for type I IFN induction [29, 30, 140]. Interestingly, UNC93B1 trafficking to these compartments is

also impaired in AP-3 deficient cells [30]. Whether UNC93B1 interacts with other components implicated in trafficking of endosomal TLRs remains to be determined.

Together, our studies show that UNC93B1 is required for multiple steps of TLR trafficking. In Chapter 3, we described a direct role for UNC93B1 in facilitating exit of TLRs from the ER. In this chapter, we describe a later role in recruitment of adaptor protein-2 (AP-2) to facilitate endocytosis of TLR9 from the plasma membrane. Surprisingly, TLR7 does not have the same requirements for UNC93B1 and utilizes distinct trafficking machinery to reach endolysosomes. Thus, our results describe how UNC93B1 controls endosomal TLR trafficking and provide the first mechanistic basis for differential regulation of these receptors.

## Results

### UNC93B1 plays a role in post-ER regulation of TLR9 trafficking

As discussed in Chapter 3, our results thus far suggest that UNC93B1 controls the function of multiple TLRs by regulating their exit from the ER. However, UNC93B1 itself also exits the ER and is present in endolysosomes (Chapter 3; Figure 3.1A, 3.1H). Moreover, we could detect both the precursor and cleaved forms of TLR9 associated with immunoprecipitated UNC93B1, suggesting that UNC93B1 and TLR9 remain associated after leaving the ER (Chapter 3; Figure 3.3E). To test whether this post-ER interaction may have functional consequences, we screened UNC93B1 mutants for any role in TLR9 function beyond ER export. Strikingly, truncation of the UNC93B1 C-terminus (Δ523 and Δ538) resulted in an accumulation of the Golgi-modified precursor form of TLR9 and a marked reduction of the cleaved receptor (Chapter 3; Figure 3.3B). This pattern suggests that TLR9 trafficking is blocked at some point after the medial Golgi, in contrast to the trafficking defect observed with N-terminal deletion mutants. Consistent with this interpretation, we observed reduced TLR9 signaling in cells expressing the Δ523 and Δ538 UNC93B1 mutants (Chapter 3; Figure 3.3C). Thus, in addition to its role in ER export, UNC93B1 appears to regulate post-ER trafficking of TLR9.

### UNC93B1 controls post-Golgi trafficking of TLR9 through recruitment of AP-2

We next sought to define the mechanism underlying the requirement for UNC93B1 in post-ER TLR9 trafficking. We focused on residues 539-542, YRYL, because they are evolutionarily conserved and fit the consensus for a YxxΦ motif (where Φ represents a hydrophobic residue), which may mediate protein interactions or serve as a site for phosphorylation [117, 141-144] (Figure 4.1A). Mutation of Tyr539 to an Ala (Y539A) resulted in accumulation of the Golgi-modified precursor form of TLR9 and reduced TLR9 cleavage, similar to the block in TLR9 trafficking observed with the Δ538 truncation mutant (Figure 4.1B). Mutation of Leu-542 to Ala (L542A) and Tyr-539 to Phe (Y539F) gave similar results, although the block was not as complete as Y539A (Figure 4.1C). Responsiveness to TLR9 ligands was also reduced in UNC93B1-Y539A expressing cells, consistent with the block of TLR9 processing (Figure 4.1D).

YxxΦ motifs can serve as binding sites for clathrin adaptor protein (AP) complexes, so we tested whether the C-terminal tail of UNC93B1 could interact with any of the four mammalian AP complexes. AP complexes consist of four subunits, of which the μ subunit typically determines cargo specificity [117, 145]. Because these interactions are often weak, we used a yeast two-hybrid (Y2H) assay in which the μ subunits of AP-1, -2, -3, and -4 were fused to the Gal4 activation domain and the UNC93B1 N- and C-terminal tails were fused to the Gal4 DNA binding domain. The C-terminal cytosolic region of UNC93B1 interacted strongly with AP-2μ, but not with the μ subunits of any of the other AP complexes (Figure 4.1E). Importantly, interaction with AP-2μ was abolished by the Δ538 truncation and the Y539A mutation (Figure 4.1F). Additionally, we were able to co-immunoprecipitate AP-2μ with UNC93B1-WT, but not with UNC93B1-Y539A (Figure 4.1G). Taken together, these data suggest that UNC93B1 directly recruits AP-2 via a YxxΦ motif present in its C-terminal cytosolic tail.

AP-2 complexes direct clathrin-mediated endocytosis of cargo from the plasma membrane. Therefore, our results suggest that UNC93B1 and TLR9 traffic together to the surface and require AP-2-mediated internalization to reach endocytic compartments. To test this

possibility, we examined whether TLR9 required UNC93B1-mediated recruitment of AP-2 to gain access to endolysosomal compartments. Using immunofluorescence microscopy, we detected reduced colocalization of TLR9 and the lysosomal marker Lamp-1 in UNC93B1-Y539A-expressing cells (Figure 4.2A). We also compared surface expression of N-terminally tagged TLR9 in cells expressing different UNC93B1 alleles. While surface TLR9 was only weakly detectable in cells expressing UNC93B1-WT, expression of UNC93B1-Y539A increased the levels of FLAG-TLR9 at the cell surface (Figure 4.2B). Furthermore, as we found for TLR9-HA, the FLAG-TLR9 Golgi-modified precursor form accumulated in UNC93B1-Y539A expressing cells (Figure 4.2C). This result suggests that disruption of the interaction between UNC93B1 and AP-2 leads to defective endocytosis of TLR9 from the cell surface. In support of this model, siRNA knockdown of AP-2μ1 resulted in a similar increase in surface expression of TLR9 (Figure 4.2D) and accumulation of the TLR9 precursor form (Figure 4.2E). As a positive control for AP-2μ1 knockdown, we observed accumulation of CD71 (transferrin receptor) at the cell surface (Figure 4.2D). Taken together, these data support a model in which UNC93B1 interacts with AP-2 to traffic TLR9 from the cell surface to endolysosomes.

**UNC93B1 differentially controls TLR7 and TLR9**

Having established the mechanisms by which UNC93B1 facilitates TLR9 delivery to endolysosomes, we next examined whether TLR7 is under similar regulation. However, for reasons that remain unclear, detection of endogenous or epitope-tagged exogenous TLR7 protein is quite challenging. Consequently, the evidence that TLR7 undergoes ectodomain processing is limited [23], and one group has reported that TLR7 is not cleaved [137]. We synthesized a TLR7 coding sequence optimized for efficient translation (see Materials and Methods) and found that our ability to detect TLR7 protein was significantly improved. Cleaved TLR7 was detected in macrophages expressing UNC93B1-WT but not in macrophages expressing UNC93B1-H412R (Figure 4.3A). Both the full-length and cleaved forms of TLR7 possessed EndoH-resistant glycans, although fewer of the TLR7 N-linked glycans acquired these modifications than for TLR9 (Figure 4.3B top). These results confirm our previous findings that TLR7 undergoes ectodomain proteolysis and traffics through the Golgi en route to endolysosomes. Importantly, our results confirm that TLR7 trafficking is dependent on UNC93B1.

We next examined whether UNC93B1 controls post-Golgi sorting of TLR7 as it does for TLR9. Similar to TLR9, both the full-length and cleaved forms of TLR7 associated with UNC93B1 suggesting that UNC93B1 traffics with TLR7 to endolysosomes (Figure 4.3C). However, unlike TLR9, the response to TLR7 ligands was normal in UNC93B1-Y539A expressing cells (Figure 4.3D). Moreover, the amount of cleaved TLR7 was unaffected, and the TLR7 Golgi-modified precursor form did not accumulate in these cells (Figure 4.3A, B). Thus, delivery of TLR7 to endolysosomes appears to be independent of the UNC93B1/AP-2 pathway.

If TLR7 does not require the UNC93B1-mediated recruitment of AP-2 for proper trafficking, then how does the receptor reach endolysosomes? We considered the possibility that TLR7 may recruit AP-2 directly, thereby obviating the need for UNC93B1. However, when we screened by Y2H for interactions between the cytosolic region of TLR7 and AP -1, -2, -3, and -4, we found that TLR7 interacted specifically with AP-4μ but not AP-2μ (Figure 4.3E). We identified 3 potential YxxΦ motifs within TLR7, and mutating one of these (Tyr-892) disrupted the interaction with AP-4 (Figure 4.3F). In addition, a TLR7-Y892A mutant no longer responded to TLR7 ligands (Figure 4.3G) and displayed reduced ectodomain processing when expressed in

bone marrow derived macrophages, suggesting that AP-4 is required for TLR7 delivery to endosomes (Figure 4.3H). AP-4 has been implicated in vesicular trafficking between the trans Golgi network (TGN) and endosomes [146-150]. Therefore, the association between AP-4 and TLR7 suggests that TLR7 is diverted from the secretory pathway at the TGN and delivered directly to endosomes while continually associating with UNC93B1. Thus, the mechanisms controlling trafficking of TLR7 and TLR9 to the compartments from which they signal are distinct.

**Several UNC93B1 dependent TLRs traffic independently of the UNC93B1/AP-2 pathway**

We next sought to determine whether the post-Golgi trafficking of other UNC93B1-dependent TLRs is similar to either of the pathways we have described for TLR7 and TLR9. First, we tested whether TLR3, TLR11, and TLR13 responses were affected in UNC93B1-Y539A expressing cells. Unfortunately, both wildtype and UNC93B1-Y539A cells were unresponsive to Poly I:C, profilin, and flagellin (data not shown), so we could not evaluate TLR3 or TLR11 signaling[48, 83, 85]. However, cells expressing wildtype UNC93B1 responded robustly to the oligoribonucleotide sequence derived from *Staphylococcus aureus* (hereafter referred to as Sa ORN) that was recently shown to stimulate TLR13[35, 88]. The response of UNC93B1-Y539A cells stimulated with Sa ORN was comparable to that of wildtype cells, suggesting that TLR13 does not require the UNC93B1/AP-2 pathway to access endosomal signaling compartments (Figure 4.4A).

We also examined trafficking of other UNC93B1-dependent TLRs biochemically in cells expressing UNC93B1-WT or UNC93B1-Y539A. TLR13 acquired EndoH-resistant glycans, and the glycosylation was unaffected in UNC93B1-Y539A expressing cells. Moreover, the full-length EndoH-resistant form did not accumulate in these cells, as we observed for TLR9. Together with the responses to TLR13 ligands, these results indicate that TLR13 traffics independently of the UNC93B1/AP-2 pathway. We performed similar experiments with TLR11 and TLR12, which both recognize profilin [34, 83]. Both of these receptors appear to undergo ectodomain cleavage, although the sizes of the cleaved receptors are quite distinct: ~45kD for TLR11 and 75kD for TLR12 (Figure 4.4C, D). Importantly, both receptors acquired EndoH-resistant glycans, and the glycosylation was unaffected in UNC93B1-Y539A expressing cells. Thus, TLR11 and TLR12 also do not require the UNC93B1/AP-2 pathway for proper trafficking.

Altogether, these results suggest that TLR9 trafficking may be unusual among the endosomal TLRs by trafficking via the plasma membrane en route to endosomes. It is important to note, though, that we have not examined TLR3 trafficking. Thus, it remains possible that TLR3 may also utilize this route, especially considering the several reports that describe TLR3 surface expression [56, 57, 60, 94].

**TLR7 and TLR9 association with UNC93B1 is mutually exclusive**

We have shown that UNC93B1 associates with both the full-length and cleaved forms of TLR9 and TLR7 (Chapter 3; Figure 3.3E and Figure 4.3C); however, the differential post-Golgi trafficking routes taken by TLR7 and TLR9 suggest that UNC93B1 must associate with TLR7 and TLR9 in separate complexes. To test this possibility directly, we examined interactions between TLR7, TLR9, and UNC93B1 by immunoprecipitation. While both TLR7 and TLR9 could precipitate UNC93B1, we could never detect interactions between the two receptors (Figure 4.5). Thus, UNC93B1 binding to TLR7 appears to preclude binding to TLR9 and vice

versa. These data support the idea that endosomal TLRs compete for binding to UNC93B1 in order to exit from the ER [107, 127, 151].

The preceding findings were documented in the publication "UNC93B1 controls the differential trafficking of endosomal TLRs" *eLife* 2013; 2: e00291. The following is a presentation of unpublished material that supports our findings that UNC93B1 controls the differential trafficking of endosomal TLRs at a post-ER step.

**TLR3 trafficking is dependent on UNC93B1 dependent but only partially dependent on the AP-2 pathway**

Expression of mouse TLR3 in a retroviral vector has presented a difficult challenge. Previous reports from our lab expressed human TLR3 in macrophage cells but to very low levels [23]. To overcome this obstacle, we optimized the mouse TLR3 codon sequence using methods previously mentioned for TLR7. C-terminally HA tagged codon optimized mouse TLR3 C-terminal tag (TLR3-HA) in the MSCV2.2 retroviral vector was successfully transduced and expressed in RAW macrophage cells and 3d iMacs (Figure 4.6A). We observed a <150KDa species, a higher mobility form running at 150kDa, and a 75kDa cleaved receptor (Figure 4.6A). Like TLR9, the cleaved receptor represents the largest portion among the three form of the receptor in macrophages (Figure 4.6A). Additionally, the high mobility "precursor" form and cleaved form of the receptor acquired EndoH resistant glycans indicating that TLR3 also transits through the Golgi (Figure 4.6A). To test whether trafficking of these forms is dependent on UNC93B1, we co-expressed TLR3 and UNC93B1-WT or UNC93B1-H412R in 3d iMacs. To our surprise, a small pool of TLR3 exited the ER independently of UNC93B1 (Figure 4.6B, lower). This pool represents a small portion of the exiting TLR because ER export was still enhanced in the presence of UNC93B1-WT (Figure 4.6B, upper). Of note, appearance of the cleaved receptor in UNC93B1-H412R expressing cells implies that this UNC93B1 independent pool was also able to traffic to endolysosomes (Figure 4.6B, lower). We next determined whether UNC93B1 dependent trafficking of TLR3 utilizes an AP-2 pathway, like TLR9. In the presence of UNC93B1-Y539A, the precursor form of TLR3 accumulated, suggesting it does use the AP-2 pathway as part of its trafficking route (Figure 4.6B). However, the amount of cleaved receptor was unimpaired, differing from the phenotype seen for TLR9. These observations may be explained by the existence of an UNC93B1-dependent and -independent route. In this case, expression of UNC93B1-Y539A may facilitate efficient ER export for both pools, and while a portion of TLR3 traffics via the AP-2 route, another portion can traffic to endolysosomes independent of UNC93B1. Because the cleaved receptor is known to be very stable, differences in the level of cleaved receptor may not be distinguishable without using methods such as pulse chase. Regardless, we conclude that TLR3 traffics via a similar pathway as TLR9, utilizing a UNC93B1/AP2 recruitment pathway, however, TLR3 is also capable of trafficking independently of UNC93B1, thus representing a unique mechanism among the UNC93B1 dependent TLRs.

**TLR5 and TLR8, but not TLR1, TLR2 and TLR4, traffic in an UNC93B1 dependent manner**

To test the remaining TLRs and their dependence on UNC93B1 and the UNC93B1/AP-2 pathway as their full-length forms, we expressed HA tagged TLRs 1, 2, 4, 5, and 8 in 3d iMac cells. As expected, TLR1, TLR2 and TLR4 trafficked entirely independent of UNC93B1 (Figure 4.7A-C). Of not, we detected a smaller cleaved receptor for TLR2 at approximately 50 kDa that was generated independent of UNC93B1 (Figure 4.7B, lower). Indeed, has been demonstrated to access endosomal compartments and could be subjected to proteolytic processing.

Next, we examined TLR5. Surface TLR5, which recognizes flagellin, acquires an EndoH resistant glycans (~125kDa) in the presence of UNC93B1-WT. However, to our surprise, this EndoH resistant TLR5 was lost in the absence of functional UNC93B1 (H412R), leaving only the ER EndoH sensitive pool (Figure 4.7D). Thus, UNC93B1 also controls the trafficking of TLR5. Additionally, TLR5 trafficking was unaffected by UNC93B1-Y539A, suggesting that the abrogation of the AP-2 pathway does not play an essential a role in TLR5 trafficking (Figure 4.7D).

Human TLR8 and UNC93B1 have been shown to interact and co-localize in similar compartments [152]. TLR8 is most closely related, phylogenetically and structurally, to TLR7. The function of TLR8 in mouse cells, however, has been controversial. Mouse TLR8 does not respond to the identified human TLR8 ligand, thus, the mouse receptor has been suggested to be non-functional [153]. Data arising from knockout studies suggests mouse TLR8 may have a functional role to prevent autoimmunity [70], however the mechanism initiating autoimmunity remains elusive. Therefore, we sought to determine the relationship between mouse TLR8 and UNC93B1. Mouse TLR8 was co-expressed with UNC93B1-WT, -H412R, or –Y539A in 3d iMacs. A cleaved form of mouse TLR8 appeared, roughly at 75kDa in the presence of UNC93B1-WT (Figure 4.7E). Additionally, the exhibited ratio of ER to cleaved pool was similar to that of TLR7. Generation of the TLR8 cleaved receptor required UNC93B1, suggesting that mouse TLR8 trafficking is entirely dependent on UNC93B1. Furthermore, the effect of UNC93B1–Y539A was minimal compared to TLR9 (Figure 4.7E). Thus, TLR8 depends on UNC93B1 similar to TLR7, and likely traffics to the same compartment. It remains to be determine whether TLR8 also relies on AP-4μ pathway to access endolysosomes.

## Discussion

Our work suggests that at least 7 endosomal TLRs are regulated by UNC93B1 in mice. TLR3, TLR7, TLR8 TLR9, TLR11, TLR12, and TLR13 require UNC93B1. To our surprise, surface localized TLR5 is also an UNC93B1-dependent TLR. We show that UNC93B1 acts at the cell surface by recruiting clathrin AP-2 to internalize TLR9 from the plasma membrane into endosomes. Perhaps most surprisingly, our results indicate that TLR7 and TLR9 have different requirements for UNC93B1 and demonstrate that the localization of these receptors is controlled through distinct post-Golgi trafficking mechanisms. This last point may provide an explanation for the contrasting roles played by TLR7 and TLR9 in SLE.

Through analysis of UNC93B1 mutants we identified an additional role for UNC93B1 in directing post-Golgi trafficking of TLR9. Unlike typical COPII loading factors, UNC93B1 remains associated with its cargo, traffics with TLR9 to the cell surface, and associates with AP-2 via a YXXΦ motif (Figure 4.8). Recruitment of AP-2 is necessary for internalization of TLR9 and subsequent trafficking to endolysosomes. This AP-2-dependent trafficking route has been described for several proteins localized to endolysosomes, including LAMP-1, LAMP-2, and MHC Class II [120-122]. In some cases, the same protein can access endocytic compartments through multiple routes. For example, LAMP-1/2 can also traffic directly from the TGN to endosomes [154]. While we cannot rule out that TLR9 may reach endolysosomes through multiple routes, AP-2-mediated internalization appears to be the main pathway of delivery, at least in the cells types we have examined. It is interesting that TLR9 and UNC93B1 would have evolved such dependency on this route, especially considering the potential for self-DNA recognition associated with surface localization of TLR9 [40, 155]. Indeed, our results appear to underscore why the requirement for ectodomain processing is a critical mechanism ensuring that receptors at the plasma membrane remain nonfunctional [24, 155].

One of the most exciting aspects of our study is the observation that trafficking of TLR7 and TLR9 are distinct. We find no evidence that TLR7 requires UNC93B1 for recruitment of AP-2. Instead, TLR7 appears to employ AP-4 in a direct route of traffic from the TGN to the endosome. These results provide the first evidence that different pathways control TLR7 and TLR9 trafficking and localization. One potential implication of this result is that these pathways may deliver TLR9 and TLR7 to distinct compartments with different access to ligands or distinct signaling properties. We find that TLR11, TLR12 and TLR13, like TLR7, do not require the UNC93B1/AP-2 pathway. However, it remains to be determined whether these TLRs utilize the AP-4 pathway or another pathway to traffic from TGN to endosomes. In contrast, TLR3 relies on the AP-2 pathway like TLR9 but only partially. It is possible that a separate pool of TLR3 is also able to employ an alternate pathway, possibly via AP-4. This finding supports the controversy over the localization of TLR3. Endosomal presence and surface presence, as well as presence in similar and distinct compartment from that of TLR9 have all been reported. Thus, future work should aim to determine whether these two pathways have different functional consequences.

Further compartmental specialization is generated by AP-3, which interacts with TLR9 and directs the receptor to endosomal compartments dedicated to type I interferon signaling [29, 30, 140]. TLR7 may also utilize AP-3 to reach this specialized compartment, although we could not detect interaction between AP-3 and TLR7 (Figure 4.3). Whether there is transport of TLRs

between each of the compartments serviced by AP-2, AP-3, and AP-4 remains an open question.

These results and our finding that TLR7 and TLR9 association with UNC93B1 is mutually exclusive suggest that each UNC93B1 molecule may interact with a single TLR. This specificity is particularly important in light of our findings that trafficking routes of TLR7 and TLR9 are distinct. Whether UNC93B1 is similarly selective for other TLRs and identification of the domains that mediate any selectivity are important topics for future studies.

The use of distinct molecular pathways to regulate endosomal TLRs may allow for differential regulation of trafficking, either in response to external cues or between different cell types. In addition, TLR7- and TLR9-containing compartments may have differing abilities to access internalized ligands, influencing responses to microbial or self-ligands. These possibilities are particularly intriguing when considering the contrasting roles played by TLR7 and TLR9 in SLE, where loss of TLR7 protects against disease while loss of TLR9 exacerbates disease [29, 30, 140] [45]. Our findings raise the possibility that distinct cell biological regulation may underlie the different roles played by these receptors in autoimmune disease. Defining the mechanisms underlying this regulation may help explain the etiology of certain autoimmune diseases as well as provide opportunities to selectively manipulate distinct aspects of TLR activation.

## Materials and Methods

### Antibodies and Reagents

The following antibodies were used for immunoblots, immunoprecipitations, or flow cytometry: anti-HA as purified antibody or matrix (3F10, Roche), anti-FLAG as purified antibody or matrix (M2 and M5, Sigma), anti-GFP (JL-8, Clontech), anti-GFP as purified or matrix (RQ2, MBL International), anti-*myc* (purified mouse, Invitrogen), anti-V5 (mouse monoclonal, Invitrogen), anti-Lamp-1 (1D4B, BD Biosciences), anti-calnexin (rabbit polyclonal, Enzo Life), anti-TNFα-PE or -APC (MP6-XT22, eBiosciences), anti-CD71-APC (OKT9, eBiosciences), goat anti-mouse IgG-AlexaFluor647 (Invitrogen), goat anti-rat-HRP, sheep anti-mouse-HRP, and donkey anti-rabbit-HRP (GE Healthcare). For immunofluorescence: rabbit anti-HA (Y11, Santa Cruz), goat anti-mouse Cy3 (Jackson Immunoresearch), goat anti-rabbit-AlexaFluor647 (Invitrogen). The following TLR ligands were used to stimulate cells: CpG ODN (TCCATGACGTTCCTGACGTT, all phosphorothioate linkages) and Sa ORN ("Sa17"[35]) (GACGGAAAGACCCCGUG RNA sequence purchased from Integrated DNA Technologies), R848 (Invivogen), and Pam3CSK4 (Invivogen). 3XFLAG peptide was purchased from Sigma. Digitonin was purchased from Wako or Calbiochem. Lipofectamine-LTX reagent (Invitrogen) was used for transient transfection of plasmid DNA. Lipofectamine RNAiMAX reagent (Invitrogen) was used for siRNA delivery. DOTAP liposomal transfection reagent (Roche) was used for transfection of Sa ORN in PBS. OptiMEM-I (Invitrogen) was used as media to form nucleic acid complexes for transient transfections.

### Mice

*Unc93b1*$^{3d/3d}$ mice[98] were obtained from the MMRRC at UC Davis. C57Bl/6 were purchased from The Jackson Laboratory. All mice were housed in the animal facilities at the University of California, Berkeley according to guidelines of the Institutional Animal Care and Use Committee.

### Plasmid Constructs

Pfu Turbo polymerase (Agilent) was used according to manufacturer's instructions for site directed mutagenesis. The following mouse stem cell virus (MSCV)-based retroviral vectors were used to express UNC93B1, TLR9, and TLR7 in cell lines: MSCV2.2 (IRES-GFP), MSCV-Thy1.1 (IRES Thy1.1), MIGR2 (IRES-hCD2). The following epitope tags were fused to the C-terminus of UNC93B1: 3XFLAG (DYKDHDGDYKDHDIDYKDDDDK), Myc (EQKLISEEDL), HA (YPYDVPDYA) and entire eGFP cDNA derived from pIRES-eGFP plasmid (Clonetech). TLR9 was fused to HA at the C-terminal end or with 3XFLAG at the N-terminal end as previously described[24, 80]. TLR7 sequence was synthesized after codon optimization by Invitrogen's GeneArt Gene Synthesis service and cloned into same vectors as TLR9 and tagged with C-terminal HA or C-terminal V5-His (GKPIPNPLLGLDST-HHHHHH). TLR11, TLR12, TLR13 was C-terminally tagged with HA and cloned into MSCV2.2. UNC93B1 shRNA and control were generated in MSCV-Lmp, as previously described. Rat AP-2m-HA containing an internal HA tag in pCDNA3 was provided by A. Sorkin (University of California, San Diego, CA, how at the University of Pittsburgh, PA)[156].

For yeast-two-hybrid assays, N-terminal (1-59 a.a.) and C-terminal (515-598 a.a.) cytosolic regions of UNC93B1 were fused to Gal4 DNA binding domain (DBD) by cloning into pGBT9

(Clontech). TLR7 cytosolic region (mouse 862-1061 a.a.), TLR9 cytosolic region (mouse 838-1032 a.a.), fused to Gal4-DBD by cloning into pGBT9. AP-1Am, AP-2m, AP-3Am, AP-3Bm, AP-4m were cloned into pACT2 (Clontech) were provided by J. Bonifacino (National Institutes of Health, Bethesda, MD).

**Cell lines and Tissue culture conditions**
HEK293T cells were obtained from American Type Culture Collection (ATCC). GP2-293 packaging cell lines were obtained from Clonetech. Phoenix-Eco (ØNX-E ) cells were provided by G. Nolan, Stanford University. The above cell lines were cultured in DMEM supplemented with 10% (vol/vol) FCS, L-glutamine, penicillin-streptomycin, sodium pyruvate, and HEPES (pH 7.2) (Invitrogen). RAW264 macrophage cell lines (ATCC) and immortalized macrophages (generated as described below) were cultured in RPMI 1640 (same supplements as above).

To generate immortalized macrophage cell lines, bone marrow from *Unc93b1*$^{3d/3d}$ mice was cultured in RPMI 1640 media supplemented with supernatant containing M-CSF, as previously described[134], as well as virus encoding both v-raf and v-myc[135]. After 8 days, macrophages were removed from M-CSF-containing media and cultured in RPMI 1640 media with added supplements as described above.

**Retroviral transduction**
For retroviral transduction of immortalized macrophages, VSV-G-psuedotyped retrovirus was made in GP2-293 packaging cells (Clontech). GP2-293 cells were transfected with retroviral vectors and pVSV-G using Lipofectamine LTX reagent. 24 hours post-transfection, cells were incubated at 32°C. 48 hours post-transfection viral supernatant (with polybrene at final 5mg/ml) and was used to infect target cells overnight at 32°C and protein expression was checked 48 hours later. Target cells were sorted on MoFlo Beckman Coulter Sorter to match expression.

For retroviral transduction of bone marrow derived macrophages, retrovirus was produced with the ØNX-E packaging line. Bone marrow cells were transduced with viral supernatant on two successive days while cultured in M-CSF containing RPMI media until harvested on day 8.

**Luciferase assays**
Activation of NF-kB in HEK293T cells was performed as previously described[24]. Briefly, transfections were performed in OptiMem (Invitrogen) with LTX transfection reagent (Invitrogen) according to manufacturer's guidelines. Cells were stimulated with 1-10μg/ml R848 after 24 h and lysed by passive lysis after an additional 12-16 h. Luciferase activity was measured on a LMaxII-384 luminometer (Molecular Devices).

**Lysate preparation, SDS-PAGE, Immunoblotting**
Cell lysates were prepared with TNT buffer (20 mM Tris [pH 8.0], 200 mM NaCl, 1% Triton X-100, 4mM EDTA and supplemented with EDTA-free complete protease inhibitor cocktail (Roche)) unless otherwise noted. Digitonin lysis buffer (50 mM Tris [pH 7.4], 150 mM NaCl, 5 mM EDTA [pH 8.0], 1% Digitonin added fresh and supplemented with EDTA-free complete protease inhibitor cocktail) was used for co-immunoprecipitations. Lysates were cleared of insoluble material by centrifugation. For immunoprecipitations, lysates were incubated with anti-

HA matrix, anti-FLAG matrix, anti-GFP matrix or with purified antibody conjugated to Protein A/G beads (Pierce) and precipitated proteins were denatured in SDS-PAGE buffer separated by SDS-PAGE (Tris-HCl self cast gels or Bio-Rad TGX precast gels), and probed by the indicated antibodies. For anti-FLAG matrix immunoprecipitations, 3XFLAG peptide (Sigma) was used to elute.

**Endoglycosidase H assay**
Immunoprecpitated proteins or total lysate were denatured and treated with Endoglycosidase H or PNGase F according to manufacturer's instructions. All enzymes and buffers were purchased from New England Biolabs.

**Flow cytometry**
To measure TNFα production, we added brefeldinA to cells 30 min after stimulation, and cells were collected after an additional 4h, and cells were stained for intracellular cytokines with a Fixation & Permeabilization kit according to manufacturer's instructions (eBioscience).
For FLAG-TLR surface expression, HEK293T cells stably expressing N-terminally tagged 3XFLAG-TLR9 were stained with anti-FLAG (M5, Sigma) antibody followed by Alexa 647 goat anti-mouse IgG secondary antibody (Invitrogen). All data were collected on LSR II (Becton Dickinson) or FC-500 (Beckman Coulter) flow cytometers and were analyzed with FloJo software (TreeStar).

**Microscopy**
Co-localization studies were performed on Leica TCS confocal microscope. The images were taken with a 40x oil immersion objective and treated with 2x digital zoom. All images were processed by Adobe photoshop. Cells were allowed to settle overnight on coverslips. Coverslips were washed with PBS, fixed with 4% paraformaldehyde/PBS, and permeabilized with 0.5% saponin/PBS. Slides were incubated in freshly made 0.1% sodium borohydride 0.1% saponin before being stained in 1% Bovine Serum Albumin (Fisher Scientific)/0.1% saponin in PBS with rabbit anti-HA(Santa Cruz), rat anti-Lamp-1 (BD Biosciences) then with secondary antibodies, goat anti-Rabbit 647 (Invitrogen) and goat anti-Rat Cy3 (Jackson Immunoresearch).

**siRNA knockdown**
3.5x10^5 HEK293Ts were plated in 2ml antibiotic free media per well in 6-well plates and reverse transfected with 5ul 20uM siRNA in 500ul OptiMEM-I and 5ul of Lipofectamine RNAiMAX for 48-96h until harvest for flow cytometry or SDS-PAGE and immunoblot analysis. siRNA duplexes against human AP-2m were purchased from Dharmacon RNAi Technologies with the following sequence: 5'-GGAGAACAGUUCUUGCGGC-3' and with the following conditions: ON-TARGET - Enhanced Antisense Loading, Standard (A4), UU added to 3' end. Control siRNA (ON-TARGETplus Non-targeting siRNA #1) was purchased from Dharmacon.

**Yeast Two-Hybrid Interaction**
Cells of an overnight culture (2.5ml) of yeast strain PJ69-4a in YPD media grown at 30°C were washed in $H_2O$ and mixed sequentially with the following: 50% PEG-3500 (Sigma), 10 mM lithium acetate in Tris-EDTA (TE) (pH 7.5), denatured salmon sperm DNA (Invitrogen) and 100ng of plasmid constructs, then mixed. Yeast were incubated for 30 min at 30°C and heat-

shocked for 15 min at 42°C. Cells were centrifuged, resuspended in $H_2O$, and spread on YNB plates with –Trp –Leu dropout mix. Liquid cultures in Trp-Leu broth were grown at 30°C overnight. Cells were normalized to 1.0 OD and 1:10 dilutions made. 4ul of each dilution was plated on –Trp–Leu–His, and –Trp–Leu–Ade at 30°C. YPD, YNB and dropout mixtures purchased from Sunrise Science. Growth on –Trp–Leu–His or –Trp–Leu–Ade plates was recorded at Day 3.

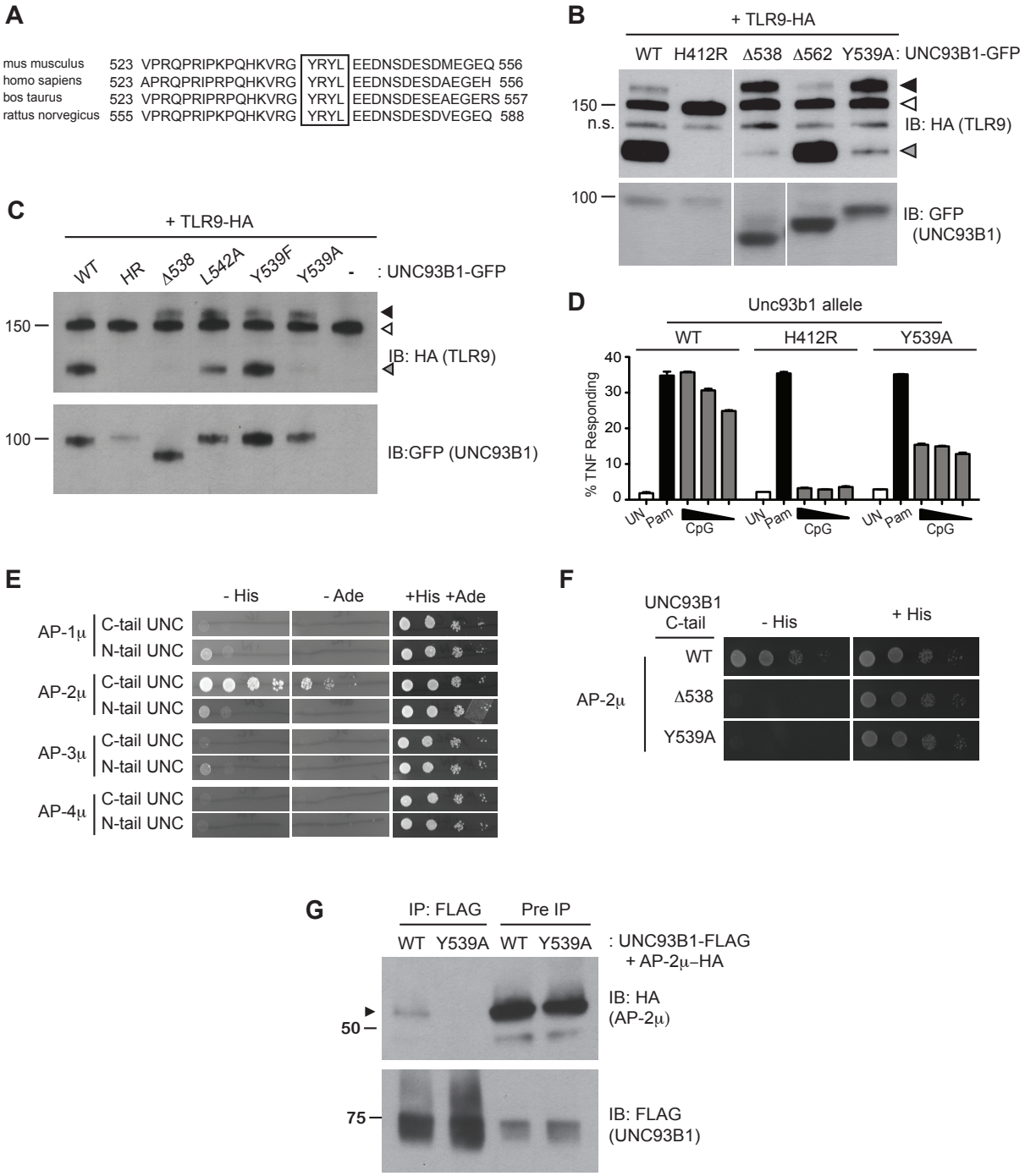
A
mus musculus 523 VPRQPRIPKPQHKVRG YRYL EEDNSDESDMEGEQ 556
homo sapiens 523 APRQPRIPRPQHKVRG YRYL EEDNSDESDAEGEH 556
bos taurus 523 VPRQPRIPRPQHKVRG YRYL EEDNSDESEAEGERS 557
rattus norvegicus 555 VPRQPRIPKPQHKVRG YRYL EEDNSDESDVEGEQ 588
B
+ TLR9-HA
WT H412R Δ538 Δ562 Y539A: UNC93B1-GFP
150
n.s.
IB: HA (TLR9)
100
IB: GFP (UNC93B1)
C
+ TLR9-HA
WT HR Δ538 L542A Y539F Y539A - : UNC93B1-GFP
150
IB: HA (TLR9)
100
IB:GFP (UNC93B1)
D
Unc93b1 allele
WT H412R Y539A
% TNF Responding
40
30
20
10
0
UN Pam CpG
E
- His - Ade +His +Ade
AP-1μ C-tail UNC N-tail UNC
AP-2μ C-tail UNC N-tail UNC
AP-3μ C-tail UNC N-tail UNC
AP-4μ C-tail UNC N-tail UNC
F
UNC93B1 C-tail
- His + His
AP-2μ
WT
Δ538
Y539A
G
IP: FLAG Pre IP
WT Y539A WT Y539A : UNC93B1-FLAG + AP-2μ–HA
50
IB: HA (AP-2μ)
75
IB: FLAG (UNC93B1)

**Figure 4.1**

**Figure 4.1 UNC93B1 controls post-Golgi trafficking of TLR9 by recruiting AP-2.**
(**A**) Multi-species protein sequence alignment of residues in the UNC93B1 C-terminal tail. The YxxΦ motif, YRYL, is boxed. (**B**) Precursor TLR9 accumulates in UNC93B1-Y539A expressing cells. Lysates from *3d* iMac cells expressing TLR9-HA were complemented with the indicated GFP tagged UNC93B1, analyzed by SDS-PAGE, and immunoblotted with anti-HA and anti-GFP antibodies. The precursor (black arrow), ER (white arrow) and cleaved (grey arrow) forms of TLR9-HA are indicated. (**C**) Mutations of YxxΦ in UNC93B1 confer partial phenotypes in TLR9 trafficking when compared with Y539A. Lysates from *3d* iMac cells expressing TLR9-HA and GFP tagged UNC93B1-WT, H412R, Δ538, L542A, Y539F, Y539A were analyzed by SDS-PAGE and immunoblotted with anti-HA and anti-GFP antibodies. Presence of precursor (black arrow), ER (white arrow) and cleaved (grey arrow) forms of TLR9 are indicated. Asterisk indicates non-specific (n.s.) band. (**D**) TLR9 signaling is impaired in UNC93B1-Y539A cells. *3d* iMac cells, complemented with GFP tagged UNC93B1-WT, -H412R, or -Y539A, were harvested for intracellular TNFα staining 5h after stimulation with 3μM CpG, 1μg/ml Pam3CSK4 (Pam) or left unstimulated. Percentages of TNF-producing cells after gating on UNC93B1-GFP positive cells are plotted. (**E**) The C-terminal tail of UNC93B1 interacts with AP-2. Results from a yeast two-hybrid assay testing for interaction between the AP (-1A, -2, -3A, -4) μ subunits and the N- or C-terminal cytosolic regions of UNC93B1 (N- or C-tail Unc), are shown. Growth on –His–Trp–Leu plates (–His) or –Ade–Trp–Leu (–Ade) indicates interaction. Growth on –Trp–Leu plates (+His+Ade) serves as a control. (**F**) The C-terminal tail of UNC93B1 interacts with AP-2. Results from a yeast two-hybrid assay testing for interaction between the AP-2 μ subunit and the C-terminal cytosolic region of UNC93B1 (UNC93B1 C-tail ) from WT, the Y539A mutant, or the Δ538 mutant are shown. Growth on –His–Trp–Leu plates (–His) indicates interaction. Growth on –Trp–Leu plates (+His) serves as a control. (**G**) Tyr-539 on UNC93B1 mediates interaction with AP-2. HEK293T were transiently transfected with AP-2μ-HA and FLAG tagged UNC93B1-WT, -Y539A, or empty vector. Cell lysates were incubated with anti-FLAG matrix, and UNC93B1-associated proteins were eluted with FLAG peptide, separated by SDS-PAGE and visualized by immunoblot with anti-HA or anti-FLAG antibodies. UNC93B1 associated AP-2μ is indicated with black arrow. All results are representative of at least three experiments (B, D-F) or two experiments (C, G).

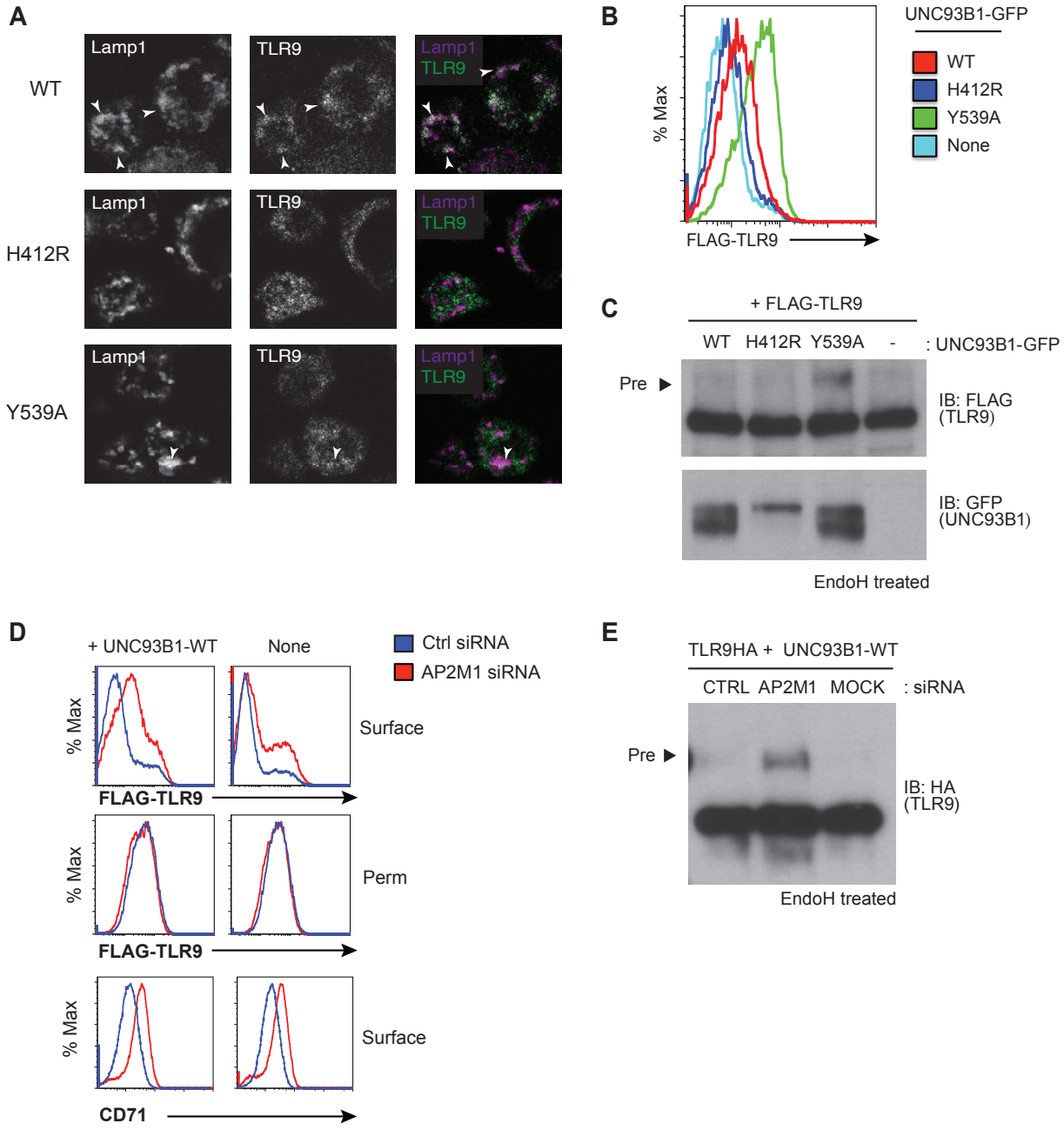
A
WT
H412R
Y539A
Lamp1
TLR9
Lamp1
TLR9
B
UNC93B1-GFP
WT
H412R
Y539A
None
% Max
FLAG-TLR9
C
+ FLAG-TLR9
WT H412R Y539A -
: UNC93B1-GFP
Pre
IB: FLAG (TLR9)
IB: GFP (UNC93B1)
EndoH treated
D
+ UNC93B1-WT
None
Ctrl siRNA
AP2M1 siRNA
% Max
Surface
FLAG-TLR9
Perm
CD71
E
TLR9HA + UNC93B1-WT
CTRL AP2M1 MOCK
: siRNA
Pre
IB: HA (TLR9)
EndoH treated

**Figure 4.2**

**Figure 4.2 Failure to recruit AP-2 by UNC93B1 results in cell surface accumulation of TLR9**

(**A**) TLR9 fails to traffic to endolysosomes in UNC93B1-Y539A expressing cells. Localization of TLR9-HA and Lamp-1 in *3d* iMac cells complemented with UNC93B1-WT, -H412R, or -Y539A was determined by immunofluorescence microscopy. Representative images of Lamp-1 (left), TLR9 (middle), and a pseudo-colored merged image for each UNC93B1 allele are shown. Arrowheads indicate areas of Lamp-1/TLR9 colocalization. (**B**) TLR9 accumulates at the cell surface in UNC93B1-Y539A expressing cells. HEK293Ts transfected with N-terminally tagged 3xFLAG-TLR9 and the indicated UNC93B1 alleles were stained with anti-FLAG and goat anti-mouse IgG secondary antibodies. FLAG staining was measured by flow cytometry. (**C**) The TLR9 precursor form accumulates in HEK293T expressing N-terminally tagged FLAG-TLR9 and UNC93B1-Y539A. Lysates from HEK293Ts stably expressing N-terminally tagged 3XFLAG TLR9 and GFP tagged UNC93B1-WT, -H412R, or -Y539A were harvested, treated with EndoH, separated by SDS-PAGE, and visualized by immunoblot with anti-FLAG and anti-GFP antibodies. (**D**) TLR9 accumulates at the cell surface in cells lacking AP-2. HEK293Ts stably expressing 3xFLAG-TLR9 with or without WT UNC93B1 were treated with AP-2μ (AP2M1) or control siRNA for 96 hrs. FLAG staining was measured on intact (surface) or permeabilized (Perm) cells as described in (G). Anti-CD71 (transferrin receptor) staining serves as a control for AP-2 knockdown. (**E**) Absence of AP-2 causes accumulation of TLR9 precursor form. HEK293Ts were treated with control or AP-2μ siRNA. After 48 hours, siRNA treated cells were transiently transfected with TLR9-HA and GFP tagged UNC93B1-WT. Lysates were harvested 24h later for EndoH assay as described in (A). The TLR9 precursor form (black arrow) is indicated in each panel. Results are representative of at least three experiments (B, D) or two (A, C, E).

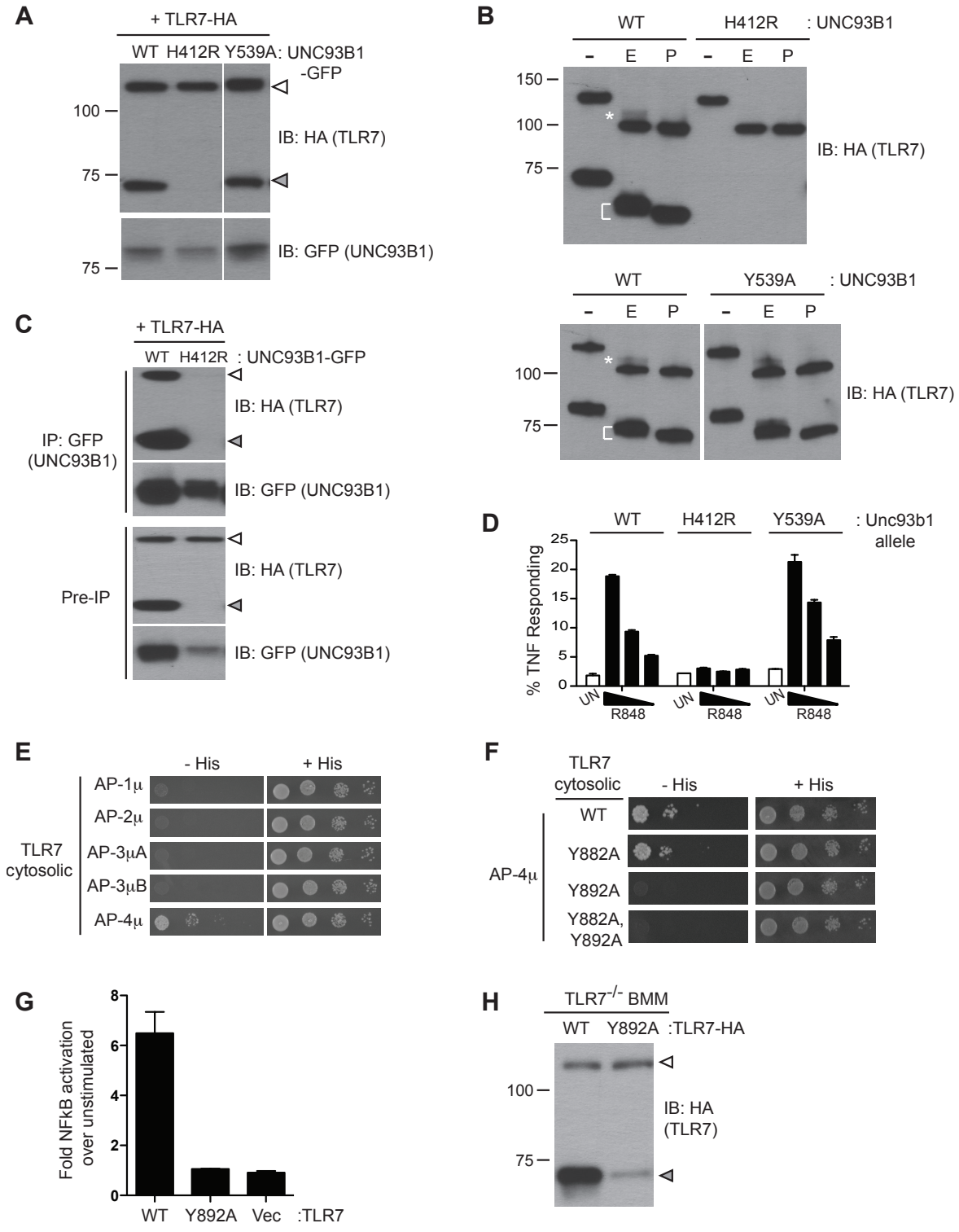
A
+ TLR7-HA
WT H412R Y539A: UNC93B1 -GFP
100
75
IB: HA (TLR7)
75
IB: GFP (UNC93B1)
B
WT
H412R
: UNC93B1
- E P - E P
150
100
75
*
IB: HA (TLR7)
WT
Y539A
: UNC93B1
- E P - E P
100
75
*
IB: HA (TLR7)
C
+ TLR7-HA
WT H412R : UNC93B1-GFP
IP: GFP (UNC93B1)
IB: HA (TLR7)
IB: GFP (UNC93B1)
Pre-IP
IB: HA (TLR7)
IB: GFP (UNC93B1)
D
WT
H412R
Y539A
: Unc93b1 allele
% TNF Responding
25
20
15
10
5
0
UN
R848
UN
R848
UN
R848
E
- His
+ His
TLR7 cytosolic
AP-1μ
AP-2μ
AP-3μA
AP-3μB
AP-4μ
F
TLR7 cytosolic
- His
+ His
AP-4μ
WT
Y882A
Y892A
Y882A, Y892A
G
Fold NFkB activation over unstimulated
8
6
4
2
0
WT
Y892A
Vec
:TLR7
H
TLR7-/- BMM
WT Y892A :TLR7-HA
100
75
IB: HA (TLR7)

**Figure 4.3**

**Figure 4.3 Differential trafficking of TLR7 and TLR9**
(**A**) TLR7 trafficking can be monitored biochemically and is UNC93B1-dependent. Lysates from *3d* iMac cells expressing TLR7-HA and complemented with GFP-tagged UNC93B1–WT, –H412R or –Y539A were separated by SDS-PAGE and immunoblotted with anti-HA and anti-GFP antibodies. ER (white arrows) and cleaved (grey arrows) forms of TLR7-HA are indicated. (**B**) TLR7 acquires EndoH resistance. TLR7-HA was immunoprecipitated from *3d* iMac cells expressing UNC93B1-WT, -H412R, or -Y539A, treated with EndoH (E), PNGaseF (P) or left untreated (-), and visualized by anti-HA immunoblot. Asterisk (*) indicates precursor form of the receptor. The bracket indicates the migration difference between EndoH-treated and PNGaseF-treated TLR7. (**C**) UNC93B1 interacts with ER and cleaved forms of TLR7. GFP-tagged UNC93B1-WT or -H412R were immunoprecipitated from *3d* iMac cells expressing TLR7-HA. UNC93B1 associated proteins were analyzed by SDS-PAGE and immunoblotted with anti-HA and anti-GFP antibodies. ER (white arrows) and cleaved (grey arrows) forms of TLR7-HA are indicated. (**D**) TLR7 signaling is normal in UNC93B1-Y539A cells. *3d* iMac cells complemented with GFP tagged UNC93B1-WT, -H412R, or -Y539A were stimulated with 100 to 25ng/ml R848 for 5h and intracellular TNFα stain was performed. Percentages of TNF-producing cells after gating on UNC93B1-GFP positive cells are plotted. (**E**) TLR7 interacts with AP-4μ. Results from a yeast two-hybrid assay testing for interaction between the AP-1, -2, -3, and -4 μ subunits and the C-terminal cytosolic region of TLR7. Growth on –His–Trp–Leu plates (–His) indicates interaction. Growth on –Trp–Leu plates (+His) serves as a control. (**F**) TLR7-Y892A is unable to interact with AP-4μ. Results from a yeast two-hybrid assay testing for interaction between the AP-4μ and TLR7 YxxΦ mutants (Y882A, Y892A, or double). Conditions are as described in (E). (**G**) TLR7-Y892A does not respond to TLR7 ligands. HEK293T cells were transiently transfected with an NF-kB luciferase reporter as well as expression plasmids encoding TLR7, TLR7-Y892A, or empty vector. Luciferase production was assayed 16h after stimulation with 10μg/ml R848. (**H-I**) TLR7-Y892A trafficking is impaired. $TLR7^{-/-}$ bone marrow derived macrophages (BMMs) (H) or RAW.264 macrophage lines (I) were transduced with HA-tagged TLR7-WT or TLR7-Y892A. Immunoprecipitated TLR7-HA (H) or cell lysates (I) were analyzed by SDS-PAGE and immunoblotted with anti-HA antibodies. ER (white arrows) and cleaved (grey arrows) forms of TLR7-HA are indicated. Results are representative of at least three experiments (A, D, E) or two experiments (B, C, F, G, I).

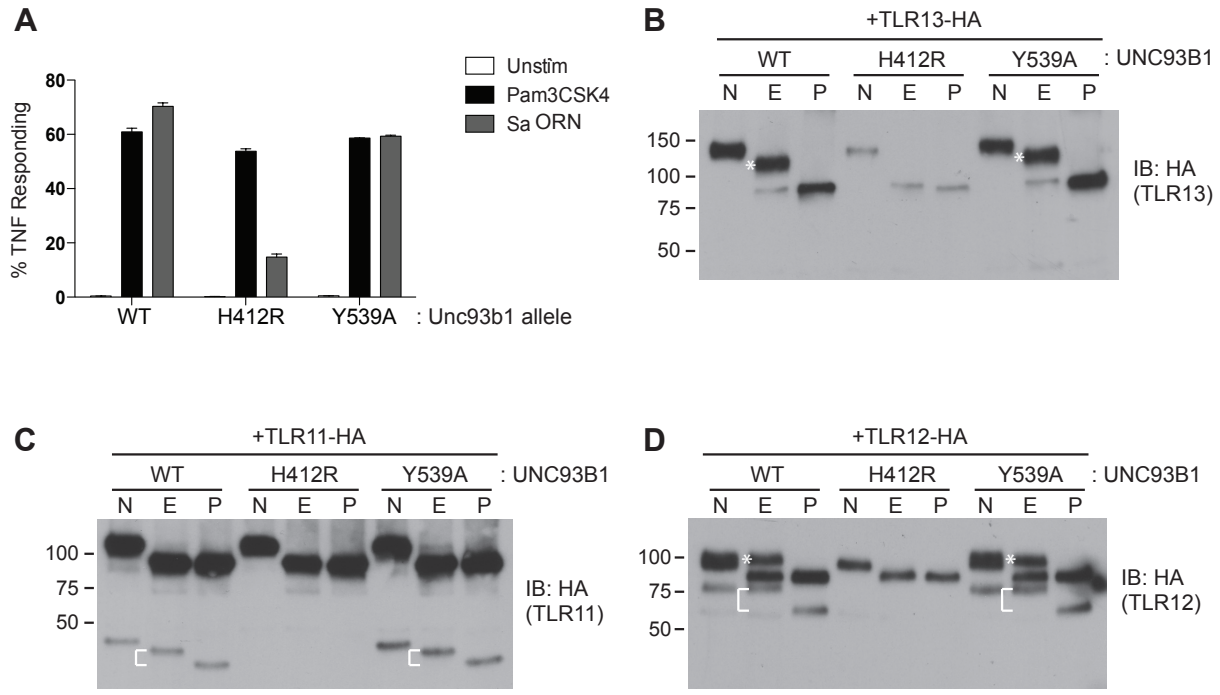


**Figure 4.4 UNC93B1 dependent TLR11, 12, and 13 traffic independently of the UNC93B1/AP-2 pathway**

(**A**) TLR13 signaling is unaffected by UNC93B1-Y539A. *3d* iMac cells expressing UNC93B1–WT, –H412R, or –Y539A were stimulated with 1μg/ml Pam3CSK4 (black) or 1*n*M Sa ORN complexed with DOTAP (grey) and harvested for intracellular TNFα staining 5h after stimulation. Percentages of TNF-producing cells are plotted. (**B**) TLR13 trafficking is unaffected by UNC93B1-Y539A. TLR13-HA was immunoprecipitated from *3d* iMac cells expressing UNC93B1-WT, -H412R, or -Y539A, treated with EndoH (E), PNGaseF (P) or left untreated (-), and visualized by anti-HA immunoblot. Asterisk (*) indicates full length EndoH resistant form of the receptor. (**C-D**) TLR11 and TLR12 trafficking is unaffected by UNC93B1-Y539A. TLR11 and TLR12 was treated as in (B). Asterisk (*) indicates full length EndoH resistant form of the receptor. The bracket indicates the migration difference between EndoH-treated and PNGaseF-treated cleaved TLR. Results are representative of at least three experiments (A) or two experiments (B-D).

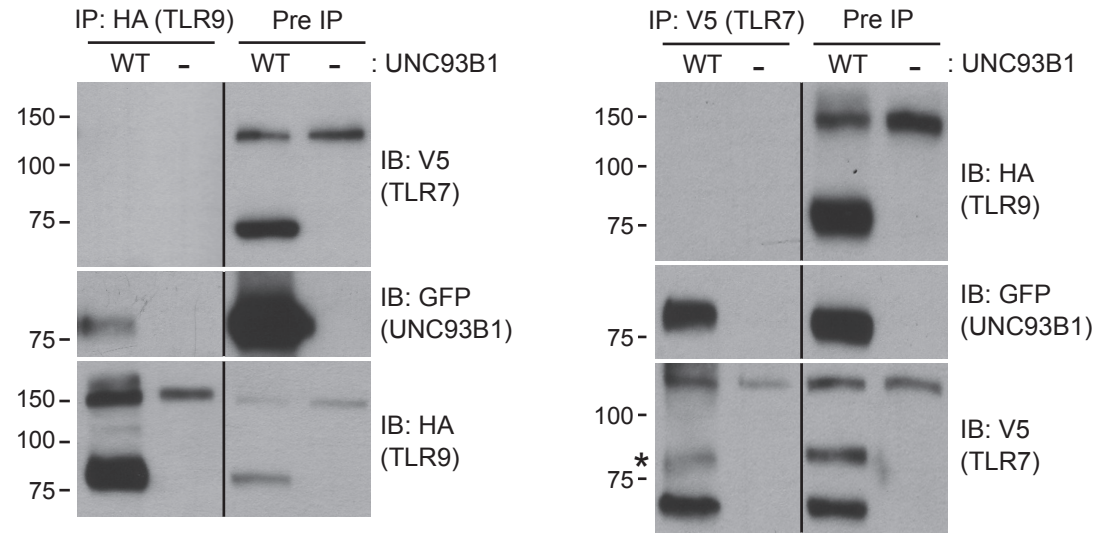


**Figure 4.5 UNC93B1 associates with TLR9 and TLR7 separately**
(**A**) TLR9 associates with UNC93B1 but not with TLR7. *3d* iMac cells expressing TLR9-HA, TLR7-V5-His, and UNC93B1-GFP were lysed in TNT buffer conditions then incubated with anti-HA matrix. Immunoprecipitated proteins were analyzed by SDS-PAGE and immunoblotted with HA, GFP and V5 antibodies. (**B**) TLR7 associates with UNC93B1 but not with TLR9. Same as (A) except with anti-V5 ProteinA/G beads. Asterisk (*) indicates remaining UNC93B1-GFP signal. Results are representative of two experiments.

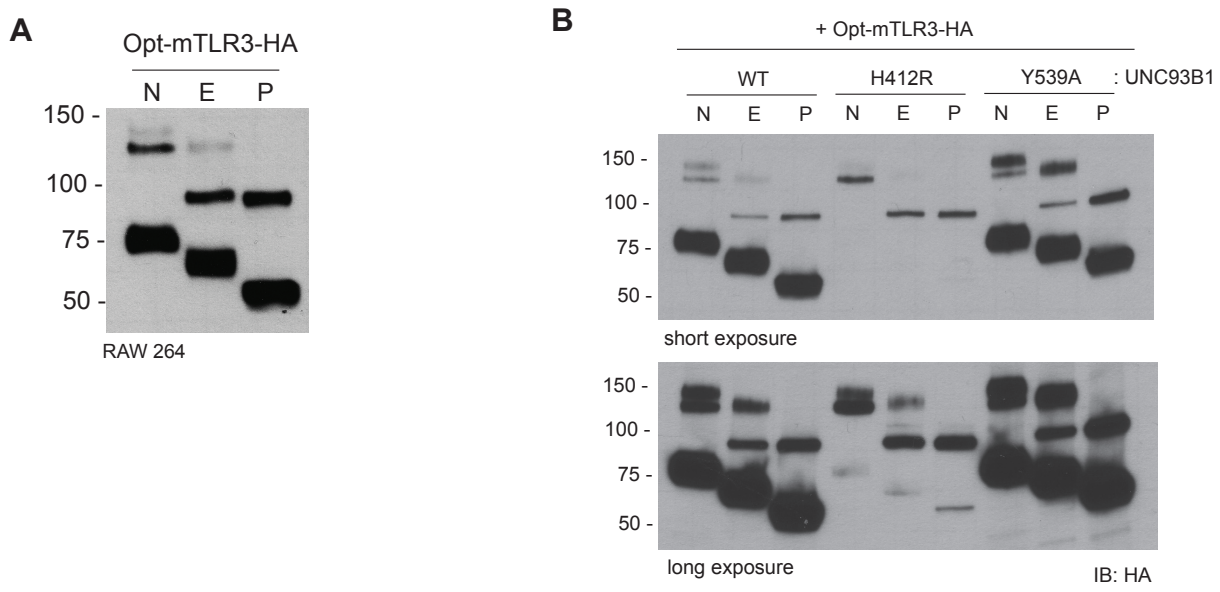


**Figure 4.6 TLR3 trafficking is partially UNC93B1 dependent**
(**A**) Mouse TLR3 protein sequence was altered to use optimal codon usage. Trafficking can be monitored biochemically in RAW264 cells. TLR3-HA from RAW cells was immunoprecipitated and treated with EndoH (E), PNGaseF (P) or left untreated (-), and visualized by anti-HA immunoblot. Asterisk (*) indicates full length EndoH resistant form of the receptor. The bracket indicates the migration difference between EndoH-treated and PNGaseF-treated cleaved TLR. (**B**) Mouse TLR3 trafficking is partially UNC93B1 dependent. TLR3-HA was immunoprecipitated from *3d* iMac cells expressing UNC93B1-WT, -H412R, or -Y539A, treated with EndoH (E), PNGaseF (P) or left untreated (-), and visualized by anti-HA immunoblot. Asterisk (*) indicates precursor form of the receptor. The bracket indicates the migration difference between EndoH-treated and PNGaseF-treated TLR3. Upper, short exposure of immunoblot. Lower, long exposure of immunoblot.

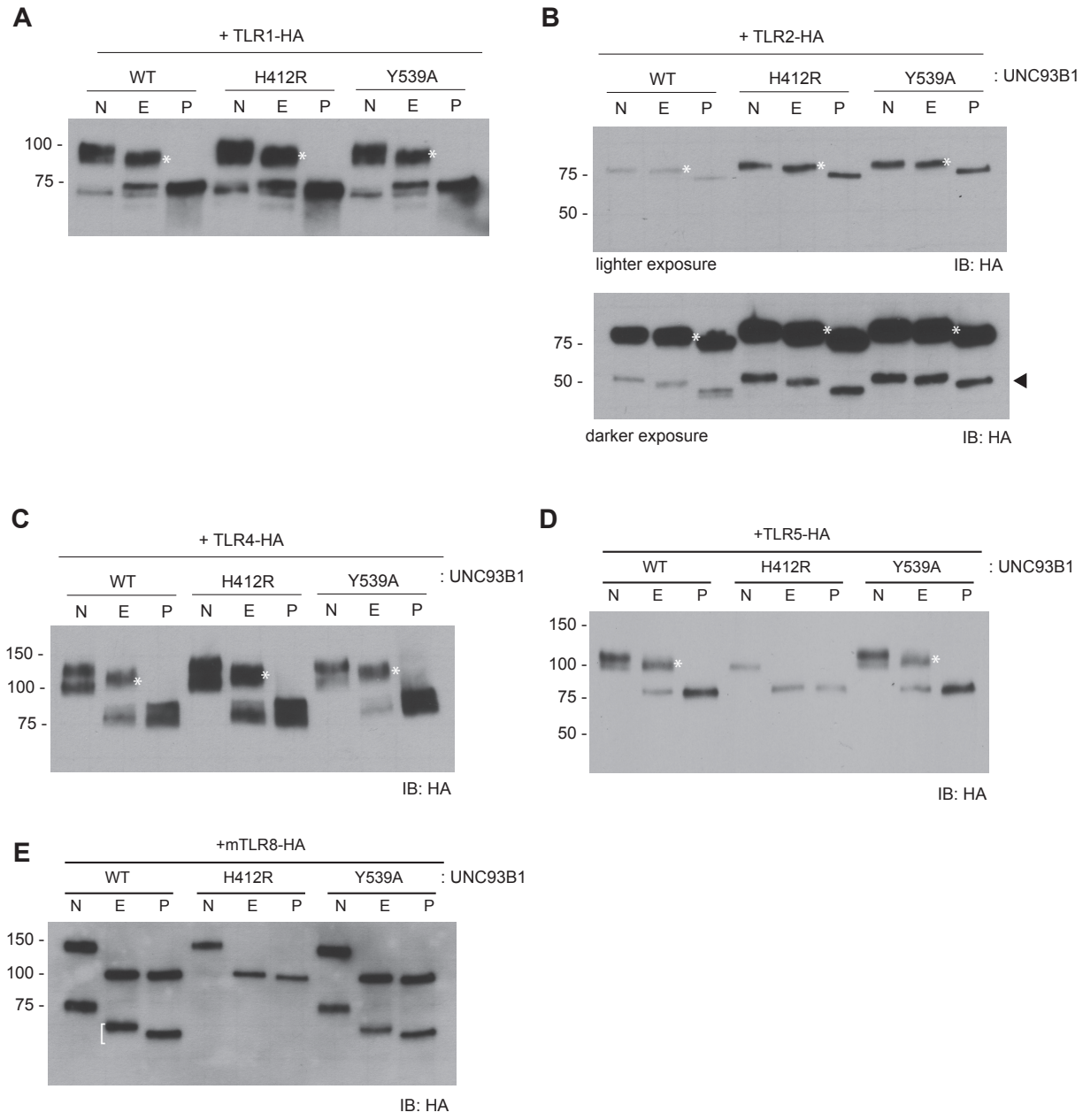


**Figure 4.7 TLR5 and TLR8, but not TLR1, TLR2 and TLR4, traffic in an UNC93B1 dependent manner**

(**A-C**) Surface TLRs 1, 2, and 4 traffic independently of UNC93B1. (**D,E**) TLR5 and TLR8 are dependent on UNC93B1. (A-E) HA tagged TLRs were immunoprecipitated from *3d* iMac cells expressing UNC93B1-WT, -H412R, or -Y539A, treated with EndoH (E), PNGaseF (P) or left untreated (-), and visualized by anti-HA immunoblot. Asterisk (*) indicates precursor form of the receptor. The bracket indicates the migration difference between EndoH-treated and PNGaseF-treated TLR.

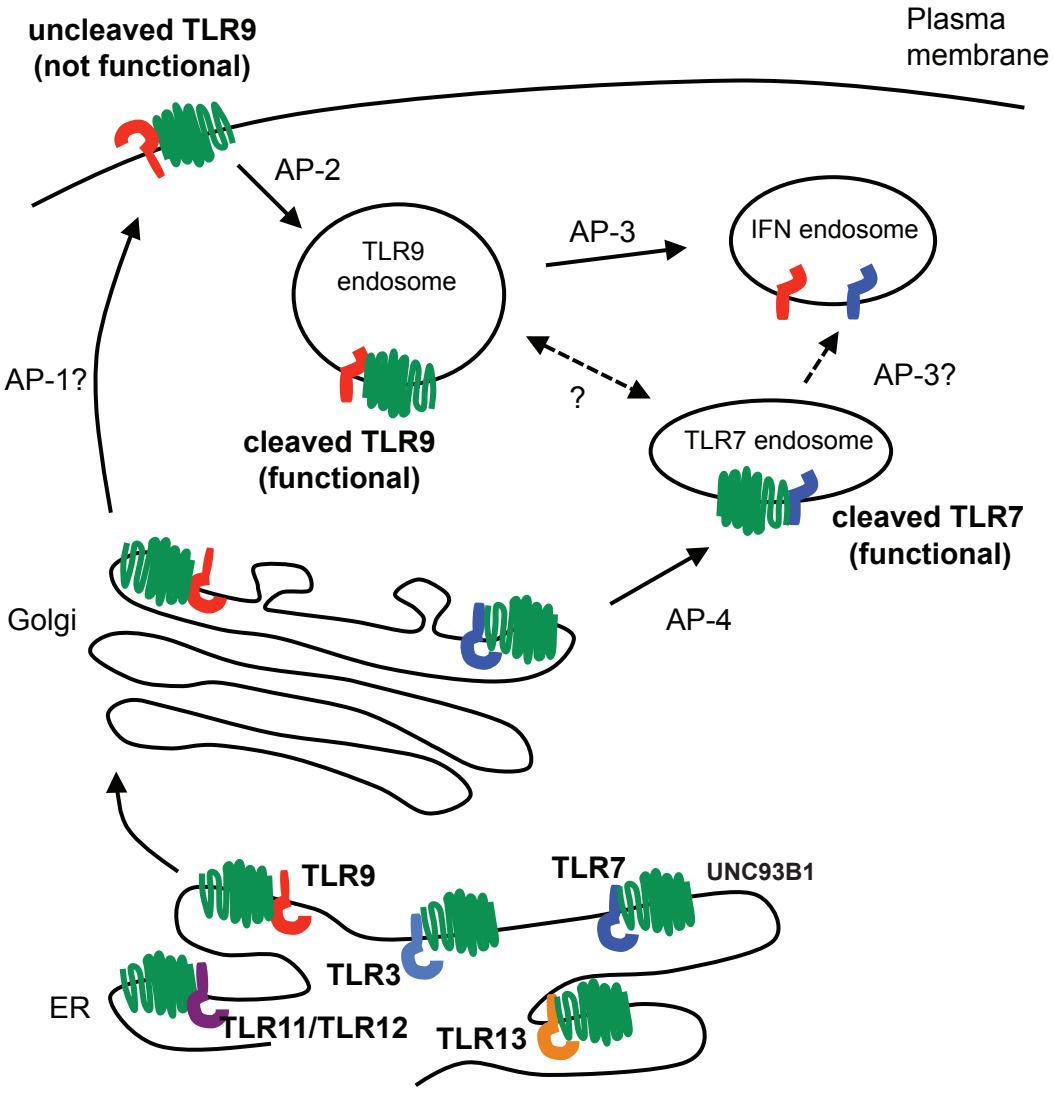


**Figure 4.8 Trafficking pathways controlling localization of endosomal TLRs**
UNC93B1 interacts with TLRs in the ER and facilitates loading into COPII vesicles. Unlike typical COPII loading factors, UNC93B1 remains associated with TLR9 and TLR7 after exit from the ER. Through its recruitment of AP-2, UNC93B1 is necessary for endocytosis of TLR9 from the plasma membrane into endosomes. TLR7 does not rely on this trafficking route. Instead, TLR7 utilizes AP-4 to bypass the cell surface and traffic directly to endosomes. This difference in trafficking may result in TLR9 and TLR7 accessing distinct compartments with unique functional properties related to the function of each receptor.

# Chapter 5: Biochemical techniques to study UNC93B1 dependent toll-like receptor trafficking

## Background

Understanding the fundamental aspects of the regulation of nucleic acid sensing TLRs will shed light on the etiology of autoimmune diseases as well as their critical role in microbial pathogenesis. Nucleic acid sensing TLRs 3, 7 and 9 traffic from the ER through the Golgi en route to endolysosomes. Mechanistic studies to determine TLR trafficking have been accomplished using many distinct and complementary techniques. Such techniques include but are not limited to: (1) immunofluorescence, (2) flow cytometry, (3) organelle fractionations, (4) biochemical analysis of glycosylation modifications, and (5) biochemical monitoring of proteolytic processing. Although many endogenous antibodies against nucleic acid sensing TLRs are commercially available, very few, if at all, are thought to be specific [9]. Due to the limitation of endogenous TLR antibodies, TLR cell biology studies have been restricted to overexpression studies with epitope tagged versions of TLRs [24, 58]. Furthermore, lack of endogenous TLR antibodies offers another limitation in identifying expressing cell populations. The extent of TLR expression studies in distinct cell types has been restricted to detection of mRNA transcript, which may yield conflicting results due to impurity of cell populations. Additionally, this technique does not provide information about protein expression. The use of an endogenous TLR antibody would enable analysis by flow cytometry or immunohistochemistry to identify exact cell types expressing the TLR based on cell surface markers. Because TLR9 and other nucleic acid TLRs are localized intracellularly, flow cytometry studies with endogenous antibodies will require fixation and permeabilization of cells, thus making it impossible to isolate viable TLR expressing cells. With these considerations in mind, we propose to generate a knock-in reporter mouse expressing a hemagglutinin (HA) epitope tagged TLR9 with an IRES GFP reporter. This knock-in allele will henceforth be referred to as $tlr9^{\text{HA-GFP}}$

A TLR9-GFP fusion transgenic mouse model has been generated another group [157]. Their findings demonstrate that TLR9 does not traffic in all cell types and this cell specificity seems to correlate with expression of UNC93B1, a factor required for the proper trafficking of TLR9 and other nucleic acid TLRs. However, because this is a transgenic overexpression model and utilizes a TLR9-GFP fusion that disrupts TLR9 signaling, it cannot be used to address TLR9 trafficking at endogenous levels and in normal conditions. Our $tlr9^{\text{HA-GFP}}$ knockin will offer the ability to analyze TLR9 trafficking biochemically at endogenous expression levels and preserve signaling capabilities. Additionally, it will allow us to identify cells that express TLR9. Indeed, determining TLR9 expression in cells other than B cells, dendritic cells and macrophages, like intestinal epithelial cells, have been difficult and controversial. Moreover, for the first time, we will be able to visualize of any dynamic changes in endogenous TLR9 expression during disease states or infection. In addition, understanding the regulatory molecules that control endogenous TLR9 trafficking will be possible through genetic ablation, such as crossing our reporter to $unc93b1^{3d/3d}$ or $ap3mb1^{pepe}$, which have defects in UNC93B1 and AP-3, respectively.

To further understand the functional relationship of UNC93B1 and the TLRs it has been shown to control (TLRs 3, 7, 8, 9, 11, 12, and 13), it will be important to develop methods to

identify the determinants on UNC93B1 required for its own trafficking as well as for TLR trafficking. To date, it has been difficult to uncouple the two. Indeed, it seems likely that proper trafficking of UNC93B1 is required to traffic TLRs out of the ER to their proper compartments [91]. UNC93B1 is a twelve pass transmembrane protein with N-and C-terminal ends predicted to face the cytosol [92]. Our previous studies determined that UNC93B1 exited the ER and entered the Golgi by detecting EndoH resistant modified glycans on UNC93B1 [158]. The H412R mutation prevents exit from the ER but also disrupts interaction with TLRs [158]. Thus, the two-fold defect in H412R cannot distinguish the role of ER exit and interaction for its function. Additionally, whether the dependency on UNC93B1 can be uncoupled at later stages beyond ER export remains an important question. Indeed, determinants necessary for trafficking beyond the ER have been identified. For example, the YxxΦ motif at the C-terminus of UNC93B1 prevents TLR9 from accessing endosomes in a post-Golgi step via AP-2 complex recruitment [158]. Additionally, it is unclear whether other regulatory mechanisms are in place to promote UNC93B1-dependent trafficking. Phosphorylation and ubiquitination are all post-translational modifications that may influence UNC93B1 trafficking and interaction with TLRs. Thus, it will be necessary to screen UNC93B1 to gain insight to these potential regulatory mechanisms.

Here I describe rapid assays to determine the consequences of UNC93B1 mutations on TLR trafficking and function. To do so, we utilized easily manipulated systems to monitor trafficking using transient transfection. We have set up two in vitro assays to monitor the trafficking of several TLRs in HEK293T cells as well as a complementary system in MEFs. Additionally, we describe the generation of selective mutations in UNC93B1 and screening for function in TLR9 trafficking. Future studies can use these assays to screen unbiased mutations of UNC93B1 generated from error-prone PCR or scanning alanine mutations for their effect UNC93B1-dependent TLR trafficking. Thus, the genetic and biochemical tools describe here will greatly enhance our understanding of the relationship between UNC93B1 and TLRs.

## Results

### TLR9 knock-in construct design

We engineered a reporter construct to include C-terminally tagged TLR9 with a HA epitope and downstream IRES GFP (Figure 5.1A). The endogenous stop codon was removed and replaced with an HA followed by a stop codon. This construct will utilize the endogenous gene regulatory elements at the *tlr9* locus for expression (Figure 5.1B). The HA epitope tag will enable detection of TLR9 with an anti-HA antibody and the GFP reporter can be detected by flow cytometry or microscopy to identify TLR9 expressing cells.

### $Tlr9^{HA\text{-}GFP}$ targeted allele and southern analysis

We have successfully targeted JM8.N4 embryonic stem cells from C57BL/6N mice [159] with our initial construct. Targeting efficiency at this locus was over 80% in several independent attempts. This may be due to the strong sequence homology of the targeting construct over exon 2 and large homology arms of ~4-5kB. The targeting was confirmed by southern analysis using a SpeI digest and the 5' probe, 3' probe, and internal "NEO" probe targeting the neomycin resistance gene (Figure 5.1B, C). We currently have several successful germline transmitted mice (Figure 5.1D). We will cross these mice to eIIa-Cre transgenic mouse, which expresses Cre at an early stage prior to embryo implantation. Several crosses will be required to subsequently lose the Cre transgene and ensure germline transmission of the deleted NEO. Of note, this deletion will leave a loxP scar between the TLR9-HA and the IRES but should have no impact on the expression of the transcript and translation of both genes. Neo deletion can be detected by southern analysis due to the change in expected size of the 3' probe and absence of NEO probe detection (Figure 5.1B).

### UNC93B1 dependent CD4-TLR trafficking

Although the use of 3d immortalized macrophages has been the most physiological system in our overexpression studies, we developed several other methods to look at trafficking and function of TLRs in the presence of UNC93B1. We generated CD4-TLR chimeras containing the ectodomain of CD4 fused to the transmembrane and entire cytosolic region of each TLR. For reasons we do not understand, co-expression of endosomal CD4-TLR chimeras and UNC93B1 results in cell surface localization of CD4-TLRs in HEK293Ts, which does not occur with full-length TLRs. This may be due to the differences in glycosylation of the CD4 molecule or the nature of a transient overexpression system in HEK293Ts. Regardless, this surface localization is only detected in the presence of UNC93B1. A fluorophore conjugated antibody against CD4 is used to determine surface localization and intracellular localization after permeabilization (Figure 5.2A). As show in Figure 5.2B, CD4-TLR surface localization is readily detected in the presence of WT UNC93B1 but not H412R. We can further confirm this by western blotting for CD4-TLR chimera and look for the presence of EndoH resistant forms (data not shown). Thus, overexpression of UNC93B1 can induce trafficking of CD4-TLRs and this provides a useful tool to detect trafficking of TLRs out of the ER in a UNC93B1 dependent manner. We have used this assay to detect differences between UNC93B1 mutants such as D34A and Y539A compared to

WT (data not shown). While UNC93B1-D34A has reduced CD4-TLR9 trafficking, UNC93B1-Y539A accumulates CD4-TLR9 at the surface, reflecting the phenotypes seen in the presence of full-length TLR9 (data not shown). Additionally, using this system, we are able to assay all endosomal TLRs and determined their dependence on UNC93B1 (Figure 5.2B). This latter point is important because UNC93B1 exhibits differential control several TLRs [158].

**Monitoring full-length UNC93B1-dependent TLR trafficking in HEK293Ts and MEFs**

Transducing macrophages requires viral packaging and cell sorting, which can introduce unnecessary lag time to screen mutations. Thus, we transiently express TLRs 3, 7 and 9 with UNC93B1 and visualized trafficking by monitoring cleaved forms of the receptors in HEK293Ts. Unlike macrophages with a predominant cleaved receptor pool, HEK293Ts generate a small, cleaved pool relative to the ER pool only in the presence of ectopically expressed UNC93B1. This difference between macrophages and 293Ts may be due to the lack of certain proteases or reduced acidic compartments as compared to macrophages. Cleaved TLR9 occurs only in the presence of WT UNC93B1 but not H412R in transient transfected HEK293Ts (Figure 5.2C). Additionally, we treated lysates with EndoH glycosidase and could visualize both the EndoH resistant full-length precursor form and cleaved form of TLR9 (Figure 5.2C). Of note, the mobility of the aforementioned forms is different from that seen in macrophages; the precursor and ER forms are not as readily resolved in HEK293Ts as in macrophages. Regardless, this assay is a sensitive method to reveal effects of different UNC93B1 mutations. For example, we can detect the same effect of the UNC93B1-Y539A mutant on TLR9 trafficking in 293Ts as in macrophages. Indeed, UNC93B1-Y539A prevents endocytosis of TLR9 causing accumulation of the precursor form and lack of a cleaved form of TLR9 in HEK293Ts (Figure 5.2D). These experiments were conducted in a 24-well format however they may be reduced to 48- or 96-well formats for more rapid screening.

We are able to conduct similar experiments in mouse embryonic fibroblasts (MEFs) however expression of TLR9 and UNC93B1 are only achieved through retroviral transduction. MEFs are readily transducible (~90%) and do not require sorting as in macrophage cell lines. Because MEFs do not express TLRs or UNC93B1, they can be used as an empty "vessel" to express combinations of TLRs and UNC93B1 and determine functional consequences. Indeed, expressing TLR9 and wildtype UNC93B1 generates a TLR9 cleaved receptor, greater than that seen in 293Ts, however lower than that of macrophages (Figure 5.2E, left lanes). No cleaved TLR9 is seen in the presence of UNC93B1-H412R (Figure 5.2E, middle lanes). Similar to macrophages, treatment with EndoH reveals a precursor form in the presence of UNC93B1-WT but not UNC93B1-HR. This method can be used to detect effects of UNC93B1 mutants on TLR9 trafficking. For example, the precursor form of TLR9 in the presence of UNC93B1-Δ523 accumulates, similar to that seen in macrophages (Figure 5.2E, right lanes). Because of the efficient transducibility of MEFs, it may be possible conduct these experiments in 48- or 96-well formats for high throughput screening of mutants. Transient transfection of MEFs is also possible, but it has not been used for visualization TLR9 trafficking.

**Selective mutagenesis approach**

We have established that UNC93B1 is necessary for both ER export and post-Golgi roles for TLR trafficking. We next sought to further define the regions that are critical for these functions. We previously generated broad truncated forms of UNC93B1 to isolate any regions required for trafficking (Chapter 3, Figure 3.3; Figure 5.3, asterisks). Additionally, we made internal deletions in inner loops (Figure 5.3, orange lines). We next sought to narrow specific sites that may provide insight to the regulatory mechanisms of UNC93B1. To do so, we used a selective mutagenesis approach to mutate residues in putative regulatory sites (Figure 5.3). A list of mutations and summary of associated phenotypes are included in Table1.1.

**Transmembrane mutations**

We hypothesized that the transmembrane domains may be important for interaction between TLRs. As Brinkmann et al. reported, the transmembrane domain of TLRs is critical for the interaction with UNC93B1. Many TLR transmembranes contain charged residues (data not shown). We hypothesized that charged residues in UNC93B1 could mediate interaction between UNC93B1 and TLR transmembranes. We mutated acidic and basic residues present in UNC93B1 putative transmembrane domains (Figure 5.3) and determined their effect on TLR trafficking and trafficking by UNC93B1 itself (Table1.1).

**Putative COPII motif mutations**

Components of the COPII vesicle machinery that promote membrane budding from the ER and transit to the Golgi recognize specific motifs on cargo proteins [110]. Sec24 homologs (A, B, C, and D) have been shown to recognize common motifs. For example, human Sec24A and Sec24B have been shown to recognize D/EXD/E motifs while Sec24C and Sec24D recognition motifs like IxM [112, 113]. Other motifs include di-acidic motifs and di-hydrophobic motifs [114, 115]. We were only able to identify D/EXD/E motifs in UNC93B1 present in cytosolic facing regions of the protein. Most of the single mutations of D/EXD/E sites did not affect trafficking of UNC93B1. However, E465A and E553A yielded partial effects, suggesting that these residues may be important for efficient ER export (Table1.1). COPII motifs may be redundant and therefore, multiple D/EXD/E motifs may need to be mutated to see a full-effect.

**Potential sites of post-translational modifications, potential proline rich region and acidic cluster mutations**

Post-translation modifications, such as phosphorylation and ubiquitination, can affect the function of a protein, leading to a multitude of activating or inhibitory outcomes. We targeted sites of potential phosphorylation at tyrosine and serine residues and ubiquitination sites at lysine residues present in UNC93B1. According to (www.phosphosite.org), mouse UNC93B1 has four phosphorylation sites and four ubiquitin sites (determined by mass spectrometry).

Additionally, we determined two proline-rich regions defined by sequential $(PXX)_n$ repeats in the N and C terminal regions of UNC93B1. In the case of Nef in HIV, proline-rich residues are important for interaction with the SH3 domain of Src family kinases [160]. We attempted to disrupt the proline rich region by mutating the prolines central to the motif. Due to the nature of the structure, single mutations may not be enough to disrupt function, and may

require larger deletions. Nevertheless, we found that P527A but not P29A has a partial effect on UNC93B1 trafficking (Table1.1).

In addition to D/EXD/E acidic residues important for interaction with COPII components, an acidic cluster is present at the N-terminal region of UNC93B1. This EEEE cluster has been reported in Nef proteins and is required for interaction with PACS1 and PACS2 proteins, a set of endosomal trafficking factors [161, 162]. Nef can downregulate MHC-I in two ways, one through interaction with PACS1/2 with its acidic cluster and second through phosphorylation of MHC-I (requiring its proline rich region) and recruitment of AP-1 to enhance trafficking of MHC-I to endosomes. Attempted disruption of the acidic cluster in UNC93B1 did not result in a disruption of function, at least in our transient studies. It has yet to be determined whether this cluster is important in other systems or for other TLRs.

## Discussion

Understanding the regulatory mechanisms involved in nucleic acid TLR trafficking, such as TLR3, TLR7, and TLR9 are of great importance because of their roles in pathogenesis and autoimmune pathologies. TLR9, which senses DNA, is capable of sensing both foreign unmethylated CpG DNA from viruses and bacteria, but also capable of sensing self-DNA present in the serum from dying cells [41]. Understanding the regulation to prevent self-recognition has been under immense study. Indeed, the current paradigm is that TLR9 and other nucleic acid TLRs are sequestered in endosomal compartments to avoid the surface where self-nucleic acids can be accessed [24, 40, 80]. Endosomal residence also serves several other purposes. For one, TLR9 needs to be proteolytically cleaved to form an active receptor [24]. Second, unprotected DNA (such as that from dying cells) are quickly degraded in the acidic and DNase-rich compartments, thus ensuring that only DNA encapsulated from viral particles can reach TLR9 receptor [163]. Third, TLR9 binding has been shown to be optimal at low pH [78]. Thus, these mechanisms seem to provide a way to prevent self-DNA recognition and optimal recognition of foreign DNA. Due to a lack of endogenous antibodies, our understanding of TLR9 trafficking originates from overexpression studies using epitope tagged TLR9. Many questions are still open in TLR9 cell biology, including what other cell types express TLR9. Therefore, we generated a knock-in mouse of HA tagged TLR9 IRES-GFP to the endogenous *tlr9* locus. As this dissertation is being written, we have achieved germline transmission of the targeted allele. Subsequent breeding to eIIa-Cre transgenic mice [164], generate the final reporter construct. This mouse will provide us the opportunity to characterize various cell types that express TLR9 and monitor any changes that may occur upon stimulation. Importantly, we will, for the first time, be able to visualize TLR9 at endogenous levels in immune cell types and determine the levels of cleaved receptor in different cell types. Additionally, we will be able to do genetic studies by crossing TLR9 to different knockout mice to determine additional factors important for trafficking.

Loss of *Unc93b1* gene prevents endosomal TLRs, including all nucleic acid sensing TLRs, from exiting the ER leading to a loss of TLR activity [91, 98]. Thus, understanding the functional relationship between UNC93B1 and TLRs is important. The most useful and physiological studies conducted by our group to address this thus far have utilized *Unc93b1*$^{3d/3d}$ immortalized macrophage lines. However, these take several rounds of retroviral transduction and cell sorting which is less efficient when screening large numbers of UNC93B1 mutants. Here, we describe rapid biochemical tools to test mutants of UNC93B1 and their consequences in trafficking TLRs. We show that nucleic acid TLR trafficking as previously shown in macrophages can be recapitulated in HEK293Ts and mouse embryonic fibroblasts. Additionally, we can utilize a chimeric CD4-TLR system to assay UNC93B1-dependent trafficking to the surface. Finally, we show that UNC93B1 has many interesting amino acid residues: charged residues in the transmembrane, di-acidic motifs for COPII binding, sites for post-translational modifications, an acidic cluster, and two proline-rich regions that could mediate binding to protein factors. By isolating the region of the respective TLRs that affect trafficking dependence on UNC93B1 we may provide a clearer model of how UNC93B1 interacts and traffics these TLRs. UNC93B1 has been shown to differentially control several TLRs. We may further be able to identify UNC93B1 mutants that reveal additional differential trafficking mechanisms.

In conclusion, UNC93B1 intimately controls the trafficking of nucleic acid TLRs, understanding the precise mechanisms of how these TLRs are activated will provide better knowledge of therapeutics for autoimmune diseases or vaccines to target cancer or pathogen infection.

## Materials and Methods

### Antibodies and Reagents

The following antibodies were used for immunoblots: anti-HA as purified antibody or matrix (3F10, Roche), anti-CD4 (RM4-5, BD Biosciences), goat anti-rat-HRP (GE Healthcare). Lipofectamine-LTX reagent (Invitrogen) was used for transient transfection of plasmid DNA. OptiMEM-I (Invitrogen) was used as media to form nucleic acid complexes for transient transfections.

### Plasmid Constructs

Pfu Turbo polymerase (Agilent) was used according to manufacturer's instructions for site directed mutagenesis. Mouse stem cell virus (MSCV)-based retroviral vectors [MSCV2.2 (IRES-GFP) and MIGR2 (IRES-hCD2)] or the mammalian expression vector, pCDNA3.1, were used to express UNC93B1 and TLR9. The following epitope tags were fused to the C-terminus of UNC93B1: 3XFLAG (DYKDHDGDYKDHDIDYKDDDDK), TLR9 was fused to HA at the C-terminal end. CD4-TLR chimeras were generated in pCDNA3.1 (Invitrogen). CD4 extracellular domain (mouse 1-390 a.a.) was fused to transmembrane domain and cytosolic regions of the following TLRs and C-terminally tagged with HA: TLR4 (620-835 a.a.), TLR9 (mouse 803-1032 a.a.), TLR3 (human 691-904 a.a.), TLR7 (human 825-1049), TLR11 (mouse 703-926 a.a.) TLR13 (mouse 770-991 a.a.).

### TLR9-HA knock-in construct

The *tlr9* locus 5' and 3' homology arms were amplified by PCR from BAC RP23-107L12 and cloned into the targeting vector (pKO915-floxNeo-DTA). The IRES-GFP fragment was subcloned from the pIRES-eGFP plasmid (Clonetech) after deletion of the SV40 PolyA tail. The construct was linearized with PvuI and electroporated into JM8.N4ES cells.

### Cell lines and Tissue culture conditions

HEK293T cells were obtained from American Type Culture Collection (ATCC). GP2-293 packaging cell lines were obtained from Clonetech. Phoenix-Eco (ØNX-E ) cells were provided by G. Nolan, Stanford University. Mouse embryonic fibroblasts (MEFs) are TLR2/TLR4 double knockout genotype immortalized with SV40 large T-antigen. The above cell lines were cultured in DMEM supplemented with 10% (vol/vol) FCS, L-glutamine, penicillin-streptomycin, sodium pyruvate, and HEPES (pH 7.2) (Invitrogen).

### Retroviral transduction

For retroviral transduction of immortalized macrophages, VSV-G-psuedotyped retrovirus was made in GP2-293 packaging cells (Clontech). GP2-293 cells were transfected with retroviral vectors and pVSV-G using Lipofectamine LTX reagent. 24 hours post-transfection, cells were incubated at 32°C. 48 hours post-transfection viral supernatant (with polybrene at final 5mg/ml) and was used to infect target cells overnight at 32°C and protein expression was checked 48 hours later. Target cells were sorted on MoFlo Beckman Coulter Sorter to match expression.

### Transient transfection

Transient transfection in HEK293T cells were performed in OptiMem (Invitrogen) with LTX transfection reagent (Invitrogen) according to manufacturer's guidelines and a ratio of 1:1 TLR and UNC93B1 plasmid DNA. Lysates were harvested 24 hours later.

**Lysate preparation, SDS-PAGE, Immunoblotting**
Cell lysates were prepared with TNT buffer (20 mM Tris [pH 8.0], 200 mM NaCl, 1% Triton X-100, 4mM EDTA and supplemented with EDTA-free complete protease inhibitor cocktail (Roche)) unless otherwise noted. For immunoprecipitations, lysates were incubated with anti-HA matrix, and precipitated proteins were subjected to EndoH assay then denatured in SDS-PAGE dye separated by SDS-PAGE (Tris-HCl self cast gels or Bio-Rad TGX precast gels), and probed by the indicated antibodies.

**Endoglycosidase H (EndoH) assay**
Immunoprecpitated proteins or total lysate were denatured and treated with Endoglycosidase H or PNGase F according to manufacturer's instructions. All enzymes and buffers were purchased from New England Biolabs.

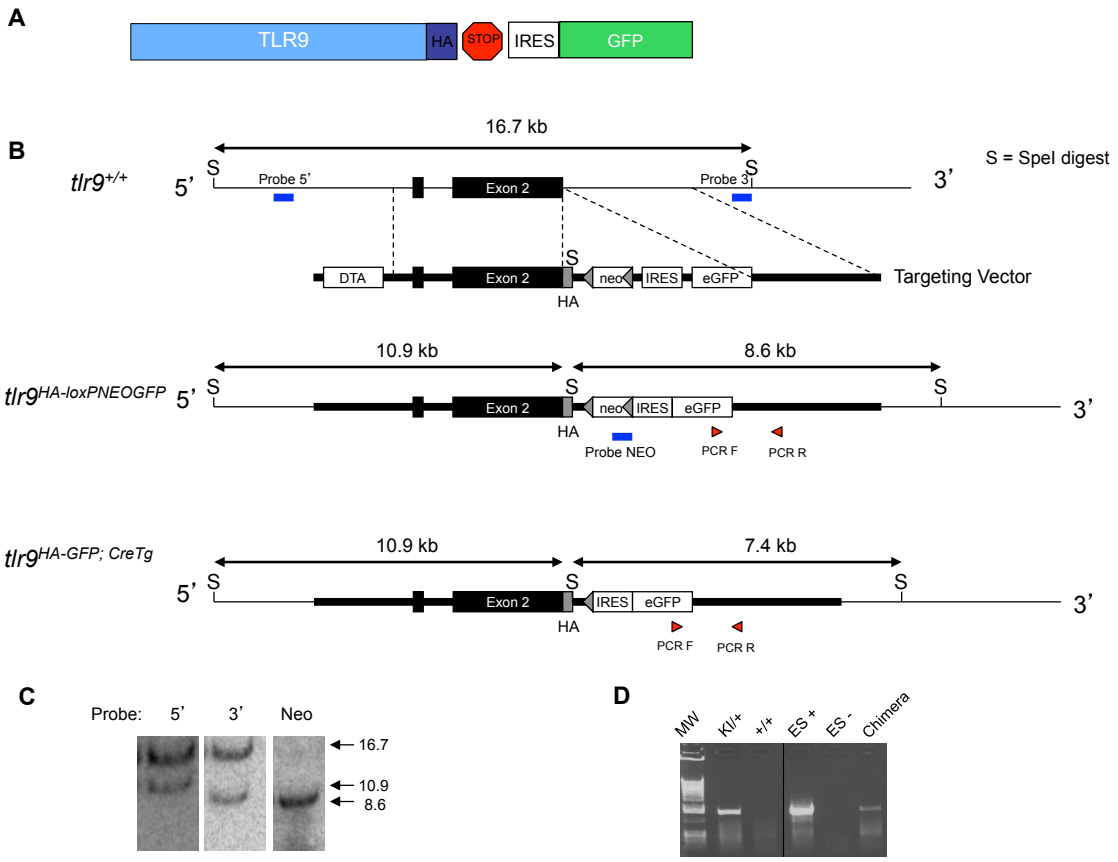


**Figure 5.1 tlr9$^{HA\text{-}GFP}$ knock-in targeting strategy**
(A) Schematic of TLR9HA-GFP reporter final expressed construct in the mouse. TLR9 is tagged with an HA epitope at the C-terminus. Downstream of TLR9-HA is an IRES-GFP on the same transcript. (B) Targeting strategy for tlr9$^{HA\text{-}GFP}$ knock-in at the tlr9 endogenous locus. SpeI digest strategy for southern analysis. Blue lines represent probes 5' and 3' of targeted locus and an internal NEO probe. Expected size bands are indicated after initial knock in ES cells (tlr9$^{HA\text{-}loxNEOGFP}$) and after crossing with EIIA-Cre Tg to generate the final reporter mouse (tlr9$^{HA\text{-}GFP}$). (C) Representative southern analysis using all three probes on a targeted of ES cell. (D) Representative PCR analysis to genotype germline transmitted mice. KI/+ is a germline transmitted mouse compared to +/+ (wildtype). ES cells and Chimera mouse are used as a control.

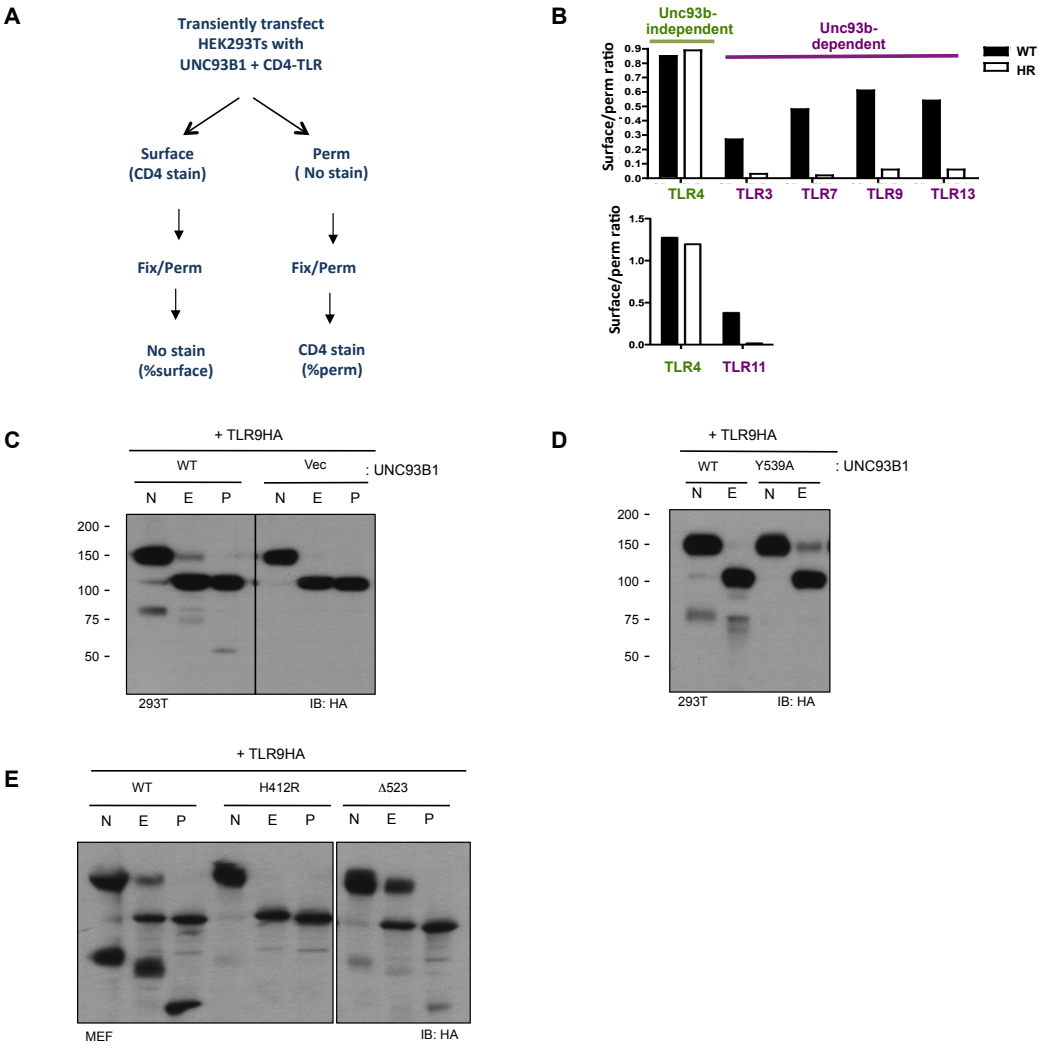
A
Transiently transfect
HEK293Ts with
UNC93B1 + CD4-TLR
Surface
(CD4 stain)
Perm
( No stain)
Fix/Perm
Fix/Perm
No stain
(%surface)
CD4 stain
(%perm)
B
Unc93b-
independent
Unc93b-
dependent
WT
HR
Surface/perm ratio
TLR4
TLR3
TLR7
TLR9
TLR13
Surface/perm ratio
TLR4
TLR11
C
+ TLR9HA
WT
Vec
: UNC93B1
N E P N E P
200 -
150 -
100 -
75 -
50 -
293T
IB: HA
D
+ TLR9HA
WT
Y539A
: UNC93B1
N E N E
200 -
150 -
100 -
75 -
50 -
293T
IB: HA
E
+ TLR9HA
WT
H412R
Δ523
N E P N E P N E P
MEF
IB: HA

**Figure 5.2**

**Figure 5.2 Assays for UNC93B1 function in TLR trafficking**
(A, B) CD4-TLR flow cytometry assay in 293Ts. A sensitive method to determine TLR trafficking out of ER and post-Golgi. (A) HEK293Ts were transiently transfected with CD4-TLRs (a chimeric protein with CD4 ectodomain and TLR transmembrane and cytosolic region) and UNC93B1. Cell population is split into "surface" and "perm" groups. "Surface" is surface stained with anti-CD4-PE and while "perm" is unstained prior to fix and permeablization. "Perm" group is stained with anti-CD4-PE after fix/perm. The ratio of surface/perm is calculated to represent the amount of CD4-TLR that has exited the ER and normalized to the total amount of CD4-TLR in the cell. (B) CD4-TLRs, 3, 7, 9, 11, and 13 exit the ER in a UNC93B1 dependent way. Surface CD4-TLR can traffic independent of UNC93B1. The surface/perm ratio of CD4 staining is graphed. (C, D) TLR9 traffics in transient transfection of HEK293Ts as in macrophages when co-expressed with UNC93B1. HEK293Ts were transiently transfected with TLR9-HA and UNC93B1. Whole cell lysates were treated with EndoH (E), PNGaseF (P) or left untreated (-), and visualized by anti-HA immunoblot. (C) WT but not H412R UNC93B1 promotes trafficking of TLR9. (D) Y539A affects the post-Golgi trafficking of TLR9-HA, similar to the phenotype seen in *3d* iMacs. (F) Mouse embryonic fibroblasts were transduced with TLR9-HA and UNC93B1. TLR9-HA was immunoprecipitated from MEFs expressing UNC93B1-WT, -H412R, or Δ523, treated with EndoH (E), PNGaseF (P) or left untreated (-), and visualized by anti-HA immunoblot. (F) NF-kB luciferase reporter system in 293Ts and MEFs to analyze UNC93B1 mutants.

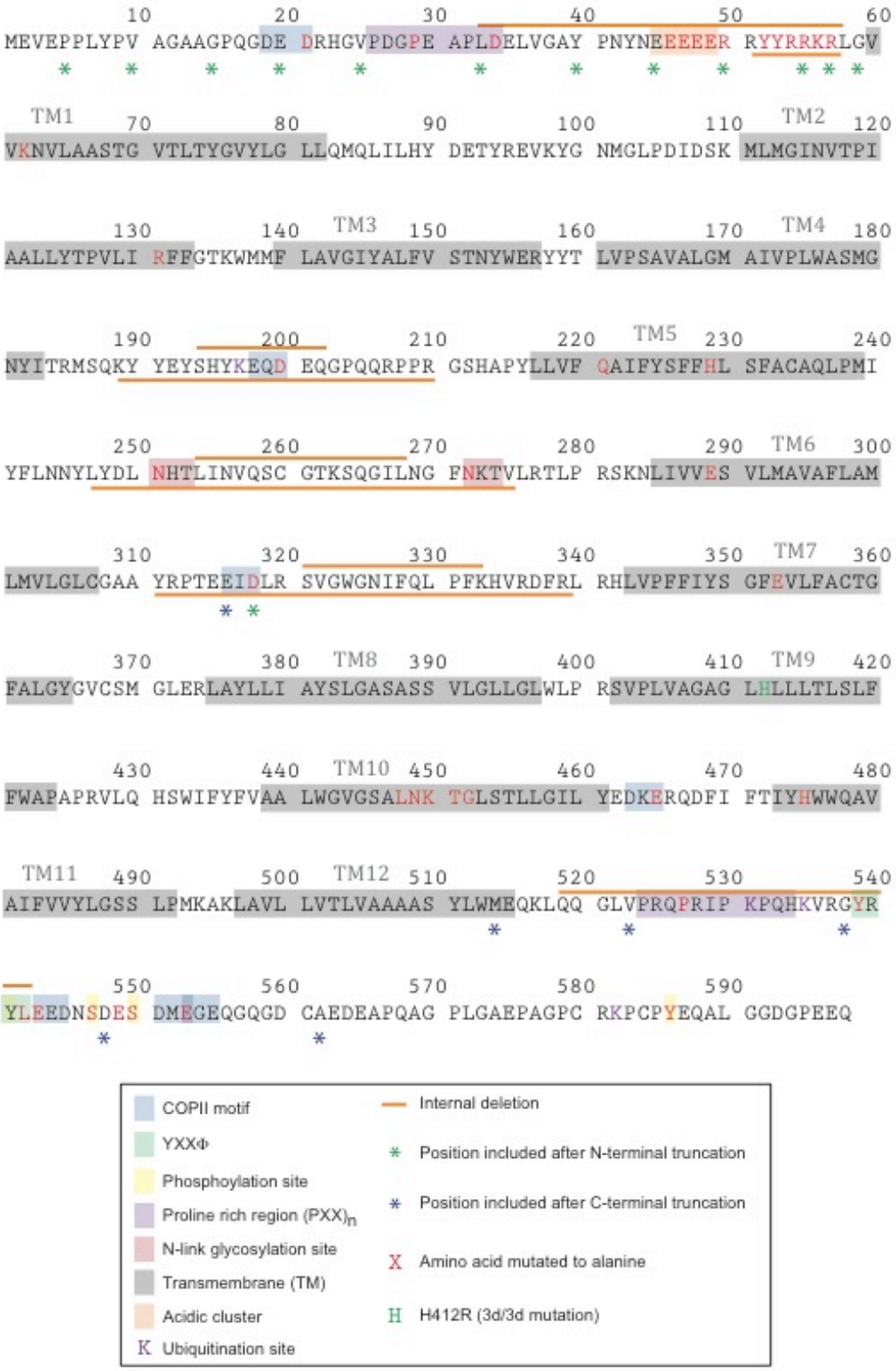


**Figure 5.3 Protein sequence of mouse UNC93B1**

Map of mouse UNC93B1 protein sequence. Shaded areas indicated potential motifs. Asterisks indicated N- or C- terminal truncations. Orange line indicates internal deletion mutants. Red lettering indicated single amino acid mutagenesis to alanine.

| UNC93B1 Mutation | Phenotypes* |
|---|---|
| Δ5N | normal TLR9 trafficking |
| Δ10N | normal TLR9 trafficking |
| Δ15N | normal TLR9 trafficking |
| Δ20N | normal TLR9 trafficking |
| Δ25N | normal TLR9 trafficking |
| Δ33N | normal TLR9 trafficking |
| Δ40N | normal TLR9 trafficking |
| Δ45N | partial effect on TLR9 trafficking |
| Δ50N | Significant loss of TLR9 trafficking, loss of UNC93B1 trafficking |
| Δ55N | loss of TLR9 trafficking, loss of UNC93B1 trafficking |
| Δ57N | loss of TLR9 trafficking, loss of UNC93B1 trafficking |
| Δ59N | loss of TLR9 trafficking, probably misfolded |
| Δ88N | loss of TLR9 trafficking; probably misfolded |
| Δ318N | loss of TLR9 trafficking; probably misfolded |
| Δ316C | loss of TLR9 trafficking; probably misfolded |
| Δ514C | loss of TLR9 trafficking; probably misfolded |
| Δ518C | enhanced TLR9 precursor, lack cleaved TLR9 receptor |
| Δ520C | enhanced TLR9 precursor, lack cleaved TLR9 receptor |
| Δ523C | enhanced TLR9 precursor, lack cleaved TLR9 receptor |
| Δ526C | enhanced TLR9 precursor, lack cleaved TLR9 receptor |
| Δ528C | enhanced TLR9 precursor, lack cleaved TLR9 receptor |
| Δ532C | enhanced TLR9 precursor, lack cleaved TLR9 receptor |
| Δ538C | enhanced TLR9 precursor, lack cleaved TLR9 receptor |
| Δ548C | normal, slight loss in amount of TLR9 cleaved receptor |
| Δ562C | normal TLR9 trafficking |
| Δ33-53 | loss of TLR9 trafficking, loss of UNC93B1 trafficking |
| Δ33-55 | loss of TLR9 trafficking, loss of UNC93B1 trafficking |
| Δ52-57 | loss of TLR9 trafficking, loss of UNC93B1 trafficking |
| Δ189-210 | loss of TLR9 trafficking |
| Δ194-202 | partial loss of cleaved TLR9 |
| Δ247-275 | loss of TLR9 trafficking |
| Δ254-268 | loss of TLR9 trafficking |
| Δ311-339 | loss of TLR9 trafficking |
| Δ320-333 | loss of TLR9 trafficking |
| Δ519-542 | enhanced TLR9 precursor, lack cleaved TLR9 receptor |
| a2C (KHILFRRRRRGFRQ) | loss of TLR9 and UNC93B1 trafficking |
| KDEL | normal TLR9 trafficking |
| KKAG | normal TLR9 trafficking |
| RKRS | normal TLR9 trafficking |
| CD3e (DLYSGLWIQT) | normal TLR9 trafficking |
| SV1 (CVLF) | normal TLR9 trafficking |

**Table 5.1 List of truncation mutants and ER retained UNC93B1**
*Red indicates effect on TLR9 and Blue indicates enhanced precursor effect

| UNC93B1 Mutation | Phenotypes* |
|---|---|
| D21A | normal TLR9 trafficking |
| P29A | normal TLR9 trafficking |
| D34A | impaired TLR9 trafficking, normal TLR7 trafficking, enhanced TLR7 signaling |
| E46A/E47A | normal TLR9 trafficking |
| EEEE/AAAA (46-49) | normal TLR9 trafficking |
| Y52A | normal TLR9 trafficking |
| Y53A | normal TLR9 trafficking |
| R54A | normal TLR9 trafficking |
| R55A | normal TLR9 trafficking |
| K56A | normal TLR9 trafficking |
| R57A | normal TLR9 trafficking |
| K62A | normal TLR9 trafficking |
| R131A | loss of TLR9 trafficking |
| D200A | normal TLR9 trafficking |
| Q221A | normal TLR9 trafficking |
| N251A | partial defect TLR9, dominant N- glycosylation site (Endo resistant) |
| N272A | partial defect TLR9 |
| E289A | normal TLR9 trafficking |
| D318A | normal TLR9 trafficking |
| E353A | loss of TLR9 trafficking |
| H412A | nonfunctional UNC93B1 |
| L448A | normal TLR9 trafficking |
| N449A | slight effect on TLR9 |
| K450A | partial effect on TLR9 |
| T451A | normal TLR9 trafficking |
| G452A | normal TLR9 trafficking |
| E465A | normal TLR9 trafficking |
| H475A | normal TLR9 trafficking |
| P527A | partial effect on TLR9 |
| Y539A | enhanced TLR9 precursor, lack cleaved TLR9 receptor |
| Y539F | enhanced TLR9 precursor, normal cleaved TLR9 receptor |
| L542A | enhanced TLR9 precursor, partial loss cleaved TLR9 receptor |
| E543A | partial effect on TLR9 and UNC93B1 trafficking |
| S547A | normal TLR9 trafficking |
| S550A | normal TLR9 trafficking |
| E553A | partial effect on TLR9 UNC93B1 trafficking |
| Y586A | normal TLR9 trafficking |

**Table 5.2 List of point mutations in UNC93B1**
*Red indicates effect on TLR9 and Blue indicates enhanced precursor effect

## Conclusion

In this dissertation, I have covered the history of innate immunity and Toll-like receptors (TLRs) and highlighted the critical roles of TLRs in immunity. Additionally, I have described important aspects of previously known endosomal TLR trafficking studies. The purpose of my work was to investigate the molecular mechanisms of UNC93B1 to better understand the control of nucleic aid sensing TLRs. Our studies have shed light on mechanisms of UNC93B1 both at the level of ER export and post-ER control. Additional roles of UNC93B1 have yet to be determined; however, because UNC93B1 associates with TLRs from ER to endolysosome, it is likely that UNC93B1 plays important roles at additional steps along the endolysosomal trafficking route. For example, does UNC93B1 help TLR9 achieve access to the surface? Does UNC93B1 participate in trafficking TLR7 from Golgi to endosome? As we gain greater insight to the various mechanisms of TLR trafficking, we must keep in mind that each TLR may use differential mechanisms to achieve proper localization. Indeed, UNC93B1 seems capable of using different determinants to traffic each TLR; however, this aspect may only be revealed by mutating important residues on UNC93B1. Certainly, it is possible that UNC93B1 interacts with each TLR by using different residues and allows for recruitment of different factors. Or perhaps UNC93B1 and TLRs both contain sorting signals and the UNC93B1-TLR complex is sorted based on the net result of all the sorting signals present. Additionally, we must be open to the idea that several mechanisms may be in place to achieve the same purpose. Multiple and redundant mechanisms to achieve proper sorting may be likely because of the potential for nucleic acid sensing TLRs to recognize self-ligands if improperly controlled. As we proceed, future studies will need to focus on a unifying model to better understand ligand binding, receptor activation, and receptor trafficking of nucleic acid sensing TLRs. These may be achieved through studying the TLR protein or studying regulatory factors such as UNC93B1 or other still unidentified factors. Significant progress in the TLR cell biology field has been met in the last 10 years, and it will be exciting to see the progress made in the next decade.

## References


1. Janeway, C.A., *Approaching the Asymptote? Evolution and Revolution in Immunology.* Cold Spring Harbor Symposia on Quantitative Biology, 1989. **54**(0): p. 1-13.
2. Lemaitre, B., *The road to Toll.* Nature reviews Immunology, 2004. **4**(7): p. 521-527.
3. Lemaitre, B., et al., *The dorsoventral regulatory gene cassette spätzle/Toll/cactus controls the potent antifungal response in Drosophila adults.* Cell, 1996. **86**(6): p. 973-983.
4. Medzhitov, R., P. Preston-Hurlburt, and C.A. Janeway, *A human homologue of the Drosophila Toll protein signals activation of adaptive immunity.* Nature, 1997. **388**(6640): p. 394-397.
5. Poltorak, A., et al., *Defective LPS signaling in C3H/HeJ and C57BL/10ScCr mice: mutations in Tlr4 gene.* Science, 1998. **282**(5396): p. 2085-8.
6. Wagner, H., *Innate immunity's path to the Nobel Prize 2011 and beyond.* European Journal of Immunology, 2012. **42**(5): p. 1089-1092.
7. Kawai, T. and S. Akira, *The role of pattern-recognition receptors in innate immunity: update on Toll-like receptors.* Nature Publishing Group, 2010. **11**(5): p. 373-384.
8. Akira, S., S. Uematsu, and O. Takeuchi, *Pathogen Recognition and Innate Immunity.* Cell, 2006. **124**(4): p. 783-801.
9. Iwasaki, A. and R. Medzhitov, *Toll-like receptor control of the adaptive immune responses.* Nature Immunology, 2004. **5**(10): p. 987-995.
10. Marques, R. and I.G. Boneca, *Expression and functional importance of innate immune receptors by intestinal epithelial cells.* Cellular and molecular life sciences : CMLS, 2011. **68**(22): p. 3661-73.
11. Asselin-Paturel, C., *Production of type I interferons: plasmacytoid dendritic cells and beyond.* Journal of Experimental Medicine, 2005. **202**(4): p. 461-465.
12. Song, D.H. and J.-O. Lee, *Sensing of microbial molecular patterns by Toll-like receptors.* Immunological reviews, 2012. **250**(1): p. 216-229.
13. Funami, K., et al., *The cytoplasmic 'linker region' in Toll-like receptor 3 controls receptor localization and signaling.* International Immunology, 2004. **16**(8): p. 1143-54.
14. Choe, J., *Crystal Structure of Human Toll-Like Receptor 3 (TLR3) Ectodomain.* Science, 2005. **309**(5734): p. 581-585.
15. Jin, M.S., et al., *Crystal Structure of the TLR1-TLR2 Heterodimer Induced by Binding of a Tri-Acylated Lipopeptide.* Cell, 2007. **130**(6): p. 1071-1082.
16. Kang, J.Y., et al., *Recognition of Lipopeptide Patterns by Toll-like Receptor 2-Toll-like Receptor 6 Heterodimer.* Immunity, 2009. **31**(6): p. 873-884.
17. Liu, L., et al., *Structural Basis of Toll-Like Receptor 3 Signaling with Double-Stranded RNA.* Science, 2008. **320**(5874): p. 379-381.
18. Lu, J. and P.D. Sun, *The Structure of the TLR5-Flagellin Complex: A New Mode of Pathogen Detection, Conserved Receptor Dimerization for Signaling.* Science Signaling, 2012. **5**(216): p. pe11-pe11.
19. Park, B.S., et al., *The structural basis of lipopolysaccharide recognition by the TLR4–MD-2 complex.* Nature, 2009. **458**(7242): p. 1191-1195.

20. Tanji, H., et al., *Structural Reorganization of the Toll-Like Receptor 8 Dimer Induced by Agonistic Ligands.* Science, 2013. **339**(6126): p. 1426-1429.
21. Latz, E., et al., *Ligand-induced conformational changes allosterically activate Toll-like receptor 9.* Nature Immunology, 2007. **8**(7): p. 772-779.
22. Latz, E., et al., *TLR9 signals after translocating from the ER to CpG DNA in the lysosome.* Nature Immunology, 2004. **5**(2): p. 190-198.
23. Ewald, S.E., et al., *Nucleic acid recognition by Toll-like receptors is coupled to stepwise processing by cathepsins and asparagine endopeptidase.* Journal of Experimental Medicine, 2011. **208**(4): p. 643-651.
24. Ewald, S.E., et al., *The ectodomain of Toll-like receptor 9 is cleaved to generate a functional receptor.* Nature, 2008. **456**(7222): p. 658-662.
25. Kaparakis, M., D.J. Philpott, and R.L. Ferrero, *Mammalian NLR proteins; discriminating foe from friend.* Immunology and cell biology, 2007. **85**(6): p. 495-502.
26. Kaisho, T. and S. Akira, *Toll-like receptor function and signaling.* Journal of Allergy and Clinical Immunology, 2006. **117**(5): p. 979-987.
27. Kagan, J.C., et al., *TRAM couples endocytosis of Toll-like receptor 4 to the induction of interferon-β.* Nature Immunology, 2008. **9**(4): p. 361-368.
28. Zanoni, I., et al., *CD14 Controls the LPS-Induced Endocytosis of Toll-like Receptor 4.* Cell, 2011. **147**(4): p. 868-880.
29. Honda, K., et al., *Spatiotemporal regulation of MyD88-IRF-7 signalling for robust type-I interferon induction.* Nature, 2005. **434**(7036): p. 1035-1040.
30. Sasai, M., M.M. Linehan, and A. Iwasaki, *Bifurcation of Toll-Like Receptor 9 Signaling by Adaptor Protein 3.* Science, 2010. **329**(5998): p. 1530-1534.
31. Barbalat, R., et al., *Toll-like receptor 2 on inflammatory monocytes induces type I interferon in response to viral but not bacterial ligands.* Nature Immunology, 2009. **10**(11): p. 1200-7.
32. Arpaia, N. and G.M. Barton, *Toll-like receptors: key players in antiviral immunity.* Current Opinion in Virology, 2011. **1**(6): p. 447-454.
33. Coban, C., et al., *Immunogenicity of whole-parasite vaccines against Plasmodium falciparum involves malarial hemozoin and host TLR9.* Cell host & microbe, 2010. **7**(1): p. 50-61.
34. Koblansky, A.A., et al., *Recognition of Profilin by Toll-like Receptor 12 Is Critical for Host Resistance to Toxoplasma gondii.* Immunity, 2013. **38**(1): p. 119-130.
35. Oldenburg, M., et al., *TLR13 Recognizes Bacterial 23S rRNA Devoid of Erythromycin Resistance-Forming Modification.* Science, 2012. **337**(6098): p. 1111-1115.
36. Pifer, R., et al., *UNC93B1 Is Essential for TLR11 Activation and IL-12-dependent Host Resistance to Toxoplasma gondii.* Journal of Biological Chemistry, 2011. **286**(5): p. 3307-3314.
37. Shi, Z., et al., *A Novel Toll-like Receptor That Recognizes Vesicular Stomatitis Virus.* Journal of Biological Chemistry, 2011. **286**(6): p. 4517-4524.
38. Yanai, H., et al., *HMGB proteins function as universal sentinels for nucleic-acid-mediated innate immune responses* Nature, 2009. **461**(7269): p. 99-103.
39. Barton, G.M. and J.C. Kagan, *A cell biological view of Toll-like receptor function: regulation through compartmentalization.* Nature reviews Immunology, 2009. **9**(8): p. 535-542.

40. Barton, G.M., J.C. Kagan, and R. Medzhitov, *Intracellular localization of Toll-like receptor 9 prevents recognition of self DNA but facilitates access to viral DNA.* Nature Immunology, 2006. **7**(1): p. 49-56.
41. Ewald, S.E. and G.M. Barton, *Nucleic acid sensing Toll-like receptors in autoimmunity.* Current Opinion in Immunology, 2011. **23**(1): p. 3-9.
42. Lande, R., et al., *Plasmacytoid dendritic cells sense self-DNA coupled with antimicrobial peptide.* Nature, 2007. **449**(7162): p. 564-9.
43. Marshak-Rothstein, A., *Toll-like receptors in systemic autoimmune disease.* Nature reviews Immunology, 2006. **6**(11): p. 823-835.
44. Napirei, M., et al., *Features of systemic lupus erythematosus in Dnase1-deficient mice.* Nature genetics, 2000. **25**(2): p. 177-81.
45. Christensen, S.R. and M.J. Shlomchik, *Regulation of lupus-related autoantibody production and clinical disease by Toll-like receptors.* Seminars in immunology, 2007. **19**(1): p. 11-23.
46. Subramanian, S., et al., *A Tlr7 translocation accelerates systemic autoimmunity in murine lupus.* Proceedings of the National Academy of Sciences, 2006. **103**(26): p. 9970-9975.
47. Marshall-Clarke, S., et al., *Polyinosinic acid is a ligand for toll-like receptor 3.* The Journal of biological chemistry, 2007. **282**(34): p. 24759-24766.
48. Alexopoulou, L., et al., *Recognition of double-stranded RNA and activation of NF-κB by Toll-like receptor 3.* Nature, 2001. **413**(6857): p. 732-738.
49. Barbalat, R., et al., *Nucleic Acid Recognition by the Innate Immune System.* Annual review of immunology, 2011. **29**(1): p. 185-214.
50. Barton, G.M., *Viral recognition by Toll-like receptors.* Seminars in immunology, 2007. **19**(1): p. 33-40.
51. Zhang, S.-Y., et al., *TLR3 immunity to infection in mice and humans.* Current Opinion in Immunology, 2013. **25**(1): p. 19-33.
52. Reinert, L.S., et al., *TLR3 deficiency renders astrocytes permissive to herpes simplex virus infection and facilitates establishment of CNS infection in mice.* Journal of Clinical Investigation, 2012. **122**(4): p. 1368-1376.
53. Lafaille, F.G., et al., *Impaired intrinsic immunity to HSV-1 in human iPSC-derived TLR3-deficient CNS cells.* Nature, 2013. **491**(7426): p. 769-773.
54. Nishiya, T., et al., *TLR3 and TLR7 are targeted to the same intracellular compartments by distinct regulatory elements.* The Journal of biological chemistry, 2005. **280**(44): p. 37107-37117.
55. Kajita, E., T. Nishiya, and S. Miwa, *The transmembrane domain directs TLR9 to intracellular compartments that contain TLR3.* Biochemical and Biophysical Research Communications, 2006. **343**(2): p. 578-584.
56. Pohar, J., et al., *The Role of UNC93B1 Protein in Surface Localization of TLR3 Receptor and in Cell Priming to Nucleic Acid Agonists.* Journal of Biological Chemistry, 2013. **288**(1): p. 442-454.
57. Qi, R., D. Singh, and C.C. Kao, *Proteolytic Processing Regulates Toll-like Receptor 3 Stability and Endosomal Localization.* Journal of Biological Chemistry, 2012. **287**(39): p. 32617-32629.
58. Toscano, F., et al., *Cleaved/Associated TLR3 Represents the Primary Form of the Signaling Receptor.* The Journal of Immunology, 2013. **190**(2): p. 764-773.

59. Fukuda, K., et al., *Modulation of Double-stranded RNA Recognition by the N-terminal Histidine-rich Region of the Human Toll-like Receptor 3.* Journal of Biological Chemistry, 2008. **283**(33): p. 22787-22794.
60. Qi, R., et al., *Secretion of the Human Toll-like Receptor 3 Ectodomain Is Affected by Single Nucleotide Polymorphisms and Regulated by Unc93b1.* Journal of Biological Chemistry, 2010. **285**(47): p. 36635-36644.
61. Lund, J.M., et al., *Recognition of single-stranded RNA viruses by Toll-like receptor 7.* Proceedings of the National Academy of Sciences of the United States of America, 2004. **101**(15): p. 5598-5603.
62. Hemmi, H., et al., *Small anti-viral compounds activate immune cells via the TLR7 MyD88–dependent signaling pathway.* Nature Immunology, 2002. **3**(2): p. 196-200.
63. Yu, P., et al., *Nucleic acid-sensing Toll-like receptors are essential for the control of endogenous retrovirus viremia and ERV-induced tumors.* Immunity, 2012. **37**(5): p. 867-79.
64. Gorden, K.B., et al., *Synthetic TLR agonists reveal functional differences between human TLR7 and TLR8.* Journal of immunology (Baltimore, Md. : 1950), 2005. **174**(3): p. 1259-1268.
65. Heil, F., et al., *The Toll-like receptor 7 (TLR7)-specific stimulus loxoribine uncovers a strong relationship within the TLR7, 8 and 9 subfamily.* European Journal of Immunology, 2003. **33**(11): p. 2987-2997.
66. Heil, F., *Species-Specific Recognition of Single-Stranded RNA via Toll-like Receptor 7 and 8.* Science, 2004. **303**(5663): p. 1526-1529.
67. Liu, T., et al., *Toll-like receptor 7 mediates pruritus.* Nature neuroscience, 2010. **13**(12): p. 1460-2.
68. Jurk, M., et al., *Human TLR7 or TLR8 independently confer responsiveness to the antiviral compound R-848.* Nature Immunology, 2002. **3**(6): p. 499.
69. Gorden, K.K.B., et al., *Cutting edge: activation of murine TLR8 by a combination of imidazoquinoline immune response modifiers and polyT oligodeoxynucleotides.* Journal of immunology (Baltimore, Md. : 1950), 2006. **177**(10): p. 6584-6587.
70. Demaria, O., et al., *TLR8 deficiency leads to autoimmunity in mice.* Journal of Clinical Investigation, 2010.
71. Hemmi, H., et al., *A Toll-like receptor recognizes bacterial DNA.* Nature, 2000. **408**(6813): p. 740-745.
72. Krug, A., *Herpes simplex virus type 1 activates murine natural interferon-producing cells through toll-like receptor 9.* Blood, 2003. **103**(4): p. 1433-1437.
73. Krug, A., et al., *TLR9-dependent recognition of MCMV by IPC and DC generates coordinated cytokine responses that activate antiviral NK cell function.* Immunity, 2004. **21**(1): p. 107-119.
74. Lund, J., et al., *Toll-like Receptor 9-mediated Recognition of Herpes Simplex Virus-2 by Plasmacytoid Dendritic Cells.* Journal of Experimental Medicine, 2003. **198**(3): p. 513-520.
75. Vollmer, J., et al., *Characterization of three CpG oligodeoxynucleotide classes with distinct immunostimulatory activities.* European Journal of Immunology, 2004. **34**(1): p. 251-262.

76. Haas, T., et al., *The DNA Sugar Backbone 2′ Deoxyribose Determines Toll-like Receptor 9 Activation.* Immunity, 2008. **28**(3): p. 315-323.
77. LAMPHIER, M.S., et al., *TLR9 and the Recognition of Self and Non-Self Nucleic Acids.* Annals of the New York Academy of Sciences, 2006. **1082**(1): p. 31-43.
78. Rutz, M., et al., *Toll-like receptor 9 binds single-stranded CpG-DNA in a sequence- and pH-dependent manner.* European Journal of Immunology, 2004. **34**(9): p. 2541-2550.
79. Krieg, A.M., et al., *CpG motifs in bacterial DNA trigger direct B-cell activation.* Nature, 1995. **374**(6522): p. 546-549.
80. Mouchess, M.L., et al., *Transmembrane Mutations in Toll-like Receptor 9 Bypass the Requirement for Ectodomain Proteolysis and Induce Fatal Inflammation.* Immunity, 2011. **35**(5): p. 721-732.
81. Peter, M.E., et al., *Identification of an N-Terminal Recognition Site in TLR9 That Contributes to CpG-DNA-Mediated Receptor Activation.* The Journal of Immunology, 2009. **182**(12): p. 7690-7697.
82. Roach, J.C., et al., *The evolution of vertebrate Toll-like receptors.* Proceedings of the National Academy of Sciences of the United States of America, 2005. **102**(27): p. 9577-9582.
83. Yarovinsky, F., *TLR11 Activation of Dendritic Cells by a Protozoan Profilin-Like Protein.* Science, 2005. **308**(5728): p. 1626-1629.
84. Zhang, D., *A Toll-like Receptor That Prevents Infection by Uropathogenic Bacteria.* Science, 2004. **303**(5663): p. 1522-1526.
85. Mathur, R., et al., *A Mouse Model of Salmonella Typhi Infection.* Cell, 2012. **151**(3): p. 590-602.
86. Andrade, W.A., et al., *Combined Action of Nucleic Acid-Sensing Toll-like Receptors and TLR11/TLR12 Heterodimers Imparts Resistance to Toxoplasma gondii in Mice.* Cell Host and Microbe, 2013. **13**(1): p. 42-53.
87. Hidmark, A., A. von Saint Paul, and A.H. Dalpke, *Cutting Edge: TLR13 Is a Receptor for Bacterial RNA.* The Journal of Immunology, 2012. **189**(6): p. 2717-2721.
88. Li, X.D. and Z.J. Chen, *Sequence specific detection of bacterial 23S ribosomal RNA by TLR13.* eLife, 2012. **1**(0): p. e00102-e00102.
89. McGettrick, A.F. and L.A.O. Neill, *Localisation and trafficking of Toll-like receptors: an important mode of regulation.* Current Opinion in Immunology, 2010. **22**(1): p. 20-27.
90. Shui, W., et al., *Membrane proteomics of phagosomes suggests a connection to autophagy.* Proceedings of the National Academy of Sciences of the United States of America, 2008. **105**(44): p. 16952-16957.
91. Kim, Y.-M., et al., *UNC93B1 delivers nucleotide-sensing toll-like receptors to endolysosomes.* Nature, 2008. **452**(7184): p. 234-238.
92. Brinkmann, M.M., et al., *The interaction between the ER membrane protein UNC93B and TLR3, 7, and 9 is crucial for TLR signaling.* The Journal of Cell Biology, 2007. **177**(2): p. 265-275.
93. Baumann, C.L., et al., *CD14 is a coreceptor of Toll-like receptors 7 and 9.* Journal of Experimental Medicine, 2010. **207**(12): p. 2689-2701.
94. Weber, C., et al., *Toll-like receptor (TLR) 3 immune modulation by unformulated small interfering RNA or DNA and the role of CD14 (in TLR-mediated effects).* Immunology, 2012. **136**(1): p. 64-77.

95. Akashi-Takamura, S. and K. Miyake, *TLR accessory molecules.* Current Opinion in Immunology, 2008. **20**(4): p. 420-425.
96. Blasius, A.L., et al., *Slc15a4, AP-3, and Hermansky-Pudlak syndrome proteins are required for Toll-like receptor signaling in plasmacytoid dendritic cells.* Proceedings of the National Academy of Sciences of the United States of America, 2010. **107**(46): p. 19973-8.
97. Chiang, C.-y., et al., *Cofactors Required for TLR7- and TLR9-Dependent Innate Immune Responses.* Cell Host and Microbe, 2012. **11**(3): p. 306-318.
98. Tabeta, K., et al., *The Unc93b1 mutation 3d disrupts exogenous antigen presentation and signaling via Toll-like receptors 3, 7 and 9.* Nature Immunology, 2006. **7**(2): p. 156-164.
99. Casrouge, A., et al., *Herpes Simplex Virus Encephalitis in Human UNC-93B Deficiency.* Science, 2006. **314**(5797): p. 308-312.
100. Schamber-Reis, B.L.F., et al., *UNC93B1 and Nucleic Acid-sensing Toll-like Receptors Mediate Host Resistance to Infection with Leishmania major.* Journal of Biological Chemistry, 2013. **288**(10): p. 7127-7136.
101. Caetano, B.C., et al., *Requirement of UNC93B1 Reveals a Critical Role for TLR7 in Host Resistance to Primary Infection with Trypanosoma cruzi.* The Journal of Immunology, 2011. **187**(4): p. 1903-1911.
102. Crane, M.J., P.J. Gaddi, and T.P. Salazar-Mather, *UNC93B1 Mediates Innate Inflammation and Antiviral Defense in the Liver during Acute Murine Cytomegalovirus Infection.* PLoS ONE, 2012. **7**(6): p. e39161.
103. Janssen, E., et al., *Efficient T cell activation via a Toll-Interleukin 1 Receptor-independent pathway.* Immunity, 2006. **24**(6): p. 787-99.
104. Koehn, J., et al., *Assessing the function of human UNC-93B in Toll-like receptor signaling and major histocompatibility complex II response.* Human Immunology, 2007. **68**(11): p. 871-878.
105. Nakano, S., et al., *Up-regulation of the endoplasmic reticulum transmembrane protein UNC93B in the B cells of patients with active systemic lupus erythematosus.* Rheumatology, 2010. **49**(5): p. 876-881.
106. Kono, D.H., et al., *Endosomal TLR signaling is required for anti-nucleic acid and rheumatoid factor autoantibodies in lupus.* Proceedings of the National Academy of Sciences of the United States of America, 2009. **106**(29): p. 12061-6.
107. Fukui, R., et al., *Unc93B1 Restricts Systemic Lethal Inflammation by Orchestrating Toll-like Receptor 7 and 9 Trafficking.* Immunity, 2011. **35**(1): p. 69-81.
108. Kashuba, V.I., et al., *hUNC93B1: a novel human gene representing a new gene family and encoding an unc-93-like protein.* Gene, 2002. **283**(1-2): p. 209-217.
109. Anelli, T. and R. Sitia, *Protein quality control in the early secretory pathway.* The EMBO Journal, 2008. **27**(2): p. 315-327.
110. Sato, K., *COPII Coat Assembly and Selective Export from the Endoplasmic Reticulum.* Journal of Biochemistry, 2004. **136**(6): p. 755-760.
111. Jensen, D. and R. Schekman, *COPII-mediated vesicle formation at a glance.* Journal of Cell Science, 2010. **124**(1): p. 1-4.
112. Zanetti, G., et al., *COPII and the regulation of protein sorting in mammals.* Nature cell biology, 2011. **14**(1): p. 20-28.

113. Mancias, J.D. and J. Goldberg, *Structural basis of cargo membrane protein discrimination by the human COPII coat machinery.* The EMBO Journal, 2008. **27**(21): p. 2918-28.
114. Barlowe, C., *Signals for COPII-dependent export from the ER: what's the ticket out?* Trends in Cell Biology, 2003. **13**(6): p. 295-300.
115. Nufer, O., et al., *Role of cytoplasmic C-terminal amino acids of membrane proteins in ER export.* Journal of Cell Science, 2002. **115**(Pt 3): p. 619-628.
116. Sun, L.-P., et al., *Sterol-regulated transport of SREBPs from endoplasmic reticulum to Golgi: Insig renders sorting signal in Scap inaccessible to COPII proteins.* Proceedings of the National Academy of Sciences of the United States of America, 2007. **104**(16): p. 6519-6526.
117. Bonifacino, J.S. and L.M. Traub, *S IGNALS FORS ORTING OFT RANSMEMBRANEP ROTEINS TOE NDOSOMES ANDL YSOSOMES*.* Annual Review of Biochemistry, 2003. **72**(1): p. 395-447.
118. Watson, R.T. and J.E. Pessin, *Transmembrane domain length determines intracellular membrane compartment localization of syntaxins 3, 4, and 5.* American journal of physiology. Cell physiology, 2001. **281**(1): p. C215-23.
119. Vagin, O., J.A. Kraut, and G. Sachs, *Role of N-glycosylation in trafficking of apical membrane proteins in epithelia.* American journal of physiology. Renal physiology, 2009. **296**(3): p. F459-69.
120. Gough, N.R., et al., *Utilization of the indirect lysosome targeting pathway by lysosome-associated membrane proteins (LAMPs) is influenced largely by the C-terminal residue of their GYXXphi targeting signals.* Journal of Cell Science, 1999. **112**(23): p. 4257-4269.
121. Janvier, K. and J.S. Bonifacino, *Role of the endocytic machinery in the sorting of lysosome-associated membrane proteins.* Molecular biology of the cell, 2005. **16**(9): p. 4231-4242.
122. McCormick, P.J., J.A. Martina, and J.S. Bonifacino, *Involvement of clathrin and AP-2 in the trafficking of MHC class II molecules to antigen-processing compartments.* Proceedings of the National Academy of Sciences of the United States of America, 2005. **102**(22): p. 7910-7915.
123. Motley, A., *Clathrin-mediated endocytosis in AP-2-depleted cells.* The Journal of Cell Biology, 2003. **162**(5): p. 909-918.
124. Boucrot, E., et al., *Roles of AP-2 in clathrin-mediated endocytosis.* PLoS ONE, 2010. **5**(5): p. e10597.
125. Guermonprez, P., et al., *ER-phagosome fusion defines an MHC class I cross-presentation compartment in dendritic cells.* Nature, 2003. **425**(6956): p. 397-402.
126. Cebrian, I., et al., *Sec22b Regulates Phagosomal Maturation and Antigen Crosspresentation by Dendritic Cells.* Cell, 2011. **147**(6): p. 1355-1368.
127. Fukui, R., et al., *Unc93B1 biases Toll-like receptor responses to nucleic acid in dendritic cells toward DNA- but against RNA-sensing.* Journal of Experimental Medicine, 2009. **206**(6): p. 1339-1350.
128. Lee, C.C., A.M. Avalos, and H.L. Ploegh, *Accessory molecules for Toll-like receptors and their function.* Nature Publishing Group, 2012. **12**(3): p. 168-179.

129. Takahashi, K., et al., *A protein associated with Toll-like receptor (TLR) 4 (PRAT4A) is required for TLR-dependent immune responses.* Journal of Experimental Medicine, 2007. **204**(12): p. 2963-2976.
130. Yang, Y., et al., *Heat Shock Protein gp96 Is a Master Chaperone for Toll-like Receptors and Is Important in the Innate Function of Macrophages.* Immunity, 2007. **26**(2): p. 215-226.
131. Kim, J., et al., *Uncoupled packaging of amyloid precursor protein and presenilin 1 into coat protein complex II vesicles.* The Journal of biological chemistry, 2005. **280**(9): p. 7758-7768.
132. Merte, J., et al., *Sec24b selectively sorts Vangl2 to regulate planar cell polarity during neural tube closure.* Nature cell biology, 2009. **12**(1): p. 41-46.
133. Melo, M.B., et al., *UNC93B1 Mediates Host Resistance to Infection with Toxoplasma gondii.* PLoS Pathogens, 2010. **6**(8): p. e1001071.
134. Arpaia, N., et al., *TLR signaling is required for Salmonella typhimurium virulence.* Cell, 2011. **144**(5): p. 675-688.
135. Blasi, E., et al., *Selective immortalization of murine macrophages from fresh bone marrow by a raf/myc recombinant murine retrovirus.* Nature, 1985. **318**(6047): p. 667-70.
136. Garcia-Cattaneo, A., et al., *Cleavage of Toll-like receptor 3 by cathepsins B and H is essential for signaling.* Proceedings of the National Academy of Sciences of the United States of America, 2012. **109**(23): p. 9053-9058.
137. Park, B., et al., *Proteolytic cleavage in an endolysosomal compartment is required for activation of Toll-like receptor 9.* Nature Immunology, 2008. **9**(12): p. 1407-1414.
138. Deane, J.A., et al., *Control of Toll-like Receptor 7 Expression Is Essential to Restrict Autoimmunity and Dendritic Cell Proliferation.* Immunity, 2007. **27**(5): p. 801-810.
139. Pisitkun, P., *Autoreactive B Cell Responses to RNA-Related Antigens Due to TLR7 Gene Duplication.* Science, 2006. **312**(5780): p. 1669-1672.
140. Blasius, A.L., et al., *Slc15a4, AP-3, and Hermansky-Pudlak syndrome proteins are required for Toll-like receptor signaling in plasmacytoid dendritic cells.* Proceedings of the National Academy of Sciences, 2010. **107**(46): p. 19973-19978.
141. Ohno, H., et al., *Interaction of tyrosine-based sorting signals with clathrin-associated proteins.* Science, 1995. **269**(5232): p. 1872-1875.
142. Crump, C.M., et al., *Inhibition of the interaction between tyrosine-based motifs and the medium chain subunit of the AP-2 adaptor complex by specific tyrphostins.* The Journal of biological chemistry, 1998. **273**(43): p. 28073-7.
143. Ohno, H., et al., *Structural determinants of interaction of tyrosine-based sorting signals with the adaptor medium chains.* The Journal of biological chemistry, 1996. **271**(46): p. 29009-15.
144. Songyang, Z., et al., *SH2 domains recognize specific phosphopeptide sequences.* Cell, 1993. **72**(5): p. 767-78.
145. Ohno, H., *Clathrin-associated adaptor protein complexes.* Journal of Cell Science, 2006. **119**(18): p. 3719-3721.
146. Aguilar, R.C., *Signal-binding Specificity of the micro4 Subunit of the Adaptor Protein Complex AP-4.* Journal of Biological Chemistry, 2001. **276**(16): p. 13145-13152.

147. Dell'Angelica, E.C., C. Mullins, and J.S. Bonifacino, *AP-4, a novel protein complex related to clathrin adaptors.* The Journal of biological chemistry, 1999. **274**(11): p. 7278-7285.
148. Simmen, T., et al., *AP-4 binds basolateral signals and participates in basolateral sorting in epithelial MDCK cells.* Nature cell biology, 2002. **4**(2): p. 154-9.
149. Barois, N. and O. Bakke, *The adaptor protein AP-4 as a component of the clathrin coat machinery: a morphological study.* The Biochemical journal, 2005. **385**(Pt 2): p. 503-10.
150. Burgos, P.V., et al., *Sorting of the Alzheimer's disease amyloid precursor protein mediated by the AP-4 complex.* Developmental cell, 2010. **18**(3): p. 425-36.
151. Wang, J., et al., *The functional effects of physical interactions among Toll-like receptors 7, 8, and 9.* The Journal of biological chemistry, 2006. **281**(49): p. 37427-37434.
152. Itoh, H., et al., *UNC93B1 physically associates with human TLR8 and regulates TLR8-mediated signaling.* PLoS ONE, 2011. **6**(12): p. e28500.
153. Cervantes, J.L., et al., *TLR8: the forgotten relative revindicated.* Cellular and Molecular Immunology, 2012. **9**(6): p. 434-438.
154. Karlsson, K. and S.R. Carlsson, *Sorting of lysosomal membrane glycoproteins lamp-1 and lamp-2 into vesicles distinct from mannose 6-phosphate receptor/gamma-adaptin vesicles at the trans-Golgi network.* The Journal of biological chemistry, 1998. **273**(30): p. 18966-18973.
155. Mouchess, M.L., et al., *Transmembrane mutations in Toll-like receptor 9 bypass the requirement for ectodomain proteolysis and induce fatal inflammation.* Immunity, 2011. **35**(5): p. 721-32.
156. Nesterov, A., et al., *Inhibition of the receptor-binding function of clathrin adaptor protein AP-2 by dominant-negative mutant mu2 subunit and its effects on endocytosis.* The EMBO Journal, 1999. **18**(9): p. 2489-2499.
157. Avalos, A.M., et al., *Cell-Specific TLR9 Trafficking in Primary APCs of Transgenic TLR9-GFP Mice.* The Journal of Immunology, 2013. **190**(2): p. 695-702.
158. Lee, B.L., et al., *UNC93B1 mediates differential trafficking of endosomal TLRs.* eLife, 2013. **2**.
159. Pettitt, S.J., et al., *Agouti C57BL/6N embryonic stem cells for mouse genetic resources.* Nature methods, 2009. **6**(7): p. 493-5.
160. Saksela, K., G. Cheng, and D. Baltimore, *Proline-rich (PxxP) motifs in HIV-1 Nef bind to SH3 domains of a subset of Src kinases and are required for the enhanced growth of Nef+ viruses but not for down-regulation of CD4.* The EMBO Journal, 1995. **14**(3): p. 484-491.
161. Piguet, V., et al., *HIV-1 Nef protein binds to the cellular protein PACS-1 to downregulate class I major histocompatibility complexes.* Nature cell biology, 2000. **2**(3): p. 163-7.
162. Crump, C.M., et al., *PACS-1 binding to adaptors is required for acidic cluster motif-mediated protein traffic.* The EMBO Journal, 2001. **20**(9): p. 2191-201.
163. Kawane, K., et al., *Cytokine-dependent but acquired immunity-independent arthritis caused by DNA escaped from degradation.* Proceedings of the National Academy of Sciences of the United States of America, 2010. **107**(45): p. 19432-7.
164. Lakso, M., et al., *Efficient in vivo manipulation of mouse genomic sequences at the zygote stage.* Proceedings of the National Academy of Sciences of the United States of America, 1996. **93**(12): p. 5860-5.